VOLUME 10 NUMBER 2 2019 ISSN 2218-7987
eISSN 2409-5508

International Journal of Mathematics and Physics

Al-Farabi Kazakh National University

The International Journal of Mathematics and Physics is a peer-reviewed international journal covering all branches of mathematics and physics. The Journal welcomes papers on modern problems of mathematics and physics, in particular, Applied Mathematics, Algebra, Mathematical Analysis, Differential Equations, Mechanics, Informatics, Mathematical Modeling, Applied Physics, Radio Physics, Thermophysics, Nuclear Physics, Nanotechnology, and etc.

International Journal of Mathematics and Physics is published twice a year by al-Farabi Kazakh National University, 71 al-Farabi ave., 050040, Almaty, Kazakhstan
website: http://ijmph.kaznu.kz/

Any inquiry for subscriptions should be send to:
Prof. Tlekkabul Ramazanov, al-Farabi Kazakh National University
71 al-Farabi ave., 050040, Almaty, Kazakhstan
e-mail: Tlekkabul.Ramazanov@kaznu.kz

EDITORIAL

The most significant scientific achievements are attained through joint efforts of different sciences, mathematics and physics are among them. Therefore publication of the Journal, which shows results of current investigations in the field of mathematics and physics, will allow wider exhibition of scientific problems, tasks and discoveries.

One of the basic goals of the Journal is to promote extensive exchange of information between scientists from all over the world. We propose publishing service for original papers and materials of Mathematical and Physical Conferences (by selection) held in different countries and in the Republic of Kazakhstan.

Creation of the special International Journal of Mathematics and Physics is of great importance because a vast amount of scientists are willing to publish their articles and it will help to widen the geography of future dissemination. We will also be glad to publish papers of scientists from all the continents.

The Journal will publish experimental and theoretical investigations on Mathematics, Physical Technology and Physics. Among the subject emphasized are modern problems of Applied Mathematics, Algebra, Mathematical Analysis, Differential Equations, Mechanics, Informatics, Mathematical Modeling, Astronomy, Space Research, Theoretical Physics, Plasma Physics, Chemical Physics, Radio Physics, Thermophysics, Nuclear Physics, Nanotechnology, and etc.

The Journal is issued on the base of al-Farabi Kazakh National University. Leading scientists from different countries of the world agreed to join the Editorial Board of the Journal.

The Journal is published twice a year by al-Farabi Kazakh National University. We hope to receive papers from many laboratories which are interested in applications of the scientific principles of mathematics and physics and are carrying out researches on such subjects as production of new materials or technological problems.

IRSTI27.29.19; 27.29.25; 27.41.19 https://doi.org/10.26577/ijmph-2019-i2-1

[1,2*]A.T.Assanova, [1,2,3]E.A.Bakirova, [1,2,4] Zh.M.Kadirbayeva

[1]Institute of Mathematics and Mathematical Modeling, Almaty, Kazakhstan;
[2]Institute of Information and Computational Technologies, Almaty, Kazakhstan;
[3]Kazakh National Women's Teacher Training University, Almaty, Kazakhstan;
[4]International Information Technology University, Almaty, Kazakhstan
[*]e-mail: assanova@math.kz

NUMERICAL SOLUTION OF A CONTROL PROBLEM FOR ORDINARY DIFFERENTIAL EQUATIONS WITH MULTIPOINT INTEGRAL CONDITION

Abstract.A linear boundary value problem with a parameter for ordinary differential equations with multipoint integral conditionis investigated.The method of parameterization is used for solving the considered problem. The linear boundary value problem with a parameter for ordinary differential equations with multipoint integral condition by introducing additional parameters at the partition points is reduced to equivalent boundary value problem with parameters. The equivalent boundary value problem with parameters consists of the Cauchy problem for the system of ordinary differential equations with parameters, multipoint integral condition and continuity conditions. The solution of the Cauchy problem for the system of ordinary differential equations with parameters is constructed using the fundamental matrix of differential equation. The system of linear algebraic equations with respect to the parameters are composed by substituting the values of the corresponding points in the built solutions to the multipoint integral condition and the continuity condition. Numerical method for finding solution of the problem is suggested, which based on the solving the constructed system and Runge-Kutta method of the 4-th order for solving Cauchy problem on the subintervals.
Key words: control problem with multipoint integral condition, numerical solution, algorithm.

Introduction

Control problems, which are also called boundary value problems with parameters and the problem of identification parameter for a system of ordinary differential and integro-differential equations with parameters, have been intensively investigated in recent years. Questions of existence, uniqueness and stability of solving problems with parameters are very important for development of numerical methods of identification of parameters of the mathematical models described by ordinary differential equations with multipoint integral condition [1-8].To solve these classes of control problems, there were used the optimization methods, topological methods, the maximum principle, etc. In spite of this, the questions of finding the effective signs of unique solvability and constructing the numerical algorithms for finding the optimal solutions of control problems for the systems of ordinary differential equations with parameters still remain open. One of the constructive methods for investigating and solving the boundary value problems with parameters for the system of ordinary differential equations is the parameterization method [9]. The parameterization method was developed for the investigating and solving the boundary value problems for the system of ordinary differential equations. On the basis of this method, coefficient criteria for the unique solvability of linear boundary value problems for the system of ordinary differential equations were obtained. Algorithms for finding the approximate solutions were also proposed and their convergence to the exact solution of the problem studied was established. Later, the parameterization method was developed for the two-point boundary value problems for the Fredholmintegro-differential equations [10-14]. Necessary and sufficient conditions for the solvability and unique solvability are established, the algorithms for finding the approximate solutions of the problems considered are the linear Fredholm integro-differential equation on the basis of new algorithms of parameterization method are constructed. This approach are applied to two-point boundary value problems for system of ordinary and ordinary loaded differential equations with parameter [16-17].

In the present paper, linear problem with a parameter for an ordinary differential equation with multipoint integral condition is investigated. Based on the parameterization method and numerical methods, the numerical method for solving the problem considered is developed, and the algorithms for their implementation are proposed. By introducing additional parameters as the values of the desired solution at some points of the interval $[0,T]$, where the problem is considered, the obtained problem is reduced to the equivalent problem consisting of a special Cauchy problem for the system of ordinary differential equations, multipoint integral conditions, and continuity conditions for the solution at the points of partition. Using the integral equation, that equivalent to the special Cauchy problem for the system of ordinary differential equation, we obtained a representation of the solution of the special Cauchy problem using the entered parameters at the assumption of invertibility of a some matrix. Based on this representation, a system of algebraic equations with respect to the parameters is constructed from the multipoint integral condition and the continuity conditions of the solution. We offer algorithm for solving the control problem for the ordinary differential equation with multipoint integral condition, and its numerical implementation.

Statement of problem and scheme of parametrization method

We consider a linear boundary value problem with a parameter for an ordinary differential equation with multipoint integral condition

$$\frac{dx}{dt} = A(t)x + A_0(t)\mu + f(t),$$

$$x \in R^n, \quad \mu \in R^m, \quad t \in (0,T), \tag{1}$$

$$\sum_{i=0}^{N+1} C_i x(t_i) + B_0\mu + \int_0^T M(t)x(t)dt = d, \quad d \in R^{n+m}, \tag{2}$$

where the $(n \times n)$-matrix $A(t)$, $(n \times m)$-matrix $A_0(t)$, $((n+m) \times n)$-matrix $M(t)$ and n-vector-function $f(t)$ are continuous on $[0,T]$, the $((n+m) \times n)$-matrices C_i, $i = \overline{0, N+1}$, the $((n+m) \times m)$-matrix B_0 are constants.

The solution to problem (1), (2) is a pair $(x^*(t), \mu^*)$, where continuous on $[0,T]$ and continuously differentiable on $(0,T)$ a function $x^*(t)$ satisfies the ordinary differential equation (1) and condition (2) with $\mu = \mu^*$.

To solve the problem with parameter (1), (2), the approach developed in [24-26] is used, based on the algorithms of the parameterization method and numerical methods for solving Cauchy problems.

Scheme of the method. Points $0 = t_0 < t_1 < \dots < t_N < t_{N+1} = T$ are taken and the interval $[0,T)$ is divided into N subintervals:

$$[0,T) = \cup_{r=1}^{N+1}[t_{r-1}, t_r).$$

Let $C([0,T], R^n)$ be the space of continuous on $[0,T]$ functions $x: [0,T] \to R^n$ with norm $\|x\|_1 = \max_{t\in[0,T]} \|x(t)\|$; $C([0,T], \Delta_N, R^{n(N+1)})$ - the space of systems of functions $x[t] = (x_1(t), x_2(t), \dots, x_{N+1}(t))$, where $x_r: [t_{r-1}, t_r) \to R^n$ are continuous on $[t_{r-1}, t_r)$ and have finite left-sided limits $\lim_{t\to t_r - 0} x_r(t)$ for all $r=\overline{1, N+1}$, with norm $\|x[\cdot]\|_2 = \max_{r=\overline{1,N+1}} \sup_{t\in[t_{r-1},t_r)} \|x_r(t)\|$.

The restriction of the function $x(t)$ to the r-th interval $[t_{r-1}, t_r)$ is denoted by $x_r(t)$, i.e. $x_r(t) = x(t)$ for $t \in [t_{r-1}, t_r)$, $r=\overline{1, N+1}$. Then we reduce problem (1), (2) to the equivalent multipoint boundary value problem

$$\frac{dx_r}{dt} = A(t)x_r + A_0(t)\mu + \mathrm{f(t)},$$

$$t \in [t_{r-1}, t_r), \quad r = \overline{1, N+1}, \tag{3}$$

$$\sum_{i=0}^{N} C_i x_{i+1}(t_i) + C_{N+1} \lim_{t\to T-0} x_{N+1}(t) + B_0\mu + \sum_{k=1}^{N+1} \int_{t_{k-1}}^{t_k} M(t)x_k(t)dt = d, \tag{4}$$

$$\lim_{t\to t_s - 0} x_s(t) = x_{s+1}(t_s), \quad s = \overline{1, N}. \tag{5}$$

where (5) are conditions for matching the solution at the interior points of partition.

The solution of problem (3) - (5) is the pair $(x^*[t], \mu^*)$ with elements $x^*[t] = (x_1^*(t), x_2^*(t), \dots, x_{N+1}^*(t)) \in C([0,T], \Delta_N, R^{n(N+1)})$, $\mu^* \in R^m$, where functions

$x_r^*(t)$, $r=\overline{1,N+1}$, are continuously differentiable on $[t_{r-1},t_r)$, which satisfies system of ordinary differential equations (3) and condition (4) with $\mu=\mu^*$ and continuity conditions (5).

We introduce additional parameters $\lambda_r=x_r(t_{r-1})$, $r=\overline{1,N+1}$, $\lambda_{N+2}=\mu$. Making the substitution $x_r(t)=u_r(t)+\lambda_r$ on every r-th interval $[t_{r-1},t_r)$, $r=\overline{1,N+1}$, we obtain multipoint boundary value problem with parameters

$$\frac{du_r}{dt}=A(t)[u_r+\lambda_r]+A_0(t)\lambda_{N+2}+\mathrm{f}(t),$$

$$t\in[t_{r-1},t_r),\ \ r=\overline{1,N+1}, \qquad (6)$$

$$u_r(t_{r-1})=0,\ r=\overline{1,N+1}, \qquad (7)$$

$$\sum_{i=0}^{N}C_i\lambda_{i+1}+C_{N+1}\lambda_{N+1}+$$

$$+C_{N+1}\lim_{t\to T-0}u_{N+1}(t)+B_0\lambda_{N+2}+$$

$$+\sum_{k=1}^{N+1}\int_{t_{k-1}}^{t_k}M(t)[u_k(t)+\lambda_k]dt=d, \qquad (8)$$

$$\lambda_s+\lim_{t\to t_s-0}u_s(t)=\lambda_{s+1},\quad s=\overline{1,N}. \qquad (9)$$

A pair $(u^*[t],\lambda^*)$ with elements $u^*[t]=(u_1^*(t),u_2^*(t),\dots,u_{N+1}^*(t))\in C([0,T],\Delta_N,R^{n(N+1)})$, $\lambda^*=(\lambda_1^*,\lambda_2^*,\dots,\lambda_{N+1}^*,\lambda_{N+2}^*)\in R^{n(N+1)+m}$ is said to be a solution to problem (6)-(9) if the functions $u_r^*(t)$, $r=\overline{1,N+1}$, are continuously differentiable on $[t_{r-1},t_r)$ and satisfy (6) and additional conditions (8), (9) with $\lambda_j=\lambda_j^*$, $j=\overline{1,N+2}$, and initial conditions (7).

If the pair $(x^*(t),\mu^*)$ is a solution of problem (1), (2), then the pair $(u^*[t],\lambda^*)$ with elements $u^*[t]=(u_1^*(t),u_2^*(t),\dots,u_{N+1}^*(t))\in C([0,T],\Delta_N,R^{n(N+1)})$, $\lambda^*=(\lambda_1^*,\lambda_2^*,\dots,\lambda_{N+1}^*,\lambda_{N+2}^*)\in R^{n(N+1)+m}$, where $\lambda_r^*=x_r^*(t_{r-1})$, $u_r^*(t)=x_r^*(t)+x_r^*(t_{r-1})$, $t\in[t_{r-1},t_r)$, $\mathrm{r}=\overline{1,N+1}$, $\lambda_{N+2}^*=\mu^*\in R^m$, is the solution of problem (3)-(6). Conversely, if a pair $(\tilde u[t],\ \tilde\lambda)$ with elements $\tilde u[t]=(\tilde u_1(t),\tilde u_2(t),\dots,\tilde u_{N+1}(t))\in C([0,T],\Delta_N,R^{n(N+1)})$, $\tilde\lambda=(\tilde\lambda_1,\tilde\lambda_2,\dots,\tilde\lambda_{N+2})\in R^{n(N+1)+m}$, is a solution of (3)-(6) , then the pair $(\tilde x(t),\tilde\mu)$ defined by the equalities $\tilde x(t)=u_r(t)+\tilde\lambda_r$, $t\in[t_{r-1},t_r)$, $\mathrm{r}=\overline{1,N+1}$, $\tilde x(T)=\lim_{t\to T-0}\tilde u_N(t)+\tilde\lambda_N$ and $\tilde\mu=\tilde\lambda_{N+2}$, will be the solution of the original boundary value problem with parameter (1), (2).

Let $X_r(t)$ be a fundamental matrix to the differential equation $\frac{dx}{dt}=A(t)x$ on $[t_{r-1},t_r)$, $\mathrm{r}=\overline{1,N+1}$.

Then the unique solution to the Cauchy problem for the system of ordinary differential equations (6), (7) at the fixed values $\lambda=(\lambda_1,\lambda_2,\dots,\lambda_{N+1},\lambda_{N+2})$ has the following form

$$u_r(t)=X_r(t)\int_{t_{r-1}}^{t}X_r^{-1}(\tau)A(\tau)d\tau\,\lambda_\mathrm{r}+X_r(t)\int_{t_{r-1}}^{t}X_r^{-1}(\tau)A_0(\tau)d\tau\,\lambda_{\mathrm{N+2}}+$$
$$+X_r(t)\int_{t_{r-1}}^{t}X_r^{-1}(\tau)f(\tau)d\tau,\quad t\in[t_{r-1},t_r),\ \mathrm{r}=\overline{1,N+1}. \qquad (10)$$

Substituting the corresponding right-hand sides of (10) into the conditions (8), (9), we obtain a system of linear algebraic equations with respect to the parameters λ_r, $r=\overline{1,N+2}$:

$$\sum_{i=0}^{N}C_i\lambda_{i+1}+C_{N+1}\lambda_{N+1}+B_0\lambda_{N+2}+C_{N+1}X_{N+1}(T)\int_{t_N}^{T}X_{N+1}^{-1}(\tau)A(\tau)d\tau\,\lambda_{\mathrm{N+1}}+$$
$$+C_{N+1}X_{N+1}(T)\int_{t_N}^{T}X_{N+1}^{-1}(\tau)A_0(\tau)d\tau\,\lambda_{\mathrm{N+2}}+$$

$$+\sum_{k=1}^{N+1}\int_{t_{k-1}}^{t_k} M(t)\left[X_k(t)\int_{t_{k-1}}^{t} X_k^{-1}(\tau)A(\tau)d\tau\,\lambda_k+\lambda_k\right]dt+$$
$$+\sum_{k=1}^{N+1}\int_{t_{k-1}}^{t_k} M(t)\left[X_k(t)\int_{t_{k-1}}^{t} X_k^{-1}(\tau)A_0(\tau)d\tau\,\lambda_{N+2}\right]dt=$$
$$=d-C_{N+1}X_{N+1}(T)\int_{t_N}^{T} X_{N+1}^{-1}(\tau)f(\tau)d\tau-$$
$$-\sum_{k=1}^{N+1}\int_{t_{k-1}}^{t_k} M(t)X_k(t)\int_{t_{k-1}}^{t} X_k^{-1}(\tau)f(\tau)d\tau\,dt, \tag{11}$$

$$\lambda_s+X_s(t_s)\int_{t_{s-1}}^{t_s} X_s^{-1}(\tau)A(\tau)d\tau\,\lambda_s+X_s(t_s)\int_{t_{s-1}}^{t_s} X_s^{-1}(\tau)A_0(\tau)d\tau\,\lambda_{N+2}-\lambda_{s+1}=$$
$$=-X_s(t_s)\int_{t_{s-1}}^{t_s} X_s^{-1}(\tau)f(\tau)d\tau,\quad s=\overline{1,N}. \tag{12}$$

We denote the matrix corresponding to the left side of the system of equations (11), (12) by $Q_*(\Delta_N)$ and write the system in the form

$$Q_*(\Delta_N)\lambda=-F_*(\Delta_N),\ \ \lambda\in R^{n(N+1)+m}, \tag{13}$$

where

$$F_*(\Delta_N)=$$
$$\begin{pmatrix} -d+C_{N+1}X_{N+1}(T)\int_{t_N}^{T} X_{N+1}^{-1}(\tau)f(\tau)d\tau+\sum_{k=1}^{N+1}\int_{t_{k-1}}^{t_k} M(t)X_k(t)\int_{t_{k-1}}^{t} X_k^{-1}(\tau)f(\tau)d\tau\,dt \\ X_1(t_1)\int_{t_0}^{t_1} X_1^{-1}(\tau)f(\tau)d\tau \\ \dots\ \ \dots\ \ \dots \\ X_N(t_N)\int_{t_{N-1}}^{t_N} X_N^{-1}(\tau)f(\tau)d\tau \end{pmatrix}.$$

It is not difficult to establish that the solvability of the boundary value problem (1), (2) is equivalent to the solvability of the system (13). The solution of the system (13) is a vector $\lambda^*=(\lambda_1^*,\lambda_2^*,\dots,\lambda_{N+1}^*,\lambda_{N+2}^*)\in R^{n(N+1)+m}$ consists of the values of the solutions of the original problem (1), (2) in the initial points of subintervals, i.e. $\lambda_r^*=x^*(t_{r-1})$, $r=\overline{1,N+1}$, $\lambda_{N+2}^*=\mu^*$.

Further we consider the Cauchy problems for ordinary differential equations on subintervals

$$\frac{dz}{dt}=A(t)z+P(t),$$

$$z(t_{r-1})=0,\quad t\in[t_{r-1},t_r],\ \ r=\overline{1,N+1}, \tag{14}$$

where $P(t)$ is either $(n\times n)$ matrix, or n vector, both continuous on $[t_{r-1},t_r]$, $r=\overline{1,N+1}$. Consequently, solution to problem (14) is a square matrix or a vector of dimension n. Denote by $a(P,t)$ the solution to the Cauchy problem (14). Obviously,

$$a(P,t)=X_r(t)\int_{t_{r-1}}^{t} X_r^{-1}(\tau)P(\tau)d\tau,$$
$$t\in[t_{r-1},t_r],$$

where $X_r(t)$ is a fundamental matrix of differential equation (14) on the r-th interval.

Numerical implementation of parametrization method

We offer the following numerical implementation of algorithm based on the Runge–Kutta method of 4th order and Simpson's method.

1. Suppose we have a partition Δ_N: $0=t_0<t_1<\dots<t_N<t_{N+1}=T$. Divide each r-th interval

$[t_{r-1},t_r]$, $r=\overline{1,N+1}$, into N_r parts with step $h_r=(t_r-t_{r-1})/N_r$. Assume on each interval $[t_{r-1},t_r]$ the variable $\hat{t}$ takes its discrete values: $\hat{t}=t_{r-1}$, $\hat{t}=t_{r-1}+h_r,\dots$, $\hat{t}=t_{r-1}+(N_r-1)h_r$, $\hat{t}=t_r$, and denote by $\{t_{r-1},t_r\}$ the set of such points.

2. Solving the Cauchy problems for ordinary differential equations

$$\frac{dz}{dt}=A(t)z+A(t),$$
$$z(t_{r-1})=0,\quad t\in[t_{r-1},t_r],$$

$$\frac{dz}{dt}=A(t)z+A_0(t),$$
$$z(t_{r-1})=0,\quad t\in[t_{r-1},t_r],$$

$$\frac{dz}{dt}=A(t)z+f(t),$$
$$z(t_{r-1})=0,\quad t\in[t_{r-1},t_r],\ \ r=\overline{1,N+1},$$

by using again the Runge–Kutta method of 4$^{\text{th}}$ order, we find the values of $(n\times n)$ matrices $a_r(A,\hat{t})$, $a_r(A_0,\hat{t})$ and n vector $a_r(f,\hat{t})$ on $\{t_{r-1},t_r\}$, $r=\overline{1,N+1}$.

3. Applying Simpson's method on the set $\{t_{r-1},t_r\}$, we evaluate the definite integrals

$$\mathrm{m}_r^{h_r}=\int_{t_{r-1}}^{t_r}\mathrm{M}(\tau)d\tau,$$

$$\mathrm{m}_r^{h_r}(\mathrm{A})=\int_{t_{r-1}}^{t_r}\mathrm{M}(\tau)a_r^{h_r}(\mathrm{A},\tau)d\tau,$$

$$\mathrm{m}_r^{h_r}(\mathrm{A}_0)=\int_{t_{r-1}}^{t_r}\mathrm{M}(\tau)a_r^{h_r}(\mathrm{A}_0,\tau)d\tau,$$

$$\mathrm{m}_r^{h_r}(f)=\int_{t_{r-1}}^{t_r}\mathrm{M}(\tau)a_r^{h_r}(f,\tau)d\tau,\ r=\overline{1,N+1}.$$

4. Construct the system of linear algebraic equations with respect to parameters

$$Q_*^{\tilde{h}}(\Delta_N)\lambda=-F_*^{\tilde{h}}(\Delta_N),\ \ \lambda\in R^{n(N+1)+m}, \quad (15)$$

Solving the system (15), we find $\lambda^{\tilde{h}}$. As noted above, the elements of $\lambda^{\tilde{h}}=(\lambda_1^{\tilde{h}},\lambda_2^{\tilde{h}},\dots,\lambda_{N+2}^{\tilde{h}})$ are the values of approximate solution to problem (1), (2) in the starting points of subintervals: $x^{\tilde{h}_r}(t_{r-1})=\lambda_r^{\tilde{h}}$, $r=\overline{1,N+1}$, $\mu^*=\lambda_{N+2}^*$.

5. To define the values of approximate solution at the remaining points of set $\{t_{r-1},t_r\}$, we solve the Cauchy problems

$$\frac{dx}{dt}=A(t)x+A_0(t)\lambda_{N+2}^{\tilde{h}}+f(t),$$

$$x(t_{r-1})=\lambda_r^{\tilde{h}},\quad t\in[t_{r-1},t_r],\ \ r=\overline{1,N+1}.$$

And the solutions to Cauchy problems are found by the Runge–Kutta method of 4th order. Thus, the algorithm allows us to find the numerical solution to the problem (1), (2).

To illustrate the proposed approach for the numerical solving linear boundary value problem with a parameter for an ordinary differential equation with multipoint integral condition (1), (2) on the basis of parameterization method, let us consider the following example.

Example. We consider a linear boundary value problem with a parameter for an ordinary differential equation with multipoint integral condition

$$\frac{dx}{dt}=A(t)x+A_0(t)\mu+f(t),$$

$$x\in R^2,\quad \mu\in R^3,\quad t\in(0,1), \qquad (16)$$

$$C_0x(t_0)+C_1x(t_1)+C_2x(t_2)+$$

$$+B_0\mu+\int_0^T M(t)x(t)dt=d,\quad d\in R^5. \quad (17)$$

Here $t_0=0,t_1=\frac{1}{2},\ t_2=1,$
$A(t)=\begin{pmatrix}t^2 & 2t\\ 1 & t+9\end{pmatrix},\quad A_0(t)=\begin{pmatrix}2 & t & t+3\\ t^2 & 0 & 3t\end{pmatrix},$

$$C_0=\begin{pmatrix}2 & 0\\ 4 & -4\\ 1 & 6\\ 0 & 2\\ 9 & 1\end{pmatrix},\ C_1=\begin{pmatrix}-3 & 1\\ 5 & 2\\ 3 & 0\\ 8 & 6\\ 1 & 9\end{pmatrix},$$

$$C_2=\begin{pmatrix}-6 & 1\\ 5 & 3\\ 8 & 1\\ 2 & 6\\ 0 & 9\end{pmatrix},B_0=\begin{pmatrix}1 & 3 & 0\\ 3 & 1 & -4\\ 0 & 7 & -6\\ -2 & 1 & 8\\ 6 & 1 & 0\end{pmatrix},$$

$$d=\begin{pmatrix}-42\\ \frac{349}{3}\\ \frac{553}{12}\\ \frac{505}{2}\\ \frac{369}{2}\end{pmatrix},\ M(t)=\begin{pmatrix}1 & 0\\ t & -2\\ t+3 & t^2\\ 0 & 9\\ -3 & 1\end{pmatrix},$$

$$f(t) = \begin{pmatrix} -8t^4 - t^3 - 25t^2 - 2t - 30 \\ -4t^4 - 36t^3 + t^2 - 107t + 20 \end{pmatrix}.$$

We use the numerical implementation of algorithm. Accuracy of solution depends on the accuracy of solving the Cauchy problem on subintervals and evaluating definite integrals. We provide the results of the numerical implementation of algorithm by partitioning the subintervals [0, 0.5], [0.5, 1] with step h = 0.025.

Solving the system of equations (15), we obtain the numerical values of the parameters

$$\lambda_1^{\tilde{h}} = \begin{pmatrix} 7.00000083 \\ -1.99999956 \end{pmatrix},$$

$$\lambda_2^{\tilde{h}} = \begin{pmatrix} 7.50000135 \\ 3.00000449 \end{pmatrix},$$

$$\lambda_3^{\tilde{h}} = \begin{pmatrix} 2.00000297 \\ -3.00000131 \\ 8.99999832 \end{pmatrix}.$$

We find the numerical solutions at the other points of the subintervals using Runge-Kutta method of the 4-th order to the following Cauchy problems

$$\frac{d\tilde{x}_r}{dt} = A(t)\tilde{x}_r + A_0(t)\lambda_3^{\tilde{h}} + f(t),$$

$$\tilde{x}_r(t_{r-1}) = \lambda_r^{\tilde{h}}, \quad t \in [t_{r-1}, t_r], \quad r = \overline{1,2}.$$

Exact solution of the problem (16), (17) is pair $(x^*(t), \mu^*)$, where $x^*(t) = \begin{pmatrix} t+7 \\ 4t^3 + 9t - 2 \end{pmatrix}$, $\mu^* = \begin{pmatrix} 2 \\ -3 \\ 9 \end{pmatrix}$.

The results of calculations of numerical solutions at the partition points are presented in the following table:

t	$\tilde{x}_1(t)$	$\tilde{x}_2(t)$	t	$\tilde{x}_1(t)$	$\tilde{x}_2(t)$
0	7.00000083	-1.99999956	0.5	7.50000135	3.00000449
0.025	7.02500086	-1.77493687	0.525	7.52500139	3.30381719
0.05	7.05000088	-1.54949918	0.55	7.55000142	3.61550487
0.075	7.0750009	-1.32331148	0.575	7.57500146	3.93544255
0.1	7.10000092	-1.09599878	0.6	7.60000149	4.26400522
0.125	7.12500094	-0.86718609	0.625	7.62500152	4.60156787
0.15	7.15000097	-0.63649839	0.65	7.65000155	4.94850549
0.175	7.17500099	-0.40356069	0.675	7.67500158	5.30519309
0.2	7.20000101	-0.16799798	0.7	7.7000016	5.67200565
0.225	7.22500104	0.07056472	0.725	7.72500161	6.04931816
0.25	7.25000106	0.31250243	0.75	7.75000162	6.4375056
0.275	7.27500109	0.55819013	0.775	7.77500161	6.83694297
0.3	7.30000111	0.80800284	0.8	7.80000158	7.24800522
0.325	7.32500114	1.06231555	0.825	7.82500153	7.67106734
0.35	7.35000117	1.32150326	0.85	7.85000144	8.10650427
0.375	7.3750012	1.58594096	0.875	7.8750013	8.55469097
0.4	7.40000123	1.85600367	0.9	7.90000111	9.01600237
0.425	7.42500126	2.13206638	0.925	7.92500083	9.49081337
0.45	7.45000129	2.41450409	0.95	7.95000044	9.97949887
0.475	7.47500132	2.70369179	0.975	7.9749999	10.48243371
0.5	7.50000135	3.00000449	1	7.99999916	10.99999269

$\tilde{\mu}_1 = \lambda_{31}^{\tilde{h}}$	$\tilde{\mu}_2 = \lambda_{32}^{\tilde{h}}$	$\tilde{\mu}_3 = \lambda_{33}^{\tilde{h}}$
2.00000297	-3.00000131	8.99999832

For the difference of the corresponding values of the exact and constructed solutions of the problem the following estimate is true:

$$\max_{j=\overline{0,40}} \|x^*(t_j) - \tilde{x}(t_j)\| < 0.000007 \text{ and}$$
$$max\|\mu^* - \tilde{\mu}\| < 0.000003.$$

Conclusion

In this work, we propose a numerical implementation of parametrization method for finding solutions to linear boundary value problem with a parameter for an ordinary differential equation with multipoint integral condition. Using the parametrization method, we reduce the considered problem to the equivalent boundary value problem with parameters. The unknown functions are determined from the Cauchy problems for the system of ordinary differential equations, and the introduced parameters are determined from the system of algebraic equations. A numerical algorithm for finding solution to the considered problem is constructed. The Cauchy problem is solved by Runge– Kutta method of 4th-order accuracy. The examples illustrating the numerical algorithms of parametrization method are provided.

Acknowledgement

The research is partially supported by grants (№№ AP05132486, AP05131220, AP05132455) of Ministry of Education and Science of the Republic of Kazakhstan (2018-2020).

References

1. Bellman R.E., Kalaba R.E. "Quasilinearization and Nonlinear Boundary-Value Problems", *American Elsevier Pub. Co.*, New York, (1965).
2. Kiguradze I.T. "Boundary value problems for systems of ordinary differential equations". *Sovremennye problemy matematiki. Noveishie dostizhenia*. (Itogi nauki i techniki. VINITI AN SSSR) (1987): 3-103 (in russian).
3. Ronto M., Samoilenko A.M. "Numerical-analytic methods in the theory of boundary-value problems", *World Scientific, River Edge* (2000).
4. Boichuk A.A., Samoilenko A.M. "Generalized inverse operators and Fredholm boundary-value problems". *VSP* (2004).
5. Brunner H. "Collocation methods for Volterra integral and related functional equations. *Cambridge University Press* (2004).
6. Wazwaz A.-M. "Linear and Nonlinear Integral Equations: Methods and Applications", *Higher Equation Press* (2011).
7. Loreti P., Sforza D. "Control problems for weakly coupled systems with memory". *J. of Diff. Equat.*, 257 (2014): 1879-1938.
8. Volpert V. "Elliptic partial differential equations Vol. 2: Reaction-Diffusing Equations". *Birkhauser Springer* (2014).
9. Dzhumabayev, D.S. "Criteria for the unique solvability of a linear boundary-value problem for an ordinary differential equation". *U.S.S.R. Computational Mathematics and Mathematical Physics* 29, 1 (1989): 34-46.
10. Dzhumabaev, D.S. "A method for solving the linear boundary value problem for an integro-differential equation". *Computational Mathematics and Mathematical Physics* 50, 7(2010): 1150-1161.
11. Dzhumabaev, D.S. "An algorithm for solving a linear two-point boundary value problem for an integro-differential equation". *Computational Mathematics and Mathematical Physics* 53, 6(2013): 736-758.
12. Dzhumabaev, D.S., Bakirova, E.A. "Criteria for the unique solvability of a linear two-point boundary value problem for systems of integro-differential equations". *Differential Equations* 49, 9(2013): 1087-1102.
13. Dzhumabaev, D.S. "Necessary and sufficient conditions for the solvability of linear boundary-value problems for the Fredholm integro-differential equations". *Ukranian Mathematical Journal* 66, 8(2015): 1200-1219.
14. Dzhumabaev, D.S. "Solvability of a linear boundary value problem for a Fredholm integro-differential equation with impulsive inputs". *Differential Equations* 51, 9(2015): 1180-1196.
15. Dzhumabaev, D.S. "On one approach to solve the linear boundary value problems for Fredholm integro-differential equations". *Journal of Computational and Applied Mathematics* 294, (2016): 342-357.
16. Dzhumabaev, D.S. Bakirova, E.A., Kadirbayeva Zh.M. "An algorithm for solving a control problem for a differential equation with a parameter". *News of the NAS RK. Phys.-Math. Series* 5, 321(2018): 25-32. DOI: https://doi.org/10.32014/2018.2518-1726.4.
17. Assanova A.T., Bakirova E.A., Kadirbayeva Zh.M. "Numerical implementation of solving a boundary value problem for a system of loaded differential equations with parameter". *News of the NAS RK. Phys.-Math. Series*. 3, 325(2019): 77-84. DOI: https://doi.org/10.32014/2019.2518-1726.27.

IRSTI 27.29.25 https://doi.org/10.26577/ijmph-2019-i2-2

[1]M. Akhmet, [2]M. Tleubergenova, [2]A. Zhamanshin

[1]Middle East Technical University, 06800 Ankara, Turkey,
e-mail: marat@metu.edu.tr,
[2]Aktobe Regional State University, Aktobe, Kazakhstan,
e-mail: madina_1970@mail.ru, akylbek78@mail.ru

Strongly unpredictable solutions of difference equations

Abstract. It so happens that the line of oscillations in the classical theory of dynamical systems, which is founded by H.Poincar´e and G.Birkhoff was broken at Poisson stable motions. The next oscillations were considered as actors of chaotic processes. This article discusses the new type of oscillations, unpredictable sequences, the presence of which proves the existence of Poincare chaos. The sequence is defined as an unpredictable function on the set of integers. The results continue the description of chaos which isinitiated from a single motion, an unpredictable one. To demonstrate the effectiveness of the approach, the existence and uniqueness of the unpredictable solution for a quasilinear difference equation are proved. An example with numerical simulations is presented to illustrate the theoretical results. Since unpredictability is request for all coordinates of solutions, the concept of strong unpredictability can be useful for investigation of neural networks, brain activity, robotics, where complexity is related to optimization and effectiveness.

Key words: Difference equations, Strongly unpredictable solutions, Existence and uniqueness, Asymptotical stability.

Introduction

Throughout the paper, $\mathbb{R}, \mathbb{N}$and $\mathbb{Z}$ will stand for the set of real, natural and integer numbers, respectively. Additionally, $x = x_i, i \in \mathbb{Z}$,and the norm$||x||_1 = \sup_{\mathbb{Z}} || x_i||$, where $x_i = (x_i^1, \dots, x_i^p), x_i^j \in \mathbb{R}, ||x_i|| = \max_{1\le j\le p}|x_i^j|, j = 1,2,\dots,p, p \in \mathbb{N}$,will be used. The following definition isone of the main in our study.

Definition 1. [1,2] A bounded sequence $\kappa_i, i \in \mathbb{Z}$, in $\mathbb{R}^p$ is called unpredictable if there exist a positive number ε_0 and sequences $\zeta_n, \eta_n, n \in \mathbb{N}$, of positive integers both of which diverge to infinity such that $\|\kappa_{i+\zeta_n} - \kappa_i\| \to 0$ as $n \to \infty$ for each i in bounded intervals of integers and $\|\kappa_{\zeta_n+\eta_n} - \kappa_{\eta_n}\| \ge \varepsilon_0$ for each $n \in \mathbb{N}$.

Some coordinates of an unpredictable sequence may be not unpredictable. This is why, in the following definition, we consider a stronger version of the concept.

Definition 2. A bounded sequence $\kappa_i, i \in \mathbb{Z}$, in $\mathbb{R}^p$ is called strongly unpredictable if there exist a positive number ε_0 and sequences $\zeta_n, \eta_n, n \in \mathbb{N}$, of positive integers both of which diverge to infinity such that $\|\kappa_{i+\zeta_n} - \kappa_i\| \to 0$ as $n \to \infty$ for each i in bounded intervals of integers and $\left|\kappa^j_{\zeta_n+\eta_n} - \kappa^j_{\eta_n}\right| \ge \varepsilon_0$ for each $j = 1, \dots, p$ and $n \in \mathbb{N}$.

Inthispaper, a strongly unpredictable sequence and a strongly unpredictable solutionare understood as mentioned in Definition 2. We investigate the existence, uniqueness andstability of strongly unpredictable solutions of a non-linear difference equation.

The research of complex dynamics as well as differential equations with singularities has been of great interest in recent decades [3-8].

Main result

Let us consider the following discrete equation

$$z_{i+1} = Bz_i + h(z_i) + \psi_i, \quad (1)$$

where$z_i = (z_i^1, \dots, z_i^p), z_i^j \in \mathbb{R}, i \in \mathbb{Z}, j = 1, \dots, p, B = diag(b_1, b_2, \dots, b_p)$ is a real valued nonsingular matrix, $h = (h_1, h_2, \dots, h_p), h: \mathbb{R}^p \to \mathbb{R}^p, p \in \mathbb{N}$, is a continuous function, and $\psi_i = (\psi_i^1, \psi_i^2, \dots, \psi_i^p), i \in \mathbb{Z}$, is a strongly unpredictable sequence.

Since $\psi_i, i \in \mathbb{Z}$, is a strongly unpredictable sequence, there exist a positive number ε_0 and

Since $\psi_i, i \in \mathbb{Z}$, is a strongly unpredictable sequence, there exist a positive number ε_0 and sequences $\zeta_n, \eta_n, n \in \mathbb{N}$, of positive integers both of which diverge to infinity such that $\|\psi_{i+\zeta_n} - \psi_i\| \to 0$ as $n \to \infty$ for each i with $\alpha \le i \le \beta, \alpha, \beta \in \mathbb{Z}$, and $\left|\psi^j_{\zeta_n+\eta_n} - \psi^j_{\eta_n}\right| \ge \varepsilon_0, j = 1, \dots, p$ for each $n \in \mathbb{N}$. Denote $M_\psi = sup_{\mathbb{R}}\|\psi_i\|$.

Let U be the set of infinite sequences $x = \{x_i\}, x_i = (x_i^1, \dots, x_i^p), x_i^j \in \mathbb{R},\ i \in \mathbb{Z}, j = 1, 2, \dots, p$, such that:

(A1) $\|x\|_1 < H$, where H is a positive real number;

(A2) There exists a sequences ζ_n, $\zeta_n \to \infty$ as $n \to \infty$ such that $\|x_{i+\zeta_n} - x_i\| \to 0$ as $n \to \infty$ on each bounded interval of integers.

The following conditions are needed throughout this paper.

(C1) There exists a positive number M_h such that $\sup_{||x||<H} ||h(x)|| < M_h$;

(C2) There exists a positive number L_h such that $\|h(x) - h(y)\| \le L_h\|x - y\|$ for all $\|x\| < H, \|y\| < H$;

(C3) $\bar{b} + L_h < 1$, where $\bar{b} = \max_k |b_k|$;

(C4) $(M_h + M_\psi)\frac{1}{1-\bar{b}} < H$;

(C5) $\frac{\epsilon_0}{2H}\left(\frac{3}{4} - \frac{\bar{b}}{2}\right) > L_h$;

(C6) $\frac{\underline{b}}{2} - \frac{2H(L_h+1)}{\epsilon_0} \ge \frac{1}{4}$, where $\underline{b} = \min_k |b_k|$.

According to the result of [9], a bounded sequence x_i is a solution of equation (1) if and only if the following relation is satisfied

$$x_i = \sum_{j=-\infty}^{i} B^{i-j}\left(h(x_{j-1}) + \psi_{j-1}\right), i \in \mathbb{Z}. \quad (2)$$

Let us rewrite equation (2) in coordinate form:

$$x_i^k = \sum_{j=-\infty}^{i} b_k^{i-j}\left(h_k(x_{j-1}) + \psi^k_{j-i}\right),$$

$$i \in \mathbb{Z},\ k = 1, \dots, p. \quad (3)$$

The sequence $\varphi \in U, \varphi = \{\varphi_i\}, \varphi_i = (\varphi_i^1, \varphi_i^2, \dots, \varphi_i^p)$. Define on U the operator Π such that $\Pi\varphi = (\Pi_1\varphi, \Pi_2\varphi, \dots, \Pi_p\varphi)$, and $\Pi_k\varphi = \{(\Pi_k\varphi)_i\}$, $1 \le k \le p, i \in \mathbb{Z}$, where

$$(\Pi_k\varphi)_i = \sum_{j=-\infty}^{i} b_k^{i-j}\left(h_k(\varphi_{j-1}) + \psi^k_{j-i}\right). \quad (4)$$

Fix a sequence $\varphi \in U$. Then one can find that

$$|(\Pi_k\varphi)_i| \le \sum_{j=-\infty}^{i} \left|b_k^{i-j}\right|(M_h + M_\psi) \le$$

$$\le (M_h + M_\psi)\frac{1}{1-\bar{b}},$$

for $1 \le k \le p, i \in \mathbb{Z}$. Thus, by condition (C4) it implies that $\Pi\varphi \in U$ and condition (A1) is satisfied.

Let us fix arbitrary positive number ε and an interval of integers $[\alpha,\ \beta]$. There exists an integer $\gamma < \alpha$ and a number $\xi > 0$, which satisfy the following inequalities,

$$\xi(L_h + 1)\frac{1}{1-\bar{b}} < \frac{\varepsilon}{2} \quad (5)$$

and

$$2(M_h + M_\psi)\frac{\bar{b}^{\alpha-\gamma}}{1-\bar{b}} < \frac{\epsilon}{2}. \quad (6)$$

There exists sufficiently large n such that $||\varphi_{i+\zeta_n-1} - \varphi_{i-1}|| < \xi$ and $||\psi_{i+\zeta_n-1} - \psi_{i-1}|| < \xi$ for $i \in [\gamma, \beta]$. Then for all $i \in [\alpha, \beta]$ we have that

$$\left|(\Pi_k\varphi)_{i+\zeta_n} - (\Pi_k\varphi)_i\right| =$$

$$= \Big|\sum_{j=-\infty}^{\gamma} b_k^{i-j}\big(h_k(\varphi_{j+\zeta_n-1}) - h_k(\varphi_{j-1}) +$$

$$+\psi^k_{j+\zeta_n-1} - \psi^k_{j-1}\big) + \sum_{j=\gamma+1}^{i} b_k^{i-j}\big(h_k(\varphi_{j+\zeta_n-1}) -$$

$$- h_k(\varphi_{j-1}) + \psi^k_{j+\zeta_n-1} - \psi^k_{j-1}\big)\Big| \le 2(M_h +$$

$$+M_\psi)\frac{\bar{b}^{\alpha-\gamma}}{1-\bar{b}} + \xi(L_h + 1)\frac{1}{1-\bar{b}}.$$

Thus, by inequalities (5) and (6), for large enough n it is true that $\left|(\Pi_k\varphi)_{i+\zeta_n} - (\Pi_k\varphi)_i\right| < \varepsilon$ for all $1 \le k \le p$ and $i \in [\alpha, \beta]$. Since ε is arbitrary small number the condition (A2) is valid.

For two sequences $a, b \in U$ the inequality

$$|(\Pi_k a)_i - (\Pi_k b)_i| =$$

$$= \left|\sum_{j=-\infty}^{i} b_k^{i-j}\left(h_k(a_j) - h_k(b_j)\right)\right| \le$$

$$\le \frac{L_h}{1-\bar{b}}||a - b||_1 \quad (7)$$

is valid for all $i \in \mathbb{Z}$. Thus, we can conclude that $||\Pi a - \Pi b||_1 \leq \frac{L_h}{1-\bar{b}} ||a - b||_1$ for all $i \in \mathbb{Z}$, and by condition (C3) the operator Π is contractive.

Theorem 1. Suppose that conditions (C1)-(C5) are valid, then the system (1) possesses unique asymptotically stable strongly unpredictable solution.

Proof. By contraction mapping theorem there exists the fixed point $\omega \in U$ of the operator Π which is a bounded solution of the system (1) and it satisfies the inequality $||\omega||_1 < H$.

Now, we prove the unpredictability of the solution $\omega = \{\omega_i\}$, $\omega_i = (\omega_i^1, \omega_i^2, \dots, \omega_i^p)$ of the system (1). The coordinates of the sequence ω satisfy the relation (1), that is

$$\omega_{i+1}^k = b_k \omega_i^k + h_k(\omega_i) + \psi_i^k,$$

$$i \in \mathbb{Z}, k = 1,2, \dots, p.$$

Fix a natural number $k = 1,2, \dots, p$, and $n \in \mathbb{N}$. Consider two alternatives, (i) $|\omega_{\zeta_n+\eta_n}^k - \omega_{\eta_n}^k| < \frac{\varepsilon_0}{2}$ and (ii) $|\omega_{\zeta_n+\eta_n}^k - \omega_{\eta_n}^k| \geq \frac{\varepsilon_0}{2}$.

(i) Using the relation

$$\omega_{\zeta_n+\eta_n+1}^k - \omega_{\eta_n+1}^k =$$

$$= b_k(\omega_{\zeta_n+\eta_n}^k - \omega_{\eta_n}^k) + h_k(\omega_{\zeta_n+\eta_n}) -$$

$$-h_k(\omega_{\eta_n}) + \psi_{\zeta_n+\eta_n}^k - \psi_{\eta_n}^k, \quad (8)$$

and condition (C5), we obtain for $n \in \mathbb{N}$ that

$$|\omega_{\zeta_n+\eta_n+1}^k - \omega_{\eta_n+1}^k| \geq$$

$$\geq |\psi_{\zeta_n+\eta_n}^k - \psi_{\eta_n}^k| - |b_k(\omega_{\zeta_n+\eta_n}^k - \omega_{\eta_n}^k)| -$$

$$-|h_k(\omega_{\zeta_n+\eta_n}) - h_k(\omega_{\eta_n})| \geq \epsilon_0 -$$

$$-\bar{b}\frac{\varepsilon_0}{2} - 2L_h H > \varepsilon_0 -$$

$$-\bar{b}\frac{\varepsilon_0}{2} - \frac{\varepsilon_0}{2H}\left(\frac{3}{4} - \frac{\bar{b}}{2}\right)2H \geq \frac{\varepsilon_0}{4}.$$

(ii) For the case $|\omega_{\zeta_n+\eta_n}^k - \omega_{\eta_n}^k| \geq \frac{\varepsilon_0}{2}$, by relation (8) and condition (C6) we have that

$$|\omega_{\zeta_n+\eta_n+1}^k - \omega_{\eta_n+1}^k| \geq \underline{b}\frac{\varepsilon_0}{2} - 2L_h H - 2H \geq$$

$$\geq \varepsilon_0\left(\frac{\underline{b}}{2} - \frac{2H(L_h + 1)}{\varepsilon_0}\right) \geq \frac{\varepsilon_0}{4}.$$

Thus, we obtained that $|\omega_{\zeta_n+\eta_n+1}^k - \omega_{\eta_n+1}^k| \geq \frac{\varepsilon_0}{4}$. That the solution ω of system (1) is strongly unpredictable with positive number $\frac{\varepsilon_0}{4}$ and sequences ζ_n and $\eta_n + 1$.

Using condition (C3) and the inequality (7), it is easy to verify that the solution ω of the system (1) is asymptotically stable [10]. The theorem is proved.

An example

Let us take into account the logistic discrete equation

$$\lambda_{i+1} = \mu\lambda_i(1 - \lambda_i). \quad (9)$$

The interval $[0, 1]$ is invariant under the iterations of (9) for $\mu \in (0,4]$ [11]. In paper [1] was proved that the equation (9) has an unpredictable solution. Let us denote by $\rho_i, i \in \mathbb{Z}$, the unpredictable solution of the logistic map (9) with $\mu = 3.91$. In this section we use the sequence ρ_i as a perturbation.

Consider the system

$$\begin{aligned} x_{i+1} &= -\frac{2}{3}x_i + k\,arctg(y_i) + l\rho_i \\ y_{i+1} &= \frac{3}{5}y_i + m\,arctg(x_i) + n\rho_i. \end{aligned} \quad (10)$$

To satisfy conditions (C1)-(C6) we need to take k, l, m, n quite small. To this end, we have chosen $k = \frac{1}{9}, l = \frac{3}{8}, m = \frac{1}{12}, n = -\frac{5}{11}$ and got the strongly unpredictable solution. Figures 1 and 2 represent the strongly unpredictable solution of the system (10) with initial data $\rho_0 = 0.35, x_0 = 0.25$ and $y_0 = -0.95$.

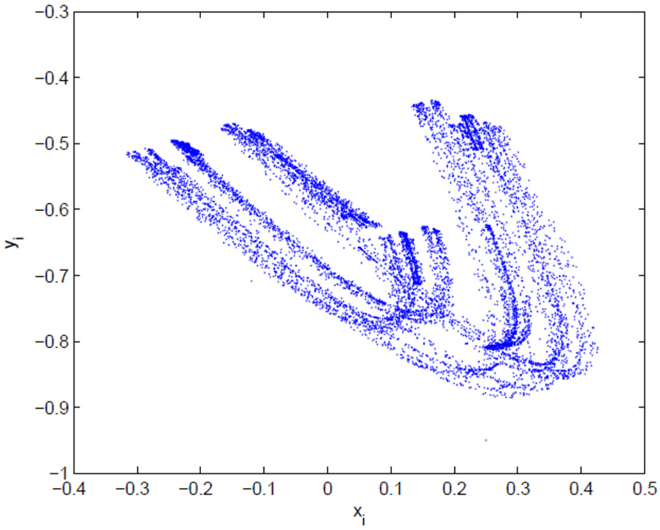

Figure 1 – The trajectory of system (10).
The figure manifests that the dynamics of system (10) is chaotic

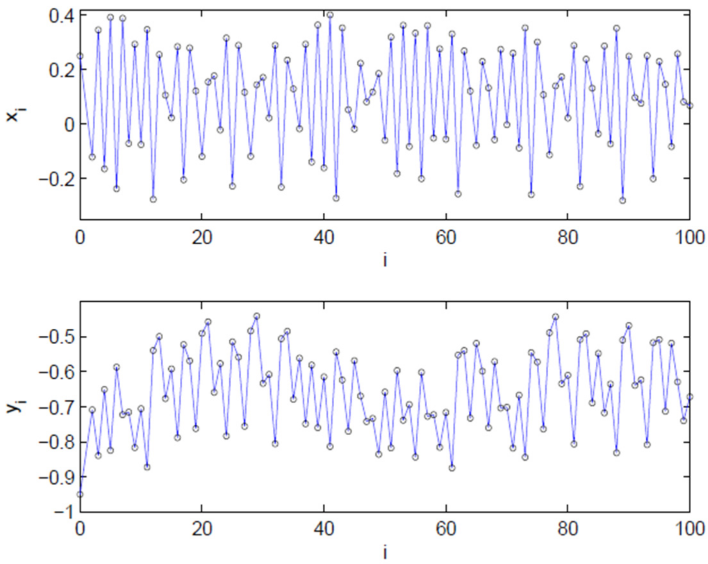

Figure 2 – The solution of system (10)
with the initial data $\rho_0 = 0.35, x_0 = 0.58$, and $y_0 = -3.95$.

Acknowledgements

M. Akhmet has been supported by a grant (118F161) from TUBITAK, the Scientific and Technological Research Council of Turkey.

M. Tleubergenova and A. Zhamanshin have been supported by the Ministry of Education and Science of the Republic of Kazakhstan under grant No. (AP05132573) "Cellular neural networks with continuous/discrete time and singular perturbations" (2018-2020).

References

1. Akhmet M.U., Fen M.O., “Poincare chaos and unpredictable functions”, *Communications in Nonlinear Science and Numerical Simulation,* vol. 48 (2017): 85-94.

2. Akhmet M. and Fen M.O., “Unpredictable points and chaos”, *Communications in Nonlinear Science and Numerical Simulation,* (2016).

3. Akhmet M., Seilova R., Tleubergenova M., Zhamanshin A., SICNNs with strongly unpredictable oscillations, *IEEE Transactions on Neural Networks and Learning Systems*, submitted (2019).

4. Aihara T., Toyoda M., Chaotic neural networks, *Physics Letters A*, vol. 144 No. 6-7 (1990): 333-340.

5. Field, R.J., Györgyi, L.: Chaos in Chemistry and Biochemistry, *World Scientific*, Singapore (1993)

6. Gonzales-Miranda, J.M.: Synchronization and Control of Chaos, *Imperial College Press*, London (2004)

7. Dauylbaev M. K., “The asymptotic behavior of solutions to singularly perturbed nonlinear integro-differential equations”*, Siberian Mathematical Journal*, vol. 41, No. 1 (2000): 49-60.

8. Akhmet M., Dauylbayev M., Mirzakulova A., A singularly perturbed differential equation with piecewise constant argument of generalized type, *Turkish Journal of Mathematics*. vol. 42. No. 4. (2018): 1680 – 1685.

9. Lakshmikantham V., Trigiante D., Theory of difference equations: numerical methods and applications, USA, Marcel Dekker, (2002).

10. Agarwal P., Difference Equations and Inequalities, Marcel Dekker, (1992).

11. Hale J., Kocak H., Dynamics and bifurcations, New York, Springer-Verlag, (1991).

IRSTI 27.03.66 https://doi.org/10.26577/ijmph-2019-i2-3

K.Zh. Kudaibergenov

KIMEP University, Almaty, Kazakhstan,
e-mail: kanat@kimep.kz

ON the *D*-saturation property

Abstract. In this paper we study the notion of a *D*-saturated model, which occupies an intermediate position between the notions of a homogeneous model and a saturated model. Both the homogeneous models and the saturated models play a very important role in model theory. For example, the saturated models are the universal domains of the corresponding theories in the sense that is used in algebraic geometry (one can also notice that the algebraically closed fields of infinite transcendence degree, which are the universal domains in algebraic geometry, are the saturated models of the theory of algebraically closed fields); this means that the saturated models realize all what is necessary for the effective study of the corresponding theory.The *D*-saturated models proved to be useful in various situations. Naturally the question arises on the conditions under which a model is *D*-saturated. In this paper we indicate some conditions of such sort for weakly o-minimal models and models of stable theories. Namely, for such models we prove that homogeneity and a certain approximation of *D*-saturation imply *D*-saturation.

Key words: *D*-saturated model, homogeneous model, weakly o-minimal model, stable theory.

Introduction

In this paper models of first-order theories are studied. The notion of a homogeneous model introduced by Vaught [1], Jonsson [2], Craig [3]plays a very important role in model theory. In particular, the saturated models which are in a sense the universal domains of the corresponding theories are also homogeneous. In [4], the notion of a *D*-saturated model which is intermediate between homogeneity and saturationwas defined and it was shown that the notion is useful. For example, for *D*-saturated models the problem of finding an elementary extension with the same diagram has a nice solution. In [5], results on the existence of *D*-saturated models in different cardinalities for stable theories were obtained. Some results on *D*-saturated models (where they are called the normal models) can be found in [6].Naturally the following question arises: under what conditions will a model be *D*-saturated? In the present paper some conditions of such sort for weakly o-minimal models (the notion of weak o-minimality was introduced in [7] and studied in detail in [8] and other papers) and models of stable theories (for a perfect presentation of stability theory see [9]) will be found. Namely, for the indicated models it will be proved that homogeneity and some approximation of *D*-saturation imply *D*-saturation.

Preliminaries

Let us fix a sufficiently saturated model of a first-order language *L*(the *universal domain*).All the models, sets, elements thatwe will work with, will be elementary sub-models, subsets, elements of the universal domain. We will use the same symbol for a model and its underlying set. The cardinality of a set *A* will be denoted by $|A|$, but for the language by $|L|$ we will denote the cardinality of the set of all its formulas. By$i, j, \alpha, \beta, \delta$ we will denote ordinals, and by κ, λ, μ infinite cardinals. The first infinite ordinal (cardinal) will be denoted by ω, and the first uncountable cardinal will be denoted by ω_1. The minimal cardinal, which is greater than λ, will be denoted by λ^+.

The definitions of all the model-theoretic notions that are used, but are not defined in this paper, can be found in [9].

Definition 1.1. (1) A model M is calledλ-*homogeneous* if for every set $A \subseteq M$ of cardinality $|A| < \lambda$ and every element $a \in M$ each elementary map from A to M extends to an elementary map from $A \cup \{a\}$ to M.

(2) A model M is called *homogeneous* if M is $|M|$-homogeneous.

Following Shelah [10], for a subset A of a model M by $D(A)$ we denote the set of all complete pure types that are realized by finite tuples of elements of M. We call the set $D = D(M)$ the *diagram* of the model M. A complete 1-type p over A is called a *D-type* over A if $D\left(A \cup \{a\}\right) \subseteq D$ for some (equivalently, every) element a that realizes p.

The following result of Keisler and Morley [11] plays an important role in the study of homogeneous models.

Lemma 1.1. *Let M be a* λ*-homogeneous model,* $A \subseteq B$, $|A| < \lambda$, $|B| \le \lambda$, *and* $D(B) \subseteq D(M)$. *Then every elementary map from A to M extends to an elementary map from B to M.*

Lemma 1.1 implies the following

Lemma 1.2. *A model N is* λ*-homogeneous if and only if for every set* $A \subseteq N$ *of cardinality* $|A|<\lambda$ *each D(N)-type over A is realized in N.*

The next statement follows from definitions.

Lemma 1.3. *The union of an increasing chain of D-types is also a D-type.*

For a 1-type p over a subset of a model M let $p(M)$ be the set of all elements in M realizing p.

Definition 1.2. A model M is called *D-saturated* if $D(M)=D$ and for every set A of cardinality $|A|<|M|$ and every non-algebraic D-type p over A we have $|p(M)|=|M|$.

Proposition 1.4. *Every countable model of a countable language has, for an appropriate D, a countable D-saturated elementary extension.*

Proof. First, for an arbitrary countable model M of a countable language we find a countable model $M^* @ M$ such that $|p(M^*)|=\omega$ for every $p \in P_M$, where P_M is the set of all $D(M)$-types over finite subsets of M. To do it, we take an ω-saturated model $M' @ M$ and for every $p \in P_M$ choose a set $A_p \subseteq p(M')$ of cardinality ω. Since P_M is countable, by Lowenheim-Skolem Theorem, there exists a countable model $M^* \,\mathrm{E}\, M'$ containing $M \cup ;\left\{A_p : p \in P_M\right\}$.

Now let N be a countable model of a countable language. By induction on $i=\omega$, we construct countable models N_i such that $N_0=N$ and $N_{i+1} = N_i^*$. Let $N_\omega = ;_{i<\omega} N_i$. Then $N \,\mathrm{E}\, N_\omega$ and N_ω is $D(N_\omega)$-saturated and countable.

Proposition 1.4 is proved.

Remark. (1) A similar construction for an uncountable model gives a D-saturated elementary extension of cardinality μ such that $\mu = \mu^{<\mu}$. The existence of such uncountable cardinals is not provable in ZFC.

(2) Some results on the existence of D-saturated models of different cardinalities for a stable theory T under the assumption that T has a D-saturated model M of a certain cardinality (say, $|M| > |T|$) can be found in [5].

***D*-saturation and weak o-minimality**

Let M be a model of a language L that contains, among others, a binary relation symbol $<$, which is interpreted as a linear order on the underlying set of the model.

A subset A of the model M is called *convex* if for any $a, b \in A$ and $c \in M$ the condition $a < c < b$ implies $c \in A$.

For example, intervals are convex sets. Singletons are also convex sets.

In the following "definable" will mean "definable with parameters".

Definition 2.1. A model is called *weakly o-minimal* if every its definable subset is the union of finitely many convex sets.

Definition 2.2. (1) We say that a model M is (κ, λ)-*normal* if for every set $A \subseteq M$ of cardinality $|A|<\kappa$ and every non-algebraic 1-type p over A, which is realized in M, we have $|p(M)| \ge \lambda$.

(2) We say that a model M is λ-*normal* if M is $(|M|, \lambda)$-normal.

(3) We say that a model M is *normal* if M is $|M|$-normal.

Lemma 2.1. *A model M is D(M)-saturated if and only if M is normal and homogeneous.*

Proof. Follows from Lemma 1.2.

Theorem 2.2. *Let M be a weakly o-minimal model. Suppose that M is λ-homogeneous and* $\left(\kappa, \left(2^{|L|}\right)^+\right)$*-normal, where* $\kappa \ge \omega$ *and* $\lambda > 2^{|L|}$. *Then M is (κ, λ)-normal.*

In order to prove Theorem 2.2, we need the following notions and results from [12].

Definition 2.3. We say that a sub-order of a given linear order is an α-*sequence* if it is isomorphic or anti-isomorphic to the ordinal α.

Lemma 2.3. *Every linear order of cardinality at least* $\left(2^\kappa\right)^+$ *contains a* κ^+*-sequence.*

Proof. See [12, Lemma 3.1].

Now let N be a weakly o-minimal model that contains a κ^+-sequence I. We can assume that I increases (the case of decrease is considered similarly). Let $L(A)$ be the set of all formulas of the language L with parameters from A. By weak o-minimality, the set, which is definable in N by a formula $\varphi(x) \in L(N)$, is the union of finitely many convex sets. Let J_φ be the rightmost of these convex sets. Then either $\left|I \cap J_\varphi\right| < \kappa^+$ and hence $\left|I \setminus J_{\neg\varphi}\right| < \kappa^+$ or $\left|I \setminus J_\varphi\right| < \kappa^+$. It follows that for any $A \subseteq N$ the set

$$AV(I, A) = \left\{\varphi(x) \in L(A) : \left|I \setminus J_\varphi\right| < \kappa^+\right\}$$

is a complete 1-type over A.

Lemma 2.4. *If $|L| < \kappa^+$, then for every $B \subseteq N$ of cardinality $|B| < \kappa^+$ there exists $I_B \subseteq I$ of cardinality $|I_B| < \kappa^+$ such that every element from $I|I_B$ realizes $AV(I,B)$.*

Proof. See [12, Lemma 3.2].

Corollary 2.5. *If I is an $|L|^+$-sequence in a model N and B is a subset of N, then $AV(I,B)$ is a $D(N)$-type.*

Proof of Theorem 2.2. Let $A \subseteq M$, $|A| < \kappa$, and let p be a non-algebraic 1-type over A that is realized in M. We must prove that $|p(M)| \geq \lambda$.

Since the model M is $\left(\kappa, \left(2^{|L|}\right)^+\right)$-normal, we have $|p(M)| \geq \left(2^{|L|}\right)^+$. Then by Lemma 2.3, $p(M)$ contains an $|L|^+$-sequence $I = \left\{a_i : i < |L|^+\right\}$. By induction on $j \geq |L|^+$, we define elements $a_j \in M$ such that a_j realizes the type $p_j = AV\left(I, \left\{a_i : i < j\right\}\right)$. We can do it for all $j < \lambda$ because M is a λ-homogeneous model and, by Corollary 2.5, p_j is a $D(M)$-type. Since $p \subseteq p_j$ for all $j < \lambda$, we have $|p(M)| \geq \lambda$. Moreover, $\left\{a_i : i < \lambda\right\}$ is a λ-sequence because the formula $a_i < x$ belongs to the type p_j and hence $a_i < a_j$ for all $i < j < \lambda$.

Theorem 2.2 is proved.

Corollary 2.6. *Let M be a weakly o-minimal model. Suppose that M is homogeneous and $\left(2^{|L|}\right)^+$-normal. Then M is $D(M)$-saturated.*

Proof. Follows from Theorem 2.2 and Lemma 2.1.

Let us notice that from the proof of Theorem 2.2 the following statement follows.

Proposition 2.7. *Let M be a weakly o-minimal model. Suppose that M is λ-homogeneous, where $\lambda > |L|$. Then every $|L|^+$-sequence in M can be extended to a λ-sequence in M.*

***D*-saturation and stability**

Let $\lambda(T)$ be the minimal cardinal in which the theory T is stable.

Theorem 3.1. *Let M be a model of a stable theory T. Then*

(1) for every $\lambda > \lambda(T)$ and $\kappa \leq \lambda$ if M is λ-homogeneous and $(\kappa, \lambda(T)^+)$-normal, then M is (κ, λ)-normal;

(2) if M is homogeneous and $\lambda(T)^+$-normal, then M is $D(M)$-saturated;

(3) *for every $\lambda > |T|$ if M is λ-homogeneous and $(|T|^+, |T|^+)$-normal, then M is $(|T|^+ \lambda)$-normal.*

In order to prove Theorem 3.1, we need the following facts.

Lemma 3.2. *Every maximal infinite indiscernible set in a λ-homogeneous model has the cardinality at least λ.*

Proof. See [5, Lemma 3.2].

Definition 3.1. We say that a sequence $\left\{b_\alpha : \alpha < \mu\right\}$ of elements of a model is a *Morley pre-sequence over A,* where A is a subset of the model, if $p_\alpha \subseteq p_\gamma$ for all $\alpha < \gamma < \mu$, where p_α is the type realized by b_α over $A \cup \left\{b_\beta : \beta < \alpha\right\}$.

In the following lemma we use the cardinal $\kappa(T)$, the definition and properties of which can be found in [9]. We only notice that $\kappa(T) \leq |T|^+$, and the equality $\kappa(T) = \omega$, is equivalent to superstability of the theory T. Let $\kappa_r(T)$ be the minimal regular cardinal that is greater than or equal to $\kappa(T)$.

Lemma 3.3. *Let $\left\{b_\alpha : \alpha < \mu\right\}$ be a Morley pre-sequence over A in a model of a stable theory T, where $\mu \geq \kappa_r(T) + \omega_1$ is a regular cardinal. Then there exists an ordinal $\alpha_0 < \mu$ such that the set $\left\{b_\alpha : \alpha_0 < \alpha < \mu\right\}$ is indiscernible over A.*

Proof. We use the notation from Definition 3.1. From the definition of $\kappa(T)$ (see [9, p. 100]) and regularity of μ, it follows that there exists an ordinal $\alpha_1 < \mu$ such that for every $\alpha \geq \alpha_1$ the type p_α does not fork over $\{b_\beta : \beta < \alpha_1\}$. By [9, Chapter III, Lemma 2.12], the type $p_{\alpha_1+\omega}$ is stationary. Then by [9, Chapter III, Lemma 1.10(1)], the set $\{b_\alpha : \alpha_1 + \omega \leq \alpha < \mu\}$ is indiscernible over A.

Lemma 3.3 is proved.

Lemma 3.4. *If M is a model of a λ-stable theory, $I \subseteq M$ and $|I| > \lambda \geq |A|$, then there exists $J \subseteq I$ such that $|J| > \lambda$ and J is indiscernible over A.*

Proof. See [9, Chapter I, Theorem 2.8].

Lemma 3.5. *Let M be a model of a stable theory T. Suppose that M is $|T|^+$-homogeneous and $(|T|^+, |T|^+)$-normal, and p is a non-algebraic 1-type over $A \subseteq M$, $|A| \leq |T|$, that is realized in M. Then p(M) contains an indiscernible set of cardinality $|T|^+$.*

Proof. By induction on $\alpha < |T|^+$, we define elements $a_\alpha \in M$ and non-algebraic *D(M)*-types p_α over $A_\alpha = A \cup \{a_\beta : \beta < \alpha\}$ as follows.

We let $p_0 = p$ and arbitrarily choose $a_0 \in p(M)$.

Suppose that the type p_α and the element $a_\alpha \in p_\alpha(M)$ have been defined. Since the model M is $(|T|^+, |T|^+)$-normal, we have $|p_\alpha(M)| < |T|$. Since $|acl(A_{\alpha+1})| \leq |T| + |A_\alpha| = |T|$, we can choose $a_{\alpha+1} \in p_\alpha(M) \setminus acl(A_{\alpha+1})$. Let $p_{\alpha+1} = tp(a_{\alpha+1} / A_{\alpha+1})$. Clearly, $p_\alpha \subseteq p_{\alpha+1}$.

Suppose that a_α and p_α have been defined for all $\alpha < \delta$, where $\delta < |T|^+$ is a limit ordinal, and $p_\alpha \subseteq p_\beta$ for all $\alpha < \beta < \delta$. Let $p_\delta = ;_{\alpha<\delta} p_\alpha$. Since for every $\alpha < \delta$ the type p_α is non-algebraic, the type p_δ is also non-algebraic. Since all the p_α are *D(M)* -types, by Lemma 1.3 the type p_δ is a *D(M)*-type over A_δ, where $|A_\delta| = |A| + |\delta| < |T|^+$. Since the model M is $|T|^+$-homogeneous, by Lemma 1.2 the type p_δ is realized by some $a_\delta \in M$.

By construction, $\{a_\alpha : \alpha < |T|^+\}$ is a Morley pre-sequence over A and hence, by Lemma 3.3, contains a set of cardinality $|T|^+$, which is indiscernible over A.

Lemma 3.5 is proved.

Proof of Theorem 3.1. (1) Let us consider a non-algebraic type p over $A \subseteq M$, $|A| < \kappa$, that is realized in M. We must prove that $|p(M)| \geq \lambda$.

Since the model M is $(\kappa, \lambda(T)^+)$-normal, we have $|p(M)| > \lambda(T)$. By Lemma 3.4, *p(M)* contains an indiscernible set I over A such that $|I| > \lambda(T)$. Let us extend I to a maximal indiscernible over A set $J \subseteq M$. Since $I \subseteq p(M)$ and J is indiscernible over A, we have $J \subseteq p(M)$. Since the model M is λ-homogeneous and $|A| < \kappa \leq \lambda$, the model $(M, a)_{a \in A}$ is also λ-homogeneous. Then by Lemma 3.2, we have $|J| \geq \lambda$ and hence $p(M) \geq \lambda$.

(2) Follows from (1) and Lemma 2.1.

(3) We repeat the proof of (1) replacing κ by $|T|^+$ and replacing $\lambda(T)$ by $|T|$, and using Lemma 3.5 instead of Lemma 3.4.

Theorem 3.1 is proved.

Conclusion

In this paper we study the notion of a *D*-saturated model. We prove that for weakly o-minimal models and models of stable theories homogeneity and some approximation of *D*-saturation imply *D*-saturation.

Acknowledgement

The work was partially supported by grant AP05130852 of the Ministry of Education and Science of the Republic of Kazakhstan.

References

1. Vaught R. "Homogeneous universal models of complete theories." Notices AMS. 5(1958): 775.
2. Jonsson B. "Homogeneous universal relational systems." Math. Scand. 8(1960): 137-142.
3. Craig W. "$\aleph_0$-homogeneous relatively universal systems." Notices AMS. 8(1961): 265.

4. Kudaibergenov K.Zh. "On extensions of homogeneous models." Algebra and Logic. 28(1)(1989): 61-74.

5. Kudaibergenov K.Zh. "Homogeneous models of stable theories." Siberian Advances in Mathematics. 3(3)(1993): 1-33.

6. Kudaibergenov K.Zh. "The small index property and the cofinality of the automorphism group." Siberian Advances in Mathematics. 27(1)(2017): 1-15.

7. Dickmann M.A. "Elimination of quantifiers for ordered valuation rings." In: Proc. of the 3rd Easter Conf. on Model Theory (Gross Koris, 1985). Berlin: Humboldt Univ. (1985): 64-88.

8. Macpherson D., Marker D., Steinhorn C. "Weakly o-minimal structures and real closed fields." Trans. Amer. Math. Soc. 352(12)(2000): 5435-5483.

9. Shelah S. Classification theory and the number of non-isomorphic models. North-Holland, Amsterdam, 1978.

10. Shelah S. "Finite diagrams stable in power." Ann. Math. Logic. 2(1970): 69-118.

11. Keisler H.J., Morley M.D. "On the number of homogeneous models of a given power." Israel J. Math. 5(2)(1967): 73-78.

12. Kudaibergenov K.Zh. "Small extensions of models of o-minimal theories and absolute homogeneity." Siberian Advances in Mathematics. 18(1)(2008): 118-123.

IRSTI 27.35.43 https://doi.org/10.26577/ijmph-2019-i2-4

Meibao Ge[1,2], Keji Liu[1,3], Dinghua Xu[1*]

[1]School of Mathematics, Shanghai University of Finance and Economics, Shanghai 200433, P.R.China.
[2] Department of Medical Imaging, Hangzhou Medical College, Zhejiang, 310053, P. R.China.
[3]Shanghai Key Laboratory of Financial Information Technology, Institute of Scientific Computation and Financial Data Analysis, Shanghai University of Finance and Economics, Shanghai 200433, P.R.China.)
e-mail:dhxu6708@mail.shufe.edu.cn, kjliu.ip@gmail.com; gemeibao@126.com

An inverse problem of dcis model based on nonlocal and terminal data

Abstract. Astheearliest period of breast cancer, the ductal carcinoma in situ (DCIS) model has wide applications in the diagnosis of breast cancer and has been attracted much attention in recent years. In this paper, a novel PSO method is developed for solving an inverse problem of the DCIS model from nonlocal and terminal data. The numerical simulations show that the proposed method is efficient, accurate, robust against noise and fast. Moreover, it is better than the optimization method in the literature [8].
Key words: free boundary problem; PSO method; ductal carcinoma in situ; numerical simulation.

1. Introduction

Ductal carcinoma in situ (DCIS) means a specific diagnosis of cancer that is isolated within the breast duct, and has not spread to other parts of the breast. Tumor growth is an important research focus of mathematical modeling in recent 40 years [1-7].

In this paper we study a model about tumor growth firstly proposed by Byrne and Chaplain in 1995 [1-3]. Ward and King developed a velocity field to handle local volume changes caused by cell movement under some reasonable assumptions [4-5]. Mathematical modeling for the dynamical growth of DCIS is a free boundary problem and was developed in [6-9]. To find possible steps to simulate the growth of the DCIS model with clinical data, Xu and his collaborators performed some mathematical analysis on the modified model and performed numerical calculations on some typical cases [6]. Li and Zhou studied an inverse problem of solving the control parameter with known moving boundaries [7]. According to one of the four inverse problems proposed by Xu [6], then Liu established the uniqueness theorem for determining the inverse problem with unknown parameters, deduced an optimization problem, and proposed an effective algorithm to solve the problem [8].

Due to the difficulties caused by the time varying boundary, numerical simulations are very limited. Especially, the effective numerical approaches for the inverse problems are indispensably and urgently needed.

In this paper, we shall present a novel efficient PSO method for solving the inverse free boundary problem. In section 2, a brief introduction of direct problem of DCIS would be exhibited. The novel PSO method would be proposed in section 3. And in section 4, a numerical example are demonstrated to show the effectiveness and robustness of our novel method.

2. A Brief Introduction of Direct Problem for DCIS

In this section, the forward problem of DCIS model would be stated. The DCIS problem of the one-dimensional case in Figure 1 is modeled by the following parabolic equation

$$c\frac{\partial v}{\partial t} = \frac{\partial^2 v}{\partial x^2} - \lambda(x)v(x,t) + F(x,t) \qquad (2.1)$$

$$0 < x < \psi(t), t > 0,$$

where $0 \le c = T_{diffusion} / T_{growth} \ll 1$ (normally, $T_{\text{diffusion}} \approx 1$ minute $T_{growth} \approx 1$ day) is the ratio of the nutrient diffusion time scale to the tumor growth time scale, v denotes the tumor growth pattern which is using dimensionless nutrient concentration, $\lambda(x)v(x,t)$ means the nutrient consumption rate, $F(x,t)$ represents the transfer of nutrient from/to the neighborhood and $\psi(t)$ are the growing boundary of the tumor. Moreover, $v(x,t)$ should satisfy the following initial and free boundary conditions,

$$v(x,0) = f(x),\ 0 < x < \psi(0),$$
$$v(0,t) = g_1(t),\ 0 < t < T, \qquad (2.3)$$
$$v(\psi(t),t) = g_2(t),\ 0 < t < T,$$

Where the final time $T < \infty$ is a constant. Furthermore, the mass conservation consideration indicates the following equality

$$\frac{d\psi(t)}{dt} = \sigma\int_0^{\psi(t)}\left(v(x,t) - s_0\right)dx, \qquad (2.3)$$

where both σ and s_0 are positive constants. The term $\sigma(v - s_0)$ in (2.3) represents the cell proliferation rate inside the tumor, and the cell birth rate is denoted as σv while the death rate is provided by σs_0. The direct problem of this model is to determine $\{v(x,t),\psi(\mathrm{t})\}$ for given $\{\lambda(x), F(x,\mathrm{t}), g_1(\mathrm{t}), g_2(\mathrm{t}), \psi(0), \sigma, s_0\}$. The direct problem can be solved by the finite difference method, we refer to the literature [8].

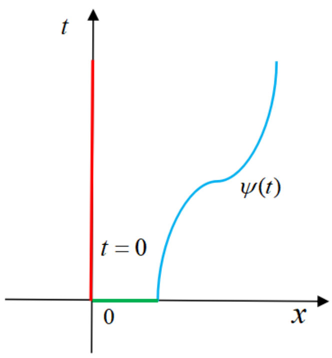

Figure 1 – The demonstration of the free boundary problem DCIS in the one dimension

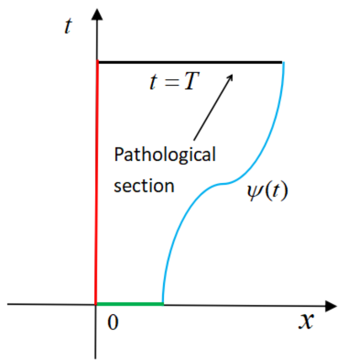

Figure 2 – The demonstration of pathological sections at time t = T

3. Inverse Problem of DCIS

In this section, the inverse problem of DCIS model would be investigated. In a routine physical examination, a possible breast tumor would be noticed, and it may be benign. The tumor would be growing bigger and bigger in the following days.

Therefore, the patient have to do an incisional biopsy to determine the DCIS pattern along with the changing rate at a fixed period (e.g. a couple of weeks). In this case, the initial data is not available, and only the information of set $\{v(x,t),\psi(\mathrm{t}),\mathrm{W}\}$ is provided by the incisional biopsy at the examine time $\mathrm{t} = T$, see Figure 2 for the demonstration.

The inverse problem of our interest is to determine the rate $\lambda(x)$ for $0 < x < \psi(T)$ from the examined data set $\{v(x,t),\psi(\mathrm{t}),\mathrm{W}\}$ and the given data set $\{\mathrm{c},\sigma,s_0 F(x,T), g_1(T), g_2(T)\}$, where the illustration of $\mathrm{W}(\xi)$ is provided in (3.1) . With the recovered $\lambda(x)$ for $0 < x < \psi(T)$ and the given data set, the process to approximate $\psi(t)|_{t>T}$ and $v(x,t)|_{t>T}$ becomes the direct problem. Finally, we are able to diagnose the breast tumor is benign or not from the information of estimate $\{\lambda(x), \psi(t)|_{t>T}, v(x,t)|_{t>T}\}$. Consequently, the inverse problem comes down to determine $\lambda(x)$ from the examined and given data. Moreover, the uniqueness of inverse problem is equivalent to the uniqueness of $\lambda(x)$.

We consider the DCIS model as follows

$$
\begin{cases}
c\dfrac{\partial v}{\partial t}=\dfrac{\partial^2 v}{\partial x^2}-\lambda(x)v(x,t)+F(x,t), \quad 0<x<\psi(t), 0<t<T, \\
v\big(0,t\big)=g_1(t), \quad 0<t<T, \\
v\big(\psi(t),t\big)=g_2(t), \quad 0<t<T, \\
\psi'(t)=\sigma\displaystyle\int_0^{\psi(t)}\big(v(x,t)-s_0\big)dx, \quad 0<t<T, \\
\displaystyle\int_0^{\psi_T} v_t(x,T)\varrho(x,\xi)dx=W(\xi), \qquad \xi\in D,
\end{cases}
\tag{3.1}
$$

where D is a parameter set, and $\{\rho(\cdot,\xi)|\xi\in D\}$ is assumed to be complete in $L^2([0,1])$. In a clinical aspect, the function represents the obtained data for the growth rate of tumor cells.

By the variables substitutions[8], the above problem (3.1) is equivalent to determine $\mu(\varsigma)$ such that

$$
\begin{cases}
\dfrac{\partial u}{\partial t}=\dfrac{1}{\psi^2(t)}\dfrac{\partial^2 u}{\partial\zeta^2}+c\dfrac{-\psi'(t)/2+\zeta\psi'(t)}{\psi(t)}\dfrac{\partial u}{\partial\zeta}-\mu(\zeta)u(\zeta,t)+H(\zeta,t), \\
u(0,t)=g_1(t), \quad 0<t<T, \\
u(1,t)=g_2(t), \quad 0<t<T, \\
u(\zeta,T)=u_T(\zeta), 0<\zeta<1, \quad \psi(T)=\psi_T, \\
\psi(t)=\psi_T e^{-\sigma\int_t^T\int_0^1\left(u(\zeta,t)-s_0\right)d\xi d\tau}, \\
W(\xi)=\int_0^1 u_t(\zeta,T)\varrho(\zeta,\xi)d\zeta, \qquad \xi\in D.
\end{cases}
\tag{3.2}
$$

where $\mu(\varsigma)$ and $H(\varsigma,t)$ are respectively presented as follows

$$\mu(\zeta)=\lambda\big(\zeta\big(\psi(t)\big)\big), \tag{3.3}$$

$$H(\zeta,t)=F\big(\zeta\big(\psi(t)\big),t\big), \tag{3.4}$$

We now consider the set $\Omega=\{\rho(\varsigma,\xi)|\varsigma\in[0,1],\xi\in D\}$ which forms a base of $L^2([0,1])$. Without loss of generality, the set is selected as $\Omega=\{\sin(\pi\varsigma\xi)|\varsigma\in[0,1],\xi=0,1,\cdots\}$.

4. PSO method for the Inverse Problem of DCIS

In this section, we convert the inverse problem of estimating $\mu(\varsigma)$ into a minimization problem and obtain the solution for the optimization problem by a stochastic search method which is known as particle swarm optimization algorithm.

The inverse problem of estimating $\mu(\varsigma)$ is expressed as follows similar to the literature [8],

$$\min_{\mu\in L^\infty([0,1])} J(\mu) \tag{4.1}$$

where

$$J(\mu)=\left\|\int_0^1\mu(\zeta)u(\zeta,T)\varrho(\zeta,\xi)\mathrm{d}\zeta-\gamma(\xi)\right\|_{L^2(D)}^2. \tag{4.1}$$

There are many approaches are existing to solve the above optimization model, we refer to [8-13]. In the reference [8], the optimization problem is transformed into a solution of linear algebraic equations by direct discrete method, and then the linear algebraic equations are solved by regularization method. In this paper, we would like to apply the PSO method which is knowns as an effective method to solve the optimization problems.

The PSO method [14-18] is an efficient technique for solving many nonlinear, nondifferentiable and multi-modal complex optimization problems. It has become very popular because its implementation is very simple and can be quickly aggregated into a good solution. It does not require any gradient information of the optimization function, and only uses the original mathematical operator. The PSO method is a stochastic algorithm, which does not depend on the initial value select, and can converge to the global optimal solution.

This group of particles is called a swarm in PSO. A swarm consists of M particles moving around in a D-dimensional search space. The position of the i-th particle can be represented $z_i=\left(z_{i_1},z_{i_2},\dots,z_{i_D}\right)$. The velocity of the i-th particle can be written as $\Delta z_i=\left(\Delta z_{i_1},\Delta z_{i_2},\dots,\Delta z_{i_D}\right)$. The optimal position so far found by particle i-th is denoted as $z_i^p=\left(z_{i_1}^p,z_{i_2}^p,\dots,z_{i_D}^p\right)$ called p_i^{best}. The best value of the all individual p_i^{best} values is denoted as the global best position $z_i^g=\left(z_{i_1}^g,z_{i_2}^g,\dots,z_{i_D}^g\right)$ and called g_i^{best}. In each iteration, the particle updates its speed and position according to the following formula:

$$\Delta z_i^{\text{new}}=w\times\Delta z_i^{\text{old}}+c_1r_1\left(p_i^{\text{best}}-z_i^{\text{old}}\right)+ \\ +c_2r_2\left(g_i^{\text{best}}-z_i^{\text{old}}\right) \tag{4.2}$$

$$z_i^{\text{new}}=z_i^{\text{old}}+\Delta z_i^{\text{new}}. \tag{4.2}$$

where r_1 and r_2 are random numbers between $[0,1]$, c_1 and c_2 are acceleration constants which control how far particles move in a single generation. Velocities Δz_i^{new} and Δz_i^{old} denote the velocities of the new and old particle respectively. z_i^{old} is the current particle position, and z_i^{new} is updated particle position. The Inertial factor w controls the impact of the previous velocity of a particle on its current one.

The algorithm only requires the fitness function of each particle, without continuity, differentiability and other assumptions, which is very useful for discontinuous functions.

5. Numerical Simulations

In this section, we would like to state a numerical example to exhibit the feasibility and effectiveness of our methods. And we would compare the reconstructions of PSO method and Liu's method of the literature [8] in the following numerical experiments.

We investigate the above DSCI model (2.1)−(2.3) with $\lambda(x)=x$, $f(x)=(1+x)e^{2x}$,

$$F(x,t)=\left[(1+x)(2-t)^2-2t+4\right]e^{(2-t)x},$$

$$g_1(t)=1,\ g_2(t)=\left(1+\frac{1}{4-2t}\right)e^{1/2},$$

$$\psi(t)=\frac{1}{4-2t},$$

then the solution can be represented as $v(x,t)=(1+x)e^{(2-t)x}$. And the parameters $c=1$, $s_0=e^{1/2}-e^{-1/2}$, $\sigma=1/(\frac{1}{2}e^{1/2}+\frac{3}{2}e^{-1/2})$. The mesh sizes of x and t variables are respectively selected as $h=0.01$ and $\tau=0.001$, and the time interval is chosen to be [0,1].

The parameters in PSO are set as $M=300, c_1=c_2=1.4962, w=0.7298$.

In order to compare the results involving random measurement noise, we add a uniform distribution uncorrelated errors. The simulated inexact measurement data can be expressed as

$$u(\zeta,T)=u(\zeta,T)[1+\delta K(\zeta)],\quad \zeta\in[0,1] \tag{5.1}$$

where $\delta=1\%$ or $\delta=3\%$ means the noise level and $K(\zeta)$ is a random number which varies from -1 to 1 and is uniformly distributed.

Given that the accurate measured data, the inversion results of the two methods are close to each other and the relative errors are not much different in Figure 3. If the measurements contain perturbations, PSO method gives better results than the method in [8] from Figures 4 and 5.

The inversion results of exact measurement data are better than the results of data containing noisy from Figure 3-5. When noisy measurements δ=1% , the results of PSO are have smaller relative errors than the results of Liu's method. The same results can be obtained with noisy measurement δ=3%.

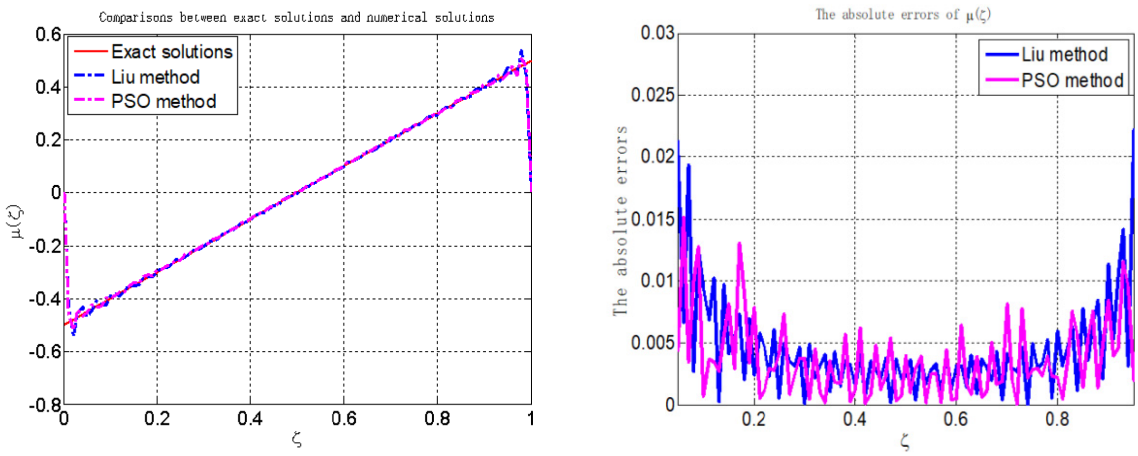

(a) Comparison results (b) Absolute errors

Figure 3 – Comparisons results and absolute errors between exact solutions and numerical solutions with exact measurements

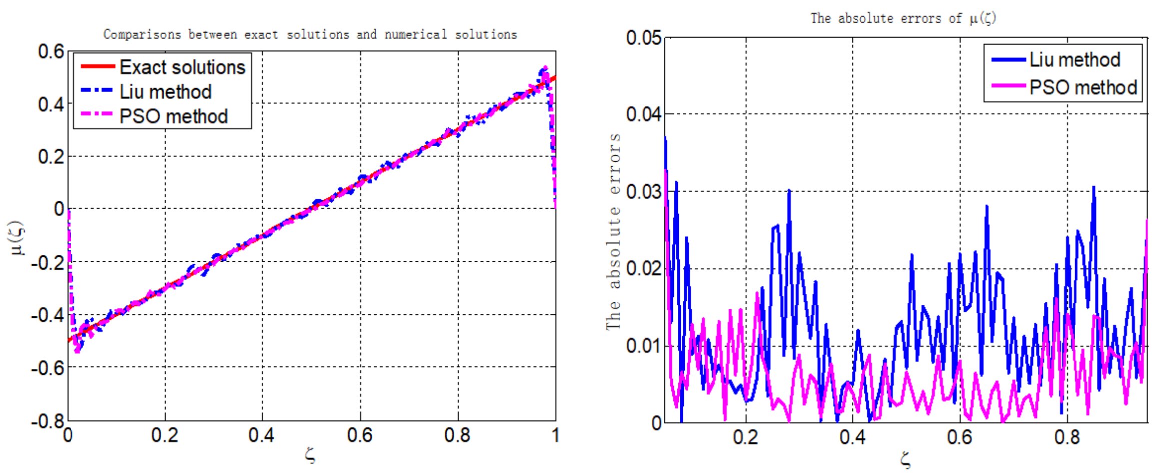

(a) Comparison results (b) Absolute errors

Figure 4 – Comparisons results and absolute errors between exact solutions and numerical solutions with noisy measurements δ=1%

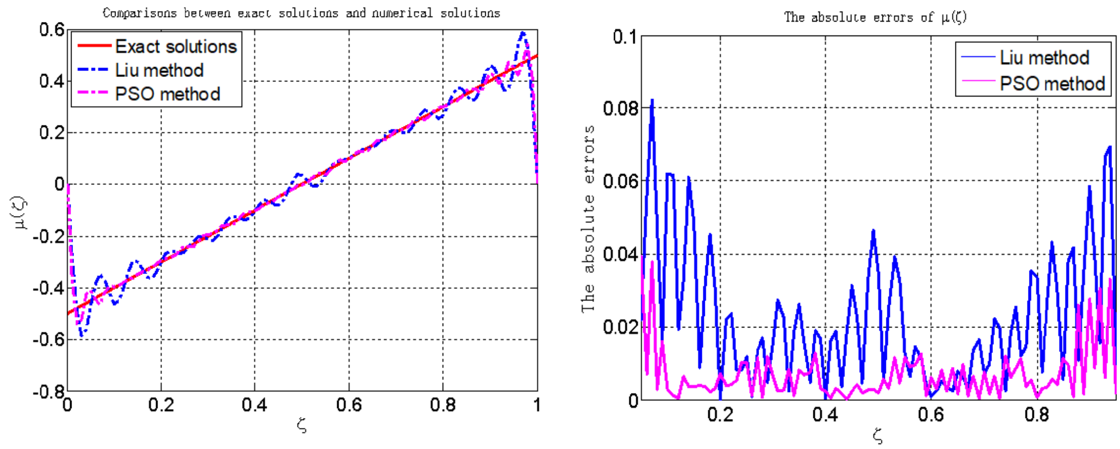

(a) Comparison results (b) Absolute errors

Figure 5 – Comparisons results and absolute errors between exact solutions and numerical solutions with noisy measurements $\delta=3\%$

6. Conclusion remarks

We adopt PSO algorithm to solve the inverse problem of DCIS model, which is converted into an optimization problem. The advantage of the characteristic of this random search method is that it does not need gradient calculation and the choice of initial guess. Therefore, even if there is a small noise, the PSO algorithm is still stable when dealing with this inverse problem. It can be observed from the numerical results that PSO method is effective and robust to solve the inverse problem of DCIS model.

Acknowledgment

The authors kindly acknowledge the help of the anonymous referees in improving the readability of the paper.

Disclosure statement

No potential conflict of interest was reported by the authors.

Funding

The work of Meibao Ge was partially supported by the Conference Funded Research Projects of School of mathematics of Shanghai University of Finance and Economics, and partially supported by Zhejiang Provincial Department of Education Research Project in 2019. The work of Keji Liu was supported by the NNSF of China under grant No. 11601308, and the Science and Technology Commission of Shanghai Municipality under the “Shanghai Rising-Star Program” No. 19QA1403400. The work of Dinghua Xu was supported by the NNSF of China [grant numbers 11871435 and 11471287].

References

1. H. Byrne, M. Chaplain. Growth of nonnecrotic tumors in the presence and absence of inhibitors. Math Biosci.130(1995):151-181.
2. H. Byrne, M. Chaplain. Growth of necrotic tumors in the presence and absence of inhibitors. Math Biosci.135(1996):187-216.
3. A. Friedman, F. Reitich, Analysis of a mathematical model for the growth of tumours,J. Math. Biol. 38(1999):262-284.
4. J.P. Ward, J.R. King, Mathematical modelling of avasculartumour growth, IMA J.Math. Appl. Med. Biol. 14(1997) :39-69.
5. J.P. Ward, J.R. King, Mathematical modelling of avasculartumour growth II: Modelling growth saturation, IMA J. Math. Appl. Med. Biol. 16 (1999):171-211.
6. Y. Xu,Gilbert R. Some inverse problems raised from a mathematical model of ductal carcinoma in situ, Math. Comp. Model. 49(2009):814-828.

7. H. Li, J. Zhou. Direct and inverse problem for the parabolic equation with initial value and time-dependent boundaries, Applicable Analysis, 95(6)(2016):1307-1326.

8. K. Liu, Y. Xu, D. Xu, Numerical algorithms for a free boundary problem model of DCIS and a related inverse problem, Applicable Analysis, DOI:10.1080/00036811.2018.1524139.

9. K. Liu, Zou J. A multilevel sampling algorithm for locating inhomogeneous media. Inv Prob. 2013;29:095003.

10. K. Liu, Xu Y, Zou J. A multilevel sampling method for detecting sources in a stratified ocean waveguide. J Comput Appl Math. 309(2017):95–110.

11. K. Liu. A simple method for detecting scatterers in a stratified ocean waveguide. Comput Math Appl. 76(2018):1791-1802.

12. D. Xu. Inverse problems of textile material design based on clothing heat-moisture comfort. Appl Anal. 93(2014):2426-2439.

13. D. Xu. Mathematical modeling of heat-moisture transfer and corresponding inverse problems in textile material design. Beijing: Science Press, 2014.

14. Kennedy J, Eberhart R. Particle swarm optimization. In: 1995 Proceedings of the IEEE International Conference on Neural Networks. 4 (1995):1942–1948.

15. Clerc M. Particle swarm optimization. 67. London: Recherche, 2006.

16. Lazinica A. Particle swarm optimization. Kirchengasse: InTech, 2009.

17. Parsopoulos K, Vrahatis M. Particle swarm optimization and intelligence: advances and applications. Chicago: Information Science Reference, 2010.

18. Y. Xu, D. Xu, L. Zhang,X. Zhou.A new inverse problem for the determination of textile fabrics thickness, Inverse Problems in Science and Engineering, DOI: 10.1080/17415977.2014.933827

IRSTI 27.35.43 https://doi.org/10.26577/ijmph-2019-i2-5

[1]Yu Jiang,[2]Junjun Lu,[3]Sihan Yin

School of Mathematics, Shanghai University of Finance and Economics, Shanghai 200433, P.R. China
e-mail:[1]jiang.yu@mail.shufe.edu.cn [2]e-mail: lujunjun0919@163.com [3]e-mail: shirleyysh@163.com

Bayesian inference approach to inverse problem in a fractional option pricing model

Abstract. As is well known to us, the Black-Scholes (B-S) model is an important and useful mathematical model for pricing a European options contract. However, because some strict assumptions in this model are not consistent with the real financial market, there are many limitations in practical applications. This paper investigates the inverse option problems (IOP) in a fractional option pricing model, which is derived from the finite moment log-stable (FMLS) model. We identify the model coefficients such as tail index α and the implied volatility σ from the measured data by using three statistical inversionschemeswhich are well known asMarkov Chain Monte Carlo (MCMC) algorithm, slice sampling algorithm and Hamiltonian/hybrid Monte Carlo (HMC) algorithm. Our numerical tests indicate that these Bayesian inference approaches can recover the unknown coefficients well.

Key words: FMLS model, statistical inversion, implied volatility, tail index, Bayesian Inference.

Introduction

As is well known to us, the Black-Scholes (B-S) model is an important and useful mathematical model for pricing a European options contract (cf. [1]). However, because some strict assumptions in this model are not consistent with the real financial market, there are many limitations in practical applications. In particular, the implied volatility of options derived from the B-S model is a constant and cannot fit to the actual "volatility smile" pattern. Recently, the fractional B-S option pricing model has begun to be widely concerned by assuming the price of the original asset is subject to the fractional Brownian motion, or even more general Lévy processes. Among these generalized B–S model, the finite moment log-stable (FMLS) model can effectively capture the leptokurtic feature observed in many financial markets (cf.[3, 4, 6 and 13]).

The stochastic differential equation corresponding to the FMLS model is as follows:

$$\frac{dS_t}{S_t} = \mu dt + \sigma dL_t^{\alpha,-1}, \tag{1}$$

where S is native asset price, t is expected return time, μ and σ are expected rate of return and asset volatility, respectively. $L_t^{\alpha,-1}$ here denotes the maximally skewed Lévy stable process with a tail index $\alpha \in (0,2)$.

By assume $x_t = \ln S_t$ and according to the argument in [4], SDE(1)can be derived into the following fractional parabolic partial differential equations with the spatial-fractional derivatives:

$$\begin{cases} \dfrac{\partial V}{\partial t} + \left(r + \dfrac{1}{2}\sigma^\alpha \sec\dfrac{\alpha\pi}{2}\right)\dfrac{\partial V}{\partial x} - \left(\dfrac{1}{2}\sigma^\alpha \sec\dfrac{\alpha\pi}{2}\right) {}_{-\infty}D_x^\alpha V - rV = 0, \\ V(x,T;\alpha) = \Pi(x) := \max(e^x - K, 0), \end{cases} \tag{2}$$

where V is option price, r is risk free rate, $\Pi(x)$ is payoff function with a given strike price K. Here ${}_{-\infty}D_x^\alpha(\cdot)$is the Weyl fractional operator defined as follows:

$${}_{-\infty}D_x^\alpha f(x) = \frac{1}{\Gamma(n-\alpha)}\frac{\partial^n}{\partial x^n}\int_{-\infty}^{x} \frac{f(y)}{(x-y)^{\alpha+1-n}}\mathrm{d}y \quad n-1 \le \mathrm{Re}(\alpha) < n.$$

Similar withthe inverse option problem basing on the B-S model pioneered by Dupire [7], we come to our inverse option problem basing on the FMSL model as follows:

Inverse Problem: Recover the tail index α and the implied volatility σ from the measured option price $V(x)$ at a given t such that $T-t$ is a fixed constant.

However, because of the nonlinear dependency of V on the coefficients α and σ, the uniqueness and stability issues of this inverse problem are quite difficult. Thus, we only desire to have a fast and stable numerical inversion algorithm for solving this inverse problem. Usually, for this purpose, a regularized iterative algorithm such as the Levenberg-Marquardt (L-M) algorithm will be the first choice ([10]). Unfortunately, without a good enough initial guess, iterations in L-M algorithm will not converge. On the other hand, a statistical inversion algorithm such as Metropolis-Hastings Markov Chain Monte Carlo (MH-MCMC) algorithm is now widely used with great success for solving a variety of inverse problems ([11]). Here in this paper we will discuss how to apply the MH-MCMC algorithm to recover the unknown α and σ.

Moreover, both L-M algorithm and MH-MCMC algorithm require for a fast forward solver, which can quickly get the accuracy numerical solution to our PDE model(2). Here we use the closed-form analytical solution given by Chen *et al.* [5] as follows:

$$V(x,t) = Ke^{-\gamma\tau}\int_{d_1}^{+\infty} f_{\alpha,0}(|m|)\mathrm{d}m - e^x\int_{d_1}^{+\infty} e^{-\tau-\tau^{1/\alpha}m} f_{\alpha,0}(|m|)\mathrm{d}m. \qquad (3)$$

where

$$d_1 = \frac{x-\ln K-(1-\gamma)\tau}{\tau^{\frac{1}{\alpha}}},$$

$$\tau = -\frac{\sigma^\alpha(T-t)}{2}\sec\frac{\alpha\pi}{2},$$

$$\gamma = -2r\left(\sigma^\alpha\sec\frac{\alpha\pi}{2}\right)^{-1},$$

and

$$f_{\alpha,0}(x) = \frac{1}{\pi}\sum_{n=1}^{\infty}\frac{\gamma(1+n/\alpha)}{n!}\sin(\frac{\pi n}{2})(-x)^{n-1}.$$

This solution will reduce to B-S formula by setting $\alpha = 2$.

The rest of this paper is organized as follows. In Section 2, three statistical inversion schemes for our inverse option problem are described and Section 3 is devoted to the numerical studies of our inversion schemes.

Statistical Inversion Schemes

In practices, the option price V is generally obtained on the different asset price $(S_1,\cdots,S_N)^{\mathrm{T}}$, and we denote:

$\mathbf{V} := (V_1,\cdots,V_N)^{\mathrm{T}} = (V(S_1),\cdots,V(S_N))^{\mathrm{T}}$.

Now our inverse problem comes to the following nonlinear inverse problem:

$$\mathbf{V} = \mathbf{F}(\mathbf{x}),$$

with respect to unknown coefficients we intend to recover:

$$\mathbf{x} := (\alpha,\sigma)^{\mathrm{T}}.$$

Here we denote the mapping $\mathbf{F}: \mathbb{R}^2 \to \mathbb{R}^N$.

We can assume the noise $\mathbf{e}$ contained in observation

$$\mathbf{V}^{\mathbf{e}} = \mathbf{V} + \mathbf{e},$$

to be Gaussian type white noise, i.e. components of the random noise $\mathbf{e}$ are independent identically distributed (i.i.d.) such that $\mathbf{e} \sim N(0,\sigma_{\mathbf{e}}^2\mathbf{I})$, where σ_e is known noise level and $\mathbf{I}$ is an identity matrix. Thus, the posterior distribution is usually formulated as follows according to the knowledge of Bayesian inference (cf. [11]):

$$p(\mathbf{x}|\mathbf{V}) \propto \exp\left(-\frac{1}{2\sigma_{\mathbf{e}}^2}\parallel \mathbf{V}^{\mathbf{e}} - \mathbf{F}(\mathbf{x})\parallel_2^2\right)p(\mathbf{x}).$$

The prior distribution here is simply assumed to be uniform, i.e.

$$p(\mathbf{x}) := \begin{cases}1, & \mathbf{x}\in D,\\ 0, & \mathbf{x}\notin D.\end{cases}$$

with a large enough admissible set D of $\mathbf{x}$. The above posterior distribution can be written into following form:

$$p(\mathbf{x}|\mathbf{V}) \propto \exp\left(-\frac{1}{2\sigma_{\mathbf{e}}^2} \parallel \mathbf{V}^e - \mathbf{F}(\mathbf{x}) \parallel_2^2\right).$$

One can get the maximum a posterior (MAP) estimator $\mathbf{x}_{\mathrm{MAP}}$ of $\mathbf{x}$ such that:

$$\mathbf{x}_{\mathrm{MAP}} = \underset{\mathbf{x}}{\operatorname{argmax}}\, p(\mathbf{x}|\mathbf{V}).$$

However, MAP estimate is *point estimate*, different measured data $\mathbf{V}$ will come to different $\mathbf{x}$. To avoid this, one can compute the posterior conditional mean (CM) estimator from various point estimators:

$$\mathbf{x}_{\mathbf{CM}} := \int_{\mathbb{R}^2} \mathbf{x}\, p(\mathbf{x}|\mathbf{V}) \mathrm{d}\mathbf{x}.$$

Furthermore, it is hard to know the explicit form of $p(\mathbf{x}|\mathbf{V})$ in practice. Some sampling algorithm can be applied to obtain a set of samples $\mathbf{x}_k$ ($k = 1, \cdots, K$) drawn independently from the distribution $p(\mathbf{x}|\mathbf{V})$ (cf. [2, 11]), and thus $\mathbf{x}_{\mathbf{CM}}$ comes to a finite sum approximately

$$\mathbf{x}_{\mathbf{CM}} \approx \frac{1}{K} \sum_{k=1}^{K} \mathbf{x}_k.$$

This is exactly the desired solution of our related inverse problem in the sense of Bayesian inference.

MH-MCMC Algorithm: in this paper, we first apply the most famous and popular sampling algorithm: Metropolis-Hastings algorithm ([8, 12]) shown as follows:

1. Generate $\mathbf{x}'$ from $q(\mathbf{x}'|\mathbf{x}_k) \sim N(\mathbf{x}_k, \Sigma)$ for given $\mathbf{x}_k$.

2. Calculate the choice

$$a(\mathbf{x}', \mathbf{x}_k) = \min\left\{1, \frac{p(\mathbf{x}'|V)}{p(\mathbf{x}_k|V)}\right\}.$$

3. Update $\mathbf{x}_k$ as $\mathbf{x}_{k+1} = \mathbf{x}'$ with probability $a(\mathbf{x}', \mathbf{x}_k)$, otherwise set $\mathbf{x}_{k+1} = \mathbf{x}_k$.

4. Here the proposal distribution $q(\mathbf{x}|\mathbf{y})$ is given as

$$q(\mathbf{x}|\mathbf{y}) \propto \exp\left(-\frac{1}{2\Sigma} \parallel \mathbf{x} - \mathbf{y} \parallel_2^2\right).$$

with given step sizes γ_α and γ_σ such that $\Sigma = \mathrm{diag}(\gamma_\alpha^2, \gamma_\sigma^2)$. For more details about MH-MCMC algorithm, we can refer to [2, 11].

However, the performance of MH-MCMC algorithm highly dependents on the specific choice of proposal distribution $q(\mathbf{x}|\mathbf{y})$. Without a carefully tuning of the step sizes γ_α and γ_σ, this algorithm will not lead to efficient samples. Therefore, we desire to have some sampling algorithm which will determine the step sizes "automatically". The following two well-known sampling algorithms introduced in [2] can be applied.

Slice Sampling Algorithm: the basic idea of this algorithm is to generate samples from the joint $(\mathbf{x}, u)$ space with an additional variable $u = p(\mathbf{x})$ where $p(\mathbf{x})$ is just the sampling distribution where we set it to the posterior distribution $p(\mathbf{x}|\mathbf{V})$. The procedure for finding the next sampling point $\mathbf{x}'$ from the current sampling point $\mathbf{x}$ is shown by following algorithm (see also Figure 1):

1. Generate a real value u from the uniform distribution $U(0, p(\mathbf{x}))$, and define the slice $S = \mathbf{x}: u < p(\mathbf{x})$.

2. Find a hyper rectangle $H := (L_1, R_1) \times \cdots \times (L_M, R_M)$ around $\mathbf{x}$, which contains the slice S as much as possible.

3. Generate the new sample $\mathbf{x}'$ uniformly in this hyperrectangle H.

Due to the existence of computational error, it is difficult to locate the hyper rectangle H exactly. A detailed numerical procedure about it can be found in [2]. Unfortunately, this numerical procedure always slows down the sampling.

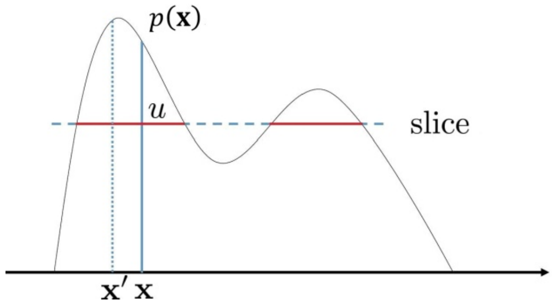

Figure 1 – Slice sampling algorithm.

Hamiltonian Monte Carlo Algorithm: this sampling algorithm is also known as Hybrid Monte Carlo (HMC) algorithm. In this algorithm, the transition of sampling points is not through the proposed distribution $q(\mathbf{x}|\mathbf{y})$, but by solving the following Hamiltoniansystem:

$$\begin{cases} \dfrac{\partial \mathbf{q}'}{\partial t} = \dfrac{\partial H}{\partial \mathbf{p}'} = \dfrac{\partial K(\mathbf{p})}{\partial \mathbf{p}'}, \\ \dfrac{\partial \mathbf{p}'}{\partial t} = \dfrac{\partial H}{\partial \mathbf{q}'} = -\dfrac{\partial U(\mathbf{q})}{\partial \mathbf{q}'}. \end{cases}$$

where $\mathbf{q}$ is a statevariable, $U(\mathbf{q})$ is the potential energy of the dynamical system when in state $\mathbf{q}$, $\mathbf{p}$ is the momentumvariable, and $K(\mathbf{p})$ is the kinetic energy. When one state $(\mathbf{q}, \mathbf{p})$ changes to another state $(\mathbf{q}', \mathbf{p}')$, the value of the following Hamiltonianisalways constant:

$$\begin{aligned} H(\mathbf{q}, \mathbf{p}) &= U(\mathbf{q}) + K(\mathbf{p}) \\ &= U(\mathbf{q}') + K(\mathbf{p}') = H(\mathbf{q}', \mathbf{p}'). \end{aligned}$$

Based on this, we have the following HMC algorithm:

1. Calculate the potential energy $U(q) = p(\mathbf{q}|\mathbf{v})$ of the current state $\mathbf{q} = \mathbf{x}$.
2. Generate the momentum $\mathbf{p}$ from a given simply normal distribution $e^{-K(\mathbf{p})}$.
3. Update the sample $\mathbf{x}' = \mathbf{q}'$ by solving the above Hamiltonian system.

However, in practice, we can only solve the Hamiltonian equations numerically by applying the leapfrog scheme. Therefore, to ensure the samples are all in the same stable Markovchain, we use the "accept-reject" criterion to accept the candidate sample $\mathbf{q}'$or not:

$$a = \min\left(1, e^{-H(\mathbf{q}', \mathbf{p}') + H(\mathbf{q}, \mathbf{p})}\right).$$

This indeed is similar to the one used in above MH-MCMC algorithm.

Numerical Test

In this section, we will test the performance of three algorithms for solving our inverse option price numerically.

Simulated Data: we firstly generate the noise free simulated data and the noisy simulated data which contains 20% relative Gaussian noise by using the closed-form analytical solution (3) (see). Here, the parameters in (3) are the same as the ones in Chen *et al.*: $K = 10$, $r = 0.1$, $T - t = 1$ (year) and $\mathbf{x} = (\alpha, \sigma)^{\mathrm{T}} = (1.75, 0.2440)^{\mathrm{T}}$.

Therefore, we test the sampling algorithms shown above under these simulated data one by one.The initial value of $\mathbf{x}_0$ is always set to $(\alpha_0, \sigma_0)^{\mathrm{T}} = (2, 0.5)^{\mathrm{T}}$.

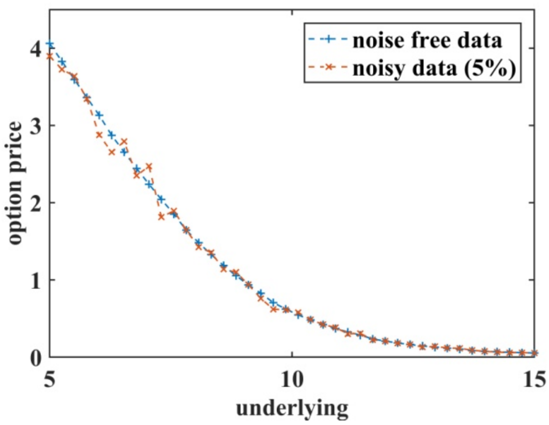

Figure 2 - Simulated data

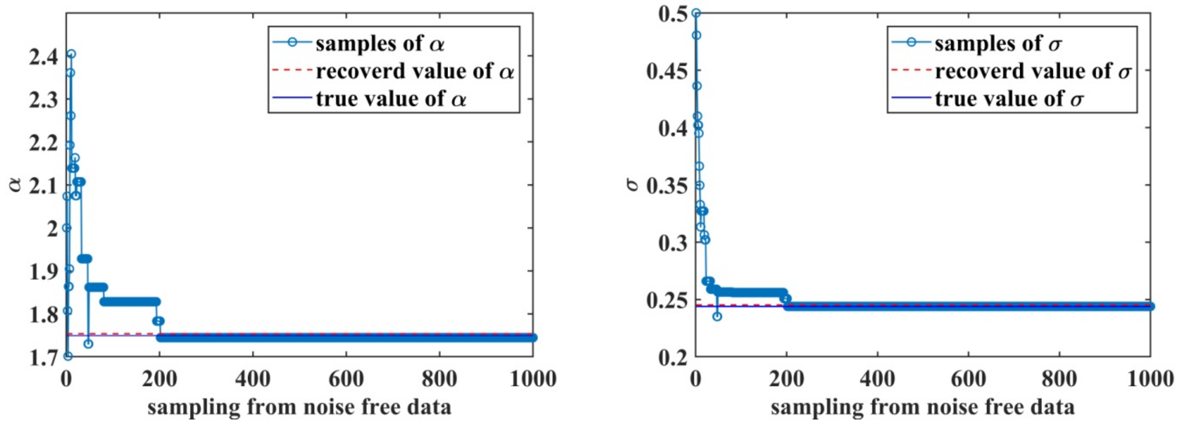

Figure 3 – Samples by applying MH-MCMC algorithm from noise free data: (up) α; (down) σ

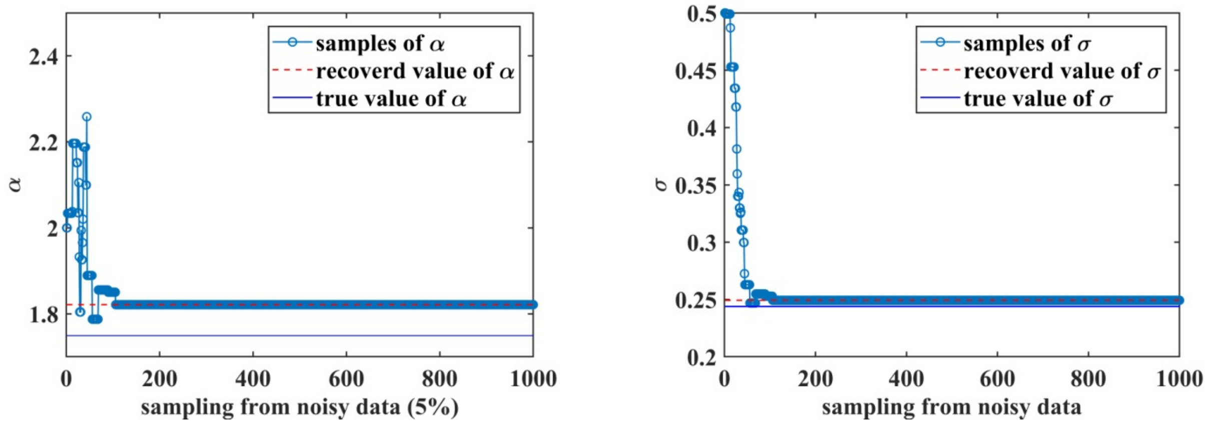

Figure 4 – Samples by applying MH-MCMC algorithm from noisy data (5%): (up) α; (down)σ

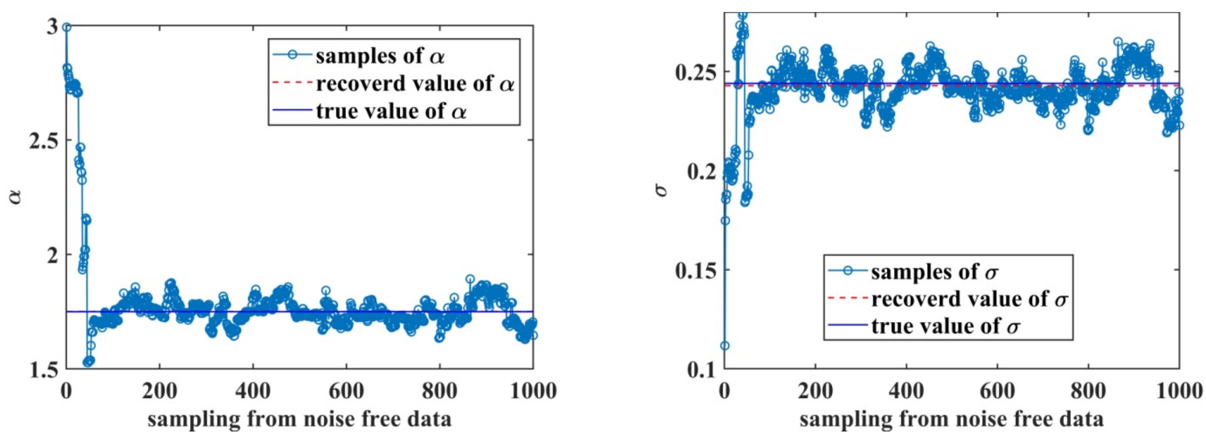

Figure 5 – Samples by applying slice sampling algorithm from noise free data: (up) α; (down) σ.

MH-MCMC Algorithm: the other hyper parameters used in MH-MCMC algorithm are set to be $\Sigma = \mathrm{diag}(0.25^2, 0.025^2)^{\mathrm{T}}$ and $\sigma_{\mathbf{e}} = 10^{-6}$. The total sampling time is 1000. Samples from noise free data are shown in, while samples from noisy data are shown in. We always set up some "burn-in" time, which is thought as the start point of stable Markov Chain. The mean value of samples among this "burn-in" time (=101) and the ending point (=1000) is computed and set to be our recovered result shown in Table 1. It is clear the MH-MCMC algorithm works well and does not trap in the any local minimums. Theoretically, a large number of samplings will final derive to a stable Markov chain, but in practice the computing cost will be very expansive, and thus we always need to manually choose the hyper parameters $\sigma_{\mathbf{e}}$ and Σ in MH-MCMC algorithm such that the Markov chain "converge" fast and stable. This is a big disadvantage of this MH-MCMC algorithm, and it will be quite interesting for us to try the other two sampling algorithms.

Slice Sampling Algorithm: the only hyper parameter needs to be set is$\sigma_{\mathbf{e}} = 10^{-3}$. The total sampling time is also 1000. Samples from noise free data are shown in, while samples from noisy data are shown in. The mean value of samples among this "burn-in" time (=101) and the ending point (=1000) is computed and set to be our recovered result shown in Table 1.

Table 1 – Recovered results by applying MH-MCMC algorithm.

	$\boldsymbol{\alpha}$	$\boldsymbol{\sigma}$
Initial value	2	0.5
Noise free data	1.7536	0.2453
Noisy data (5%)	1.8215	0.2493
True value	1.75	0.244

Table 2 – Recovered results by applying slice sampling algorithm.

	$\boldsymbol{\alpha}$	$\boldsymbol{\sigma}$
Initial value	2	0.5
Noise free data	1.7509	0.2429
Noisy data (5%)	2.0617	0.2529
True value	1.75	0.244

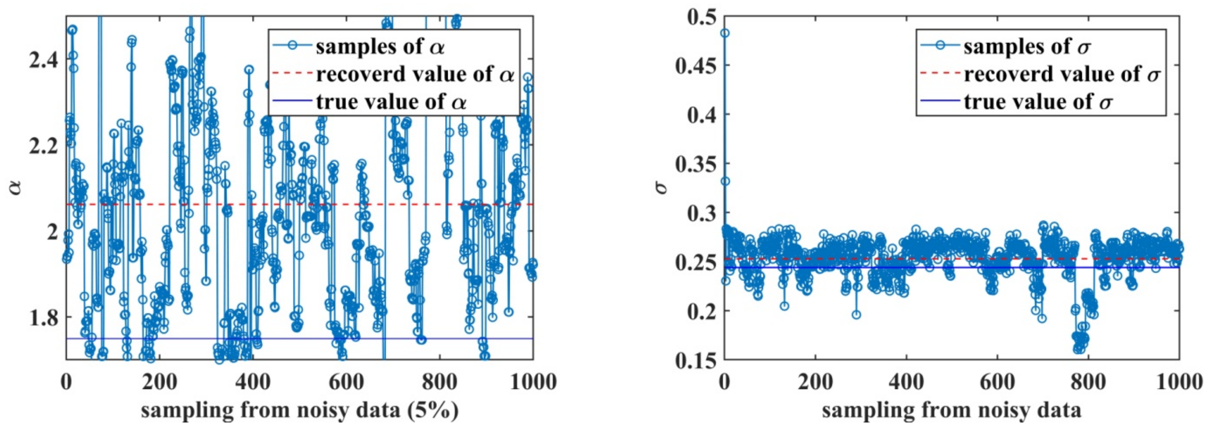

Figure 6 – Samples by applying slice sampling algorithmfrom noisy data (5%): (up) α; (down) σ

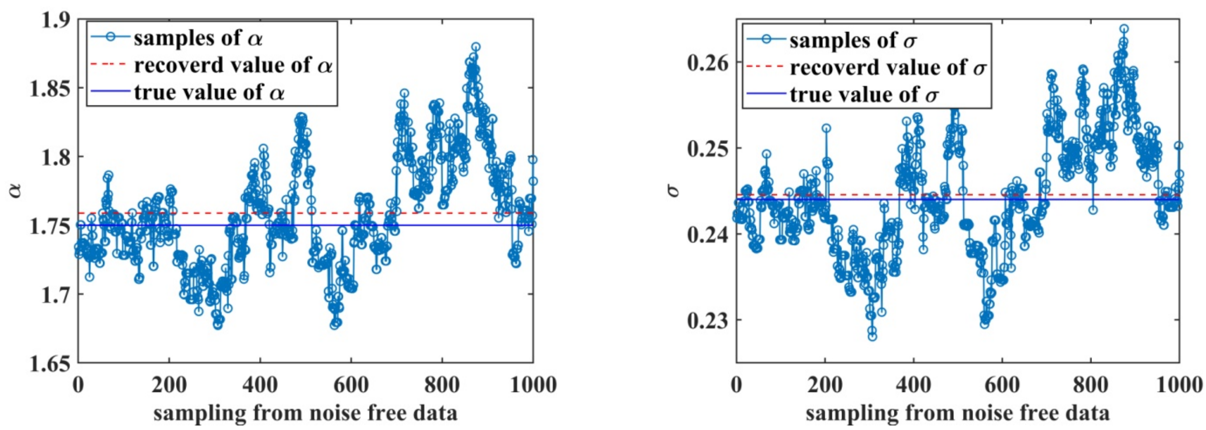

Figure 7 – Samples by applying HMC algorithm from noise free data: (up) α; (down) σ

It is clear that the samples always transit with probability one without stopping. Therefore, these samples generated by slice sampling algorithm can exhibit the real random characteristics of the posterior distribution $p(\mathbf{x}|\mathbf{V})$ we desire to recover in every statistical inverse problem.

Hamiltonian Monte Carlo Algorithm: similar to slice sampling algorithm, the only hyper parameter needs to be set is $\sigma_{\mathbf{e}} = 10^{-1}$. The total sampling time is again 1000. Samples from noise free data are shown in, while samples from noisy data are shown in. The mean value of samples among this "burn-in" time (=101) and the ending point (=1000) is computed and set to be our recovered result shown in Table 1.

Similar to slice sampling algorithm, the samples draw by HMC algorithm usually transit stalely without stopping. These samples generated can also exhibit the real random characteristics of the posterior distribution $p(\mathbf{x}|\mathbf{V})$ we desire to recover. However, the numerical computation of Hamiltonian system in each sampling is quite time consuming, and thus HMC algorithm is much slower than the other two in this paper.

Table 3 – Recovered results by applying HMC algorithm

	$\boldsymbol{\alpha}$	$\boldsymbol{\sigma}$
Initial value	2	0.5
Noise free data	1.7588	0.2446
Noisy data (5%)	1.9255	0.2539
True value	1.75	0.244

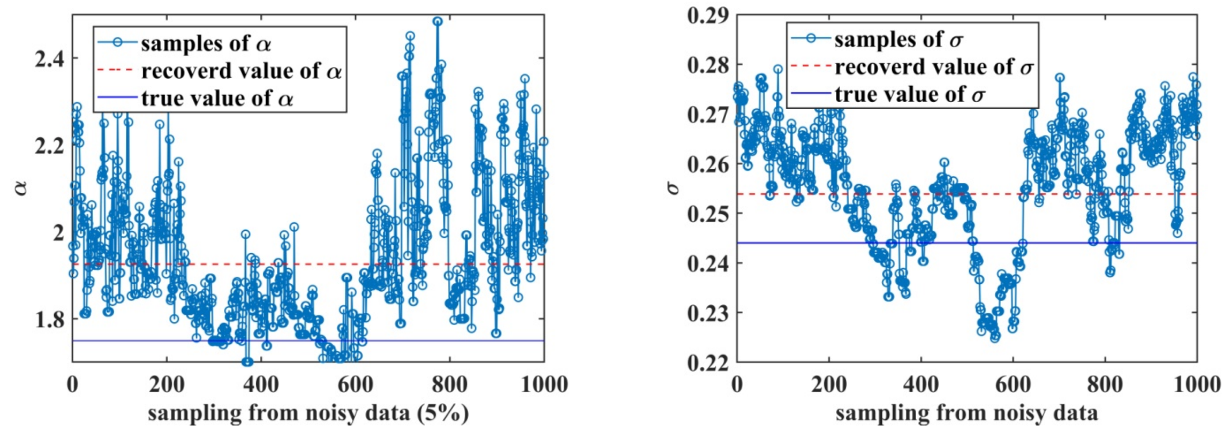

Figure 8 – Samples by applying HMC algorithm from noisy data (5%): (up) α; (down) σ

Conclusion: all of these three sampling algorithms can solve our invers option problem well. The recovery of the implied volatility σ is much better than the recovery of the tail index αbecause of the high nonlinearity of the problem corresponding to α.

Also, here isa short summary of the main advantage and disadvantage of inversion algorithms involved in this paper:

L-M algorithm

Disadvantage: good initial value $\mathbf{x}_0$ is required, otherwise it is easy to fall into local minimum.

Advantage: if the initial value is properly selected, the convergence speed is fast and the result is accuracy.

MH-MCMC algorithm

Disadvantage: need to carefully choose a proposal distribution, otherwise the rejected rate will be quite high and need to have a large number of samples to draw/recover the posterior distribution $p(\mathbf{x}|\mathbf{V})$.

Advantage: if the proposal distribution is properly chosen, the recovered posterior distribution $p(\mathbf{x}|\mathbf{V})$ is good.

Slice sampling algorithm

Disadvantage: finding a proper slice in each sampling is time consuming.

Advantage: no need of the proposal distribution and the recovered posterior distribution $p(\mathbf{x}|\mathbf{V})$ is good.

HMC algorithm

Disadvantage: numerical computation of Hamiltonian system in each sampling is quite time consuming.

Advantage: no need of the proposal distribution and the recovered posterior distribution $p(\mathbf{x}|\mathbf{V})$ is good.

Acknowledgment

This research was supported by National Natural Science Foundation of China (No. 11971121).

Reference

1. Black F., Scholes M.S., "The Pricing of Options and Corporate Liabilities." *Journal of Political Economy* vol. 81, no. 3 (1973):637-654.

2. Bishop C.M., *Pattern Recognition and Machine Learning*. NewYork: Springer-Verlag Inc.,2006.

3. Carr P., Wu L., "The Finite Moment Log Stable Process and Option Pricing." *Journal of Finance* vol.58, no. 2 (2003):753-778.

4. Cartea A., Del-Castillo-Negrete D., "Fractional Diffusion Models of Option Prices in Markets with Jumps." *Birkbeck Working Papers in Economics and Finance* vol.374, no. 2 (2006):749-763.

5. Chen W., Xu X., Zhu S.P., "Analytically pricing European-style options under the modified Black-Scholes equation with a spatial-fractional derivative." *Quarterly of Applied Mathematics* vol. 72, no. 3 (2014):597-611.

6. Cont R., Tankov P.,*Financial Modelling with Jump Processes*. London: Chapman & Hall/CRC Press, 2003.

7. Dupire B., "Price with a smile." *RISK*vol. 7, (1994): 18-20.

8. Hastings W.K., "Monte Carlo Sampling Methods Using Markov Chains and Their Applications."*Biometrika* vol.57, no 1 (1970):97-109.

9. Liu J.S.,*Monte Carlo Strategies in Scientific Computing*. New York: Springer-Verlag Inc.,2004.

10. Kaltenbacher B., Neubauer A., Scherzer O.,*Iterative regularization methods for nonlinear ill-posed problems.*KG Berlin: Walter de Gruyter GmbH & Co,2008.

11. Kaipio J.P., Somersalo E., *Statistical and Computational Inverse Problems.* New York: Springer-Verlag Inc., 2005.

12. Metropolis N., Rosenbluth A.W., Rosenbluth M.N., et al. "Equation of State Calculations by Fast Computing Machines." *The Journal of Chemical Physics*vol. 21(2004):1087-1092.

13. Schoutens W., *Lévy Processes in Finance: Pricing Financial Derivatives.*Hoboken: John Wiley & Sons Inc., 2003.

IRSTI 27.35.46 https://doi.org/10.26577/ijmph-2019-i2-6

A. Abdibekova, D. Zhakebayev, A. Zhumali

Al-Farabi Kazakh National University, Almaty, Kazakhstan,
e-mail: Dauren.Zhakebaev@kaznu.kz,

Stuart number effect on 3-d mhd convection in a cubic area

Abstract. In this paper mathematical modeling of magnetohydrodynamics natural convection in three dimensional area at different Stuart numbers has been considered. The magnetic field is considered vertically and results have been shown at different planes of 3-D enclosure. The modeling of natural convection is based on the solution of a filtered unsteady three - dimensional Navier- Stokes equation and the equation for temperature. The problem is solved numerically: the equations of motion and temperature – by a finite-difference method in combination with penta-diagonal matrix using the Adams-Bashfort scheme, the equation for pressure – by spectral Fourier method with combination of matrix factorization. Change the dynamic of natural convection is gained over the time depending on the different values of Stuart numbers. As result of modelling, isothermal surfaces, velocity and temerature contoures, also profiles for different Sturart numbers are obtained.

Key words. Natural convection, magnetohydrodynamics, finite difference method, spectral method.

Introduction

Natural convection is a phenomenon that occurs in many engineering applications, resulting in airflow near surfaces of solid particles or liquids, such as airflow in double-glazed windows, airflow in double-glazed doors of refrigerated display cases and airflow in gaps or cavities building walls. To clearly understand, many researchers have devoted themselves to the study of this phenomenon in order to enhance or reduce this heat transfer mode. Natural convection of the flow is one of the most important problems in fluid mechanics and [1,2].

Magnetic field convection has been developed and has been used in recent decades [3-7]. In [8], two-dimensional mixed convection in a chamber was solved using the finite volume method. They examined the sinusoidal boundary condition and the effect of the ratio of amplitudes, phase deviation, Richardson number and Hartmann number on the heat transfer rate. Their results show that the Nusselt number increases in amplitude ratio. In addition, the Nusselt number increases with the phase deviation to $\varphi = \pi / 2$, and then decreases. In [9], the results for a laminar mixed convection flow in the presence of a magnetic field in the upper cavity controlled by a cover with a set of Graskoff and Hartmann numbers are presented. They used the finite volume method to model the equations and concluded that the transfer rate decreases with the Hartmann number.

In [10], the Boltzmann MRT double lattice method was applied to simulate three-dimensional MHD of natural convection flow in a cubic cavity. Two different populations with models D3Q19 and D3Q7 were used to determine the flow field and temperature, respectively. The effect of the Hartmann and Grashof numbers on the projection of the flow trace and the heat transfer rate on various surfaces of the cavity, where the flow structure and isotherms in different planes of the casing change sharply due to an increase in the Hartmann and Grashof numbers, since the magnetic field is strong, the rates are suppressed.

Three-dimensional nanofluidic non-Darsian natural convection is presented in the presence of Lorentz forces [11]. The lattice Boltzmann method is selected for mesoscopic analysis. The simulation results are presented for various amounts of Darcy, Rayleigh, and Hartmann numbers, and the volume fraction of Al2O3. The results show that convection dominates at large Darcy and Rayleigh numbers; therefore, distorted isotherms are observed at high Darcy and Rayleigh numbers. The motion of the nanofluid increases with increasing volume fraction, the Rayleigh and Darcy numbers, but decreases with increasing Hartmann number. The temperature gradient on a hot surface decreases with increasing

Hartmann number, while it increases with increasing Darcy number, Rayleigh number. The influence of the use of nanoparticles reaches a maximum degree for the maximum Hartmann value and the minimum value of the Darcy and Rayleigh numbers.

In [12], convective flows and heat transfer in a magnetic field were studied. They also use the finite volume method and report that the heat transfer rate is increasing. In [13], the LBM method was used to solve a two-dimensional MHD flow in an inclined cavity with four heat sources. They thought that the double model of multiple time relaxation models the equations of momentum and energy, and explores the effect of the Hartmann number on fluid flow and heat transfer. They show that the average Nusselt number decreases due to an increase in the Hartmann number for all Rayleigh numbers.

In [14], MHD natural convection in a three-dimensional square cavity with a sinusoidal temperature distribution on one side wall was investigated using the new Boltzmann lattice method with a double relaxation time model using nano-liquid copper-water. The influence of various parameters, such as the Rayleigh and Hartmann numbers, the volume fraction of nanoparticles, and the phase deviation on heat transfer, was considered. Concerning the present results, the following conclusions are drawn: Convection heat transfer decreases with increasing Hartmann number, and the average Nusselt number decreases for both the left and right walls, but the decrease for the right wall is greater than for the left. When the Hartmann number increases from 0 to 50, the average Nusentt number decreases by 64% and 70% for the left and right walls, respectively.

In this paper, we consider a mathematical model of the problem of natural convection under the influence of a vertical magnetic field, where the effect of the Start number on convection of the MHD flow was obtained.

The applied magnetic field $B = -H_0\vec{j}$ effect in the Navier-Stokes equations is the inclusion of the Lorentz force to the momentum equations $F_l = J \times B$, where $J = \sigma(E + V \times B)$ -is electric current density, E - is electric field strength, which we set equal to zero, and σ is electric conductivity, $V = u_1\vec{i} + u_2\vec{j} + u_3\vec{k}$ velocity of fluid, and all of these in combination we obtain $F_l = \sigma(V \times B) \times B$ – Lorentz force, where $F_l = \sigma\left[(u_1\vec{i} + u_2\vec{j} + u_3\vec{k}) \times (-H_0\vec{j})\right] \times (-H_0\vec{j})$ is in detail, after using the properties of the multiplication of unit vectors, we obtain $F_l = \sigma(u_1 H_0\vec{k} - u_3 H_0\vec{i}) \times (-H_0\vec{j})$, or $F_l = \sigma(-u_1 H_0^2\vec{i} - u_3 H_0^2\vec{k})$, and $F_l = F_1 + F_2 + F_3$, where $F_1 = -\sigma u_1 H_0^2,\ F_2 = 0,\ F_3 = -\sigma u_3 H_0^2$.

The problem is based on solving non-stationary equations of magnetohydrodynamics with filtration in combination with the continuity equation, equations for temperature, equations of motion of charged particles, taking into account the continuity equation in a Cartesian coordinate system in dimensionless form

$$\begin{cases} \dfrac{\partial \overline{u}_i}{\partial t} + \dfrac{\partial(\overline{u}_i\overline{u}_j)}{\partial x_j} = -\dfrac{\partial \overline{p}}{\partial x_i} + \dfrac{1}{\mathrm{Re}}\dfrac{\partial}{\partial x_j}\left(\dfrac{\partial \overline{u}_i}{\partial x_j}\right) + F_i + \dfrac{Ra}{\mathrm{Re}^2\,\mathrm{Pr}}\overline{\theta}, \\ \dfrac{\partial \overline{u}_i}{\partial x_i} = 0, \\ \dfrac{\partial \overline{\theta}}{\partial t} + \dfrac{\partial(\overline{u}_i\overline{\theta})}{\partial x_j} = \dfrac{1}{\mathrm{Re}\,\mathrm{Pr}}\dfrac{\partial}{\partial x_j}\left(\dfrac{\partial \overline{\theta}}{\partial x_j}\right), \end{cases} \tag{1}$$

where $\overline{u}_i\ (i = 1,2,3)$ are the velocity components, $\overline{F}_1 = -N\overline{u}_1, \overline{F}_2 = 0, \overline{F}_3 = -N\overline{u}_3$ -non-dimensional Lorentz force [10], $N = \dfrac{\sigma L H_0^2}{\rho \nu_0} = \dfrac{Ha^2}{\mathrm{Re}}$ is the Stuart number, where $Ha = H_0 L\sqrt{\sigma/\mu}$ – Hartmann number, H - magnetic field strength, σ is the conductivity of the medium, which is determinedfrom plasma physics.

$U_0 = \sqrt{\alpha D(T_1 - T_0)L_3}$ – characteristically velocity, $\overline{p}$ is the full pressure, t is the time, $\overline{\theta} = (T - T_0)/(T_1 - T_0)$ – non-dimensional temperature in ionosphere, where T_0 and T_1 are the respective temperatures of the minimum and maximum of the area, $Ra = \dfrac{\alpha g (T_1 - T_0)L_3^3}{\nu D}$ -Rayleigh, where α is volumetric thermal expansion coefficient, g – acceleration due to gravity, $\mathrm{Re} = \sqrt{\dfrac{Ra}{\mathrm{Pr}}}$ is the Reynolds number, $\mathrm{Pr} = \dfrac{\nu}{D}$ – Prandtl number, D – diffusion coefficient, L is the typical length, ν is the kinematic viscosity coefficient, ρ is the density of the flow.

A schematic picture of the computational domain is shown in Figure 1, where the left wall - indicated by the blue color, corresponds to the low temperature of flow. The right wall layer - highlighted in red, corresponds to high temperature of the flow.

Initial conditions for temperature, velocity components are set zero in all directions of the domain. The boundary conditions imposed for temperature is Dirichlet on the right and left boundary, and Neumann on the other directions of the domain. The velocity components are equal to 0 in all directions.

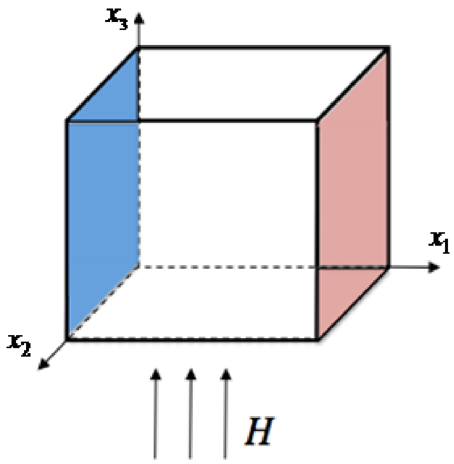

Figure 1 – Illustration of the problem statement

Numerical method

To solve the problem of homogeneous incompressible MHD turbulence, a scheme of splitting by physical parameters is used:

I. $$\frac{(\vec{u}^*)^{n+1} - (\vec{u})^n}{\Delta t} - \frac{1}{2\,\mathrm{Re}}\nabla^2 (\vec{u}^*)^{n+1} = \frac{1}{2\,\mathrm{Re}}\nabla^2 (\vec{u})^n + \frac{3}{2}K^n - \frac{1}{2}K^{n-1},$$

II. $$\Delta p = \frac{\nabla (\vec{u}^*)^{n+1}}{\tau},$$

III. $$\frac{(\vec{u})^{n+1} - (\vec{u}^*)^{n+1}}{\Delta t} = -\nabla p,$$

IV. $$\frac{\overline{\theta}^{n+1} - \overline{\theta}^n}{\Delta t} - \frac{1}{2Pe}\nabla^2 \overline{\theta}^{n+1} = \frac{1}{2Pe}\nabla^2 \overline{\theta}^n + \left(\frac{3}{2}G^n - \frac{1}{2}G^{n-1}\right)$$

where

$$K^n = -(\vec{u}^n \nabla)\vec{u}^n + F^n + \frac{Ra}{\mathrm{Re}^2\,\mathrm{Pr}}\theta^n,$$

$G^n = -(\vec{u}^n \nabla)\theta^n$ where $Pe = \mathrm{Re}\,\mathrm{Pr}$ – Peclet number.

During the first stage, the full magneto hydrodynamic equation system is solved without the pressure consideration. For approximation of the convective and diffusion terms of the intermediate velocity field a finite-difference method in combination with penta-diagonal matrix is used,which allowed to increase the order of accuracy in space. The numerical algorithm for the solution of incompressible MHD turbulence is considered at [15].

At the second step, the pressure Poisson equation is solved, which ensures that the continuity equation is satisfied. The Poisson equation is transformed from the physical space into the spectral space by using a Fourier transform. To solve the three-dimensional Poisson equation, the spectral conversion in combination with matrix sweeping algorithm is developed [15]. The resulting pressure field in the third stage is used to recalculate the final velocity field [16].

At the fourth stage, the equation for temperature is solved by using Adams-Bashforth scheme.

Consider the temperature distribution in the horizontal direction at the point i, j, k :

$$\frac{\partial\theta}{\partial t}+\frac{\partial(u_1\theta)}{\partial x_1}+\frac{\partial(u_2\theta)}{\partial x_2}+\frac{\partial(u_3\theta)}{\partial x_3}= =\frac{1}{\mathrm{Re}\,\mathrm{Pr}}\left(\frac{\partial^2\theta}{\partial x_1^2}+\frac{\partial^2\theta}{\partial x_2^2}+\frac{\partial^2\theta}{\partial x_3^2}\right) \quad (2)$$

When using the explicit Adams-Bashfort scheme for convective terms and the implicit Crank-Nicholson scheme for viscous terms, equation (2) takes the form:

$$\theta^{n+1}_{i,j,k}-\theta^{n}_{i,j,k}=-\frac{3\Delta t}{2}[hr]^n_{i,j,k}+ +\frac{\Delta t}{2}[hr]^{n-1}_{i,j,k}+\frac{\Delta t}{2}[ar]^n_{i,j,k}+\frac{\Delta t}{2}\cdot\frac{1}{\mathrm{Re}\,\mathrm{Pr}}\times \times\left[\left(\frac{\partial^2\theta}{\partial x_1^2}\right)^{n+1}_{i,j,k}+\left(\frac{\partial^2\theta}{\partial x_2^2}\right)^{n+1}_{i,j,k}+\left(\frac{\partial^2\theta}{\partial x_3^2}\right)^{n+1}_{i,j,k}\right] \quad (3)$$

where

$$[hr]^n_{i,j,k}=\left(\frac{\partial(u_1\theta)}{\partial x_1}\right)^{n+1}_{i,j,k}+ +\left(\frac{\partial(u_2\theta)}{\partial x_2}\right)^{n+1}_{i,j,k}+\left(\frac{\partial(u_3\theta)}{\partial x_3}\right)^{n+1}_{i,j,k}$$

$$[ar]^n_{i+\frac{1}{2},j,k}=\frac{1}{\mathrm{Re}\,\mathrm{Pr}}\times \times\left[\left(\frac{\partial^2\theta}{\partial x_1^2}\right)^{n}_{i,j,k}+\left(\frac{\partial^2\theta}{\partial x_2^2}\right)^{n}_{i,j,k}+\left(\frac{\partial^2\theta}{\partial x_3^2}\right)^{n}_{i,j,k}\right]$$

Discretization of convective expressions looks like this:

$$\left(\frac{\partial u_1\theta}{\partial x_1}\right)\bigg|_{i,j,k}=\frac{-(u_1\theta)_{i+2,j,k}+27(u_1\theta)_{i+1,j,k}-27(u_1\theta)_{i,j,k}+(u_1\theta)_{i-1,j,k}}{24\Delta x_1}+O(\Delta x_1^4),$$

$$\left(\frac{\partial u_2\theta}{\partial x_2}\right)\bigg|_{i,j,k}=\frac{(u_2\theta)_{i+1,j-2,k}-27(u_2\theta)_{i,j-1,k}}{24\Delta x_2}+\frac{27(u_2\theta)_{i,j,k}-(u_2\theta)_{i,j+1,k}}{24\Delta x_2}+O(\Delta x_2^4)$$

$$\left(\frac{\partial u_3\theta}{\partial x_3}\right)\bigg|_{i,j,k}=\frac{(u_3\theta)_{i,j,k-2}-27(u_3\theta)_{i,j,k-1}}{24\Delta x_3}+\frac{27(u_3\theta)_{i,j,k}-(u_3\theta)_{i,j,k+1}}{24\Delta x_3}+O(\Delta x_3^4).$$

Discretization of diffusion conditions looks like this:

$$\left(\frac{\partial^2\theta}{\partial x_1^2}\right)\bigg|_{i,j,k}=\frac{-(\theta)_{i+2,j,k}+16\cdot(\theta)_{i+1,j,k}-30\cdot(\theta)_{i,j,k}+16\cdot(\theta)_{i-1,j,k}-(\theta)_{i-2,j,k}}{12\Delta x_1^2};$$

$$\left(\frac{\partial^2\theta}{\partial x_2^2}\right)\bigg|_{i,j+\frac{1}{2},k}=\frac{-(\theta)_{i,j+2,k}+16\cdot(\theta)_{i,j+1,k}-30\cdot(\theta)_{i,j,k}+16\cdot(\theta)_{i,j-1,k}-(\theta)_{i,j-2,k}}{12\Delta x_2^2};$$

$$\left.\left(\frac{\partial^2\theta}{\partial x_3^2}\right)\right|_{i,j,k+\frac{1}{2}} = \frac{-(\theta)_{i,j,k+2}+16\cdot(\theta)_{i,j,k+1}-30\cdot(\theta)_{i,j,k}+16\cdot(\theta)_{i,j,k-1}-(\theta)_{i,j,k-2}}{12\Delta x_3^2};$$

where

$$(u_1\theta)_{i,j,k} = \left(\frac{-u_{1_{i+1,j,k}}+9u_{1_{i,j,k}}+9u_{1_{i-1,j,k}}-u_{1_{i-2,j,k}}}{16}\right)\cdot\left(\frac{-\theta_{i+1,j,k}+9\theta_{i,j,k}+9\theta_{i-1,j,k}-\theta_{i-2,j,k}}{16}\right);$$

$$(u_2\theta)_{i,j,k} = \left(\frac{-\theta_{i,j+2,k}+9\theta_{i,j+1,k}+9\theta_{i,j,k}-\theta_{i-1,j-1,k}}{16}\right)\cdot\left(\frac{-u_{2_{i+2,j,k}}+9u_{2_{i+1,j,k}}+9u_{2_{i,j,k}}-u_{2_{i-1,j,k}}}{16}\right);$$

$$(u_3\theta)_{i,j,k} = \left(\frac{-\theta_{i,j,k+2}+9\theta_{i,j,k+1}+9\theta_{i,j,k}-\theta_{i-1,j,k-1}}{16}\right)\cdot\left(\frac{-u_{3_{i+2,j,k}}+9u_{3_{i+1,j,k}}+9u_{3_{i,j,k}}-u_{3_{i-1,j,k}}}{16}\right);$$

Then the left side of equation (3) is denoted by $q_{i,j,k}$

$$q_{i,j,k} \equiv \theta^{n+1}_{i+1,j,k} - \theta^{n}_{i,j,k} \tag{4}$$

From equation (4) we find $\theta^{n+1}_{i,j,k}$

$$\theta^{n+1}_{i,j,k} = q_{i,j,k} + \theta^{n}_{i,j,k}$$

Replacing all $\theta^{n+1}_{i,j,k}$ from the equations (13), we obtain

$$q_{i,j,k} - \frac{\Delta t}{2}\cdot\frac{1}{\mathrm{Re}\,\mathrm{Pr}}\cdot\left(\frac{\partial^2 q}{\partial x_1^2}\right)_{i,j,k} - \frac{\Delta t}{2}\cdot\frac{1}{\mathrm{Re}\,\mathrm{Pr}}\cdot\left(\frac{\partial^2 q}{\partial x_2^2}\right)_{i,j,k} - \frac{\Delta t}{2}\cdot\frac{1}{\mathrm{Re}\,\mathrm{Pr}}\cdot\left(\frac{\partial^2 q}{\partial x_3^2}\right)_{i,j,k} = -\frac{3\Delta t}{2}[hr]^n_{i,j,k} + \frac{\Delta t}{2}[hr]^{n-1}_{i,j,k} + \Delta t[ar]^n_{i,j,k}$$

Equation (5) is converted to

$$\left[1-\frac{\Delta t}{2}\cdot\frac{1}{\mathrm{Re}\,\mathrm{Pr}}\cdot\frac{\partial^2}{\partial x_1^2}-\frac{\Delta t}{2}\cdot\frac{1}{\mathrm{Re}\,\mathrm{Pr}}\cdot\frac{\partial^2}{\partial x_2^2}-\frac{\Delta t}{2}\cdot\frac{1}{\mathrm{Re}\,\mathrm{Pr}}\cdot\frac{\partial^2}{\partial x_3^2}\right]q_{i,j,k} = d_{i,j,k} \tag{6}$$

where

$$d_{i,j,k} = -\frac{3\Delta t}{2}[hr]^n_{i,j,k} + \frac{\Delta t}{2}[hr]^{n-1}_{i,j,k} + \Delta t[ar]^n_{i,j,k}$$

Assuming that equation (6) has second-order accuracy in time, we can instead solve the following equation:

$$\left[1-\frac{\Delta t}{2}\cdot\frac{1}{\mathrm{Re}\,\mathrm{Pr}}\cdot\frac{\partial^2}{\partial x_1^2}\right]\left[1-\frac{\Delta t}{2}\cdot\frac{1}{\mathrm{Re}\,\mathrm{Pr}}\cdot\frac{\partial^2}{\partial x_2^2}\right]\left[1-\frac{\Delta t}{2}\cdot\frac{1}{\mathrm{Re}\,\mathrm{Pr}}\cdot\frac{\partial^2}{\partial x_3^2}\right]q^*_{i,j,k}=d_{i,j,k} \qquad (7)$$

We can show that equation (7) is an approximation $O\left(\Delta t^4\right)$ to equation (6).

Since the difference between $q^*_{i,j,k}$ and $q_{i,j,k}$ has a higher order, we return to the same notation and just use $q_{i,j,k}$.

To determine $q_{i+\frac{1}{2},j,k}$ the equation (7) is solved in 3 stages:

$$\left[1-\frac{\Delta t}{2}\cdot\frac{1}{\mathrm{Re}\,\mathrm{Pr}}\cdot\frac{\partial^2}{\partial x_1^2}\right]A_{i,j,k}=d_{i,j,k} \qquad (8)$$

$$\left[1-\frac{\Delta t}{2}\cdot\frac{1}{\mathrm{Re}\,\mathrm{Pr}}\cdot\frac{\partial^2}{\partial x_2^2}\right]B_{i,j,k}=A_{i,j,k} \qquad (9)$$

$$\left[1-\frac{\Delta t}{2}\cdot\frac{1}{\mathrm{Re}\,\mathrm{Pr}}\cdot\frac{\partial^2}{\partial x_3^2}\right]q_{i,j,k}=B_{i,j,k} \qquad (10)$$

At the first stage, the $A_{i,j,k}$ search is carried out in the direction of the x_1 coordinates:

$$\left[1-\frac{\Delta t}{2}\cdot\frac{1}{\mathrm{Re}\,\mathrm{Pr}}\cdot\frac{\partial^2}{\partial x_1^2}\right]A_{i,j,k}=d_{i,j,k}$$

$$A_{i,j,k}-\frac{\Delta t}{2}\cdot\frac{1}{\mathrm{Re}\,\mathrm{Pr}}\cdot\left(\frac{\partial^2 A}{\partial x_1^2}\right)^{n+1}_{i,j,k}=d_{i,j,k}$$

$$A_{i,j,k}-\frac{\Delta t}{2}\cdot\frac{1}{\mathrm{Re}\,\mathrm{Pr}}\cdot\frac{-A_{i+2,j,k}+16\cdot A_{i+1,j,k}-30\cdot A_{i,j,k}+16\cdot A_{i-1,j,k}-A_{i-2,j,k}}{12\Delta x_1^2}=d_{i,j,k}$$

$$s_1\cdot A_{i+2,j,k}-16\cdot s_1\cdot A_{i+1,j,k}+(1+30\cdot s_1)\cdot A_{i,j,k}-16\cdot s_1\cdot A_{i-1,j,k}+s_1\cdot A_{i-2,j,k}=d_{i,j,k} \qquad (11)$$

where $s_1=\dfrac{\Delta t}{24\cdot \mathrm{Re}\cdot \mathrm{Pr}\cdot \Delta x_1}$.

This equation (11) is solved by the method of the penta-diagonal matrix, which determines $A_{i,j,k}$.

The same procedure is repeated further for directions x_2 in the second stage, namely, $B_{i,j,k}$ is determined by solving equation (9), and the solution from the first stage, as the coefficient on the right, and the s_1 coefficient in the penta-diagonal matrix are replaced by $s_2=\dfrac{\Delta t}{24\cdot \mathrm{Re}\cdot \mathrm{Pr}\cdot \Delta x_2}$. Finally, in the third stage, $q_{i,j,k}$ is solved using a similar penta-diagonal system shown in equation (9).

Once we have determined the value $q_{i,j,k}$, we find $\theta^{n+1}_{i,j,k}$

$$\theta^{n+1}_{i,j,k}=q_{i,j,k}+\theta^{n}_{i,j,k}$$

The other components of temperature θ^{n+1}_{ijk} are solved in a similar way.

Simulation results

The results of modeling the imposition of a vertical magnetic field is obtained,where the lateral distribution of the temperature field is pronounced. The Grashof number is chosen $Gr=20000$, the Prandtl number Pr =0.09, the Stuart number has the following values: 1) N = 0; 2) N = 0.09; 3) N = 2.16, kinematic viscosity $\nu = 0.013$ diffusion coefficient equal to $D = 0.14$ For calculations, the mesh size is $34 \times 34 \times 34$. The size of the computational domain is equal to $L_1 = 2\pi,\ L_2 = 2\pi,\ L_3 = 2\pi$, which corresponds to the directions x_1, x_2 and x_3.

In this paper effect of Stuart number on isothermal surfaces for differentStuart numbers is shown at Figure 2. It is seen that isothermal surfaces changeconsiderably and gradient of the boundary layer declines with increasing of Stuartnumber, so heat transfer rate, which depends on the temperature gradient, graduallydecreases with increasing magnetic field, which indicates a weakening of the overallheat transfer effect. These trends were also discovered [17–19], who also studiednatural convection or Rayleigh Bernard convection under the influence of a magneticfield.

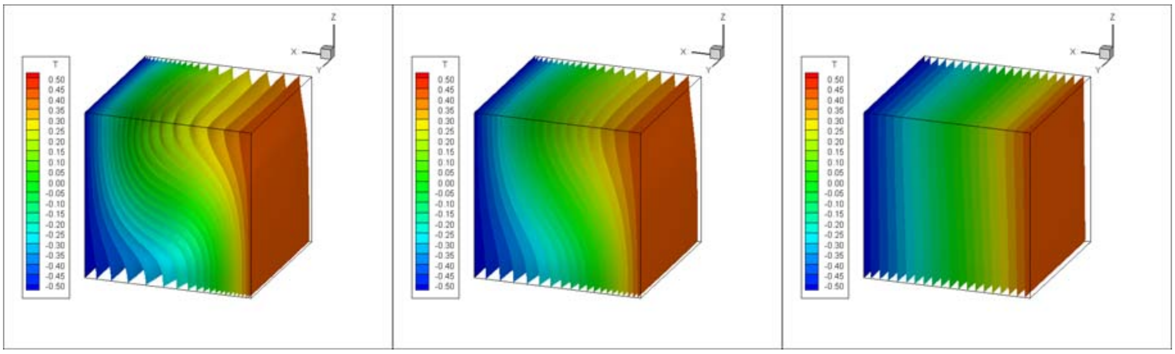

a) b) c)

Figure 2 – Isothermal surfaces for various Stuart coefficients
a) $N = 0$; b) $N = 0.09$;c) $N = 2.16$ at $Gr = 20000$

The contours of vertical velocity components, and temperature contours on the different planes of the enclosure are very important for understanding the trend offlow, so present results for the different locations of the cavity have been shown infigures 4 and 5. It is shown at figures 4-5 that, increasing Stuart number isothermallines become parallel to the walls and temperature gradient on the wall declines, therefore heat transfer rate decreases.

As for the physics of the influence of MHD on the structure of natural convection flows and heat transfer, this is due to the fact that in MHD flows the motion of vortex structures perpendicular to magnetic fields, i.e. horizontally oriented vortex cells, strongly suppressed due to the anisotropic effect of the magnetic field. This is recognized by the universal effect of magnetic fields, which is theoretically interpreted in [20]. Moreover, another important characteristic of the effect of the vertical magnetic field is that when the magnetic fields are stronger, the vortex structures will be more regular and will be shown parallel to each other.

Consequently, thermal convection caused by the movement of the vortex cells will decrease due to the amplification of magnetic fields.

Figures 6-7 show a longitudinal dimensionless temperature and velocity profile, respectively, for a different number of Stuart 1) $N = 0$; 2) $N = 0.09$ 3) $N = 2.16$. It is observed that the solution has a linear velocity dependence along the transverse direction.

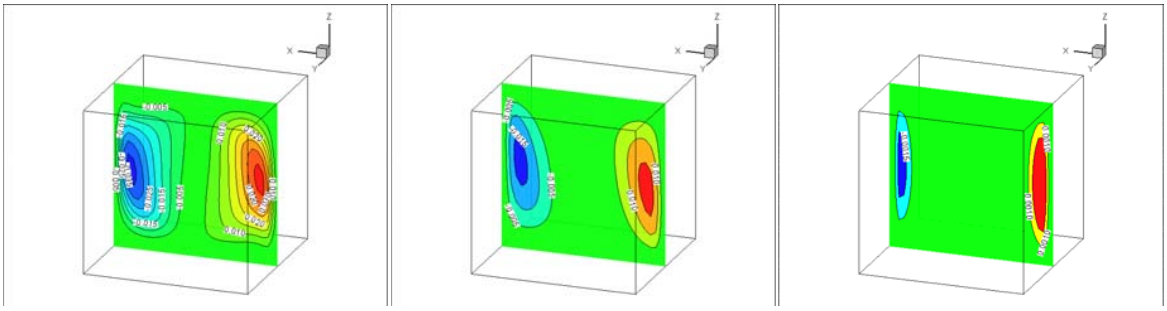

a) b) c)

Figure 3 – Contours of x_3 vertical velocity components on $x_2 = 0.5$ plane for different Stuart numbersa) $N = 0$; b) $N = 0.09$;c) $N = 2.16$ at $Gr = 20000$

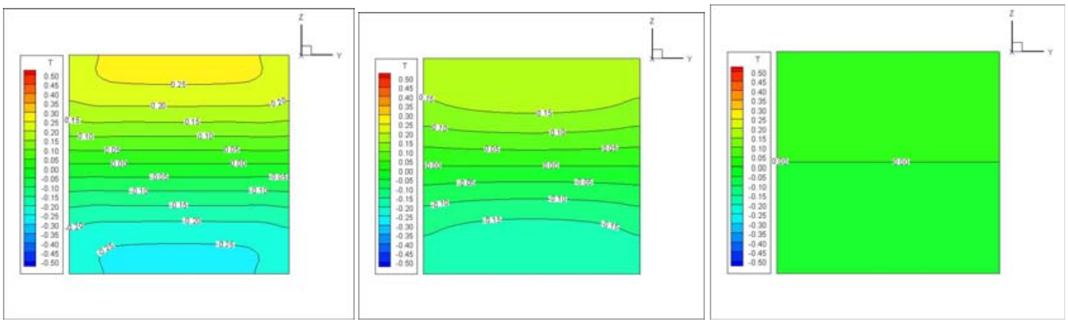

a) b) c)

Figure 4 – Temperature contours on $x_1 = 0.5$ plane for different Stuart numbersa) $N = 0$; b) $N = 0.09$;c) $N = 2.16$ at $Gr = 20000$

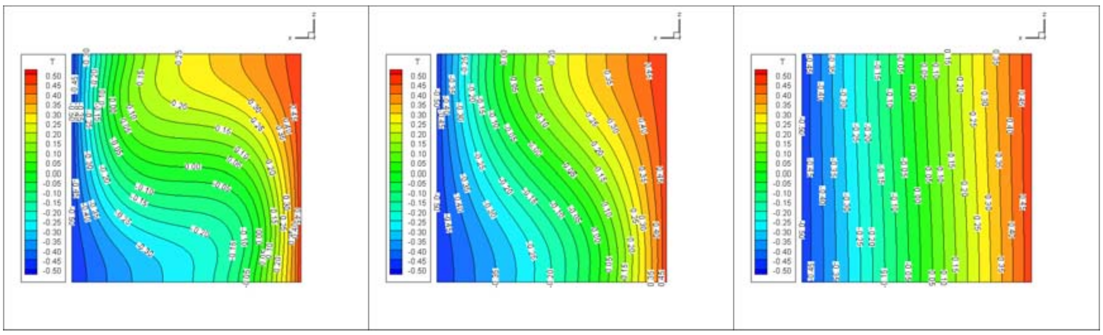

a) b) c)

Figure 5 – Temperature contours on $x_2 = 0.5$ plane for different Stuart numbersa) $N = 0$; b) $N = 0.09$;c) $N = 2.16$ at $Gr = 20000$

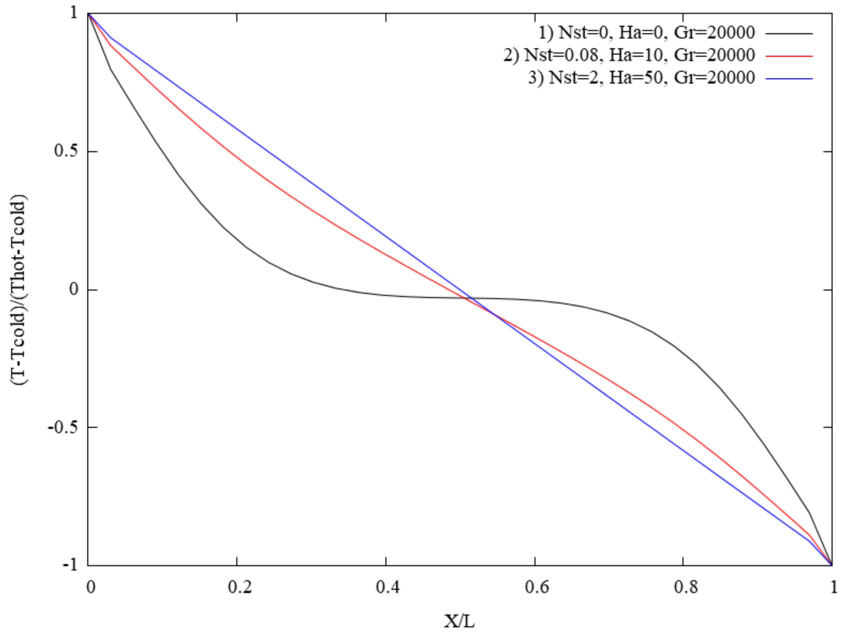

Figure 6 – Temperature profile for different values of the Stuart number
1) $N = 0$; 2) $N = 0.09$; 3) $N = 2.16$ at $Gr = 20000$.

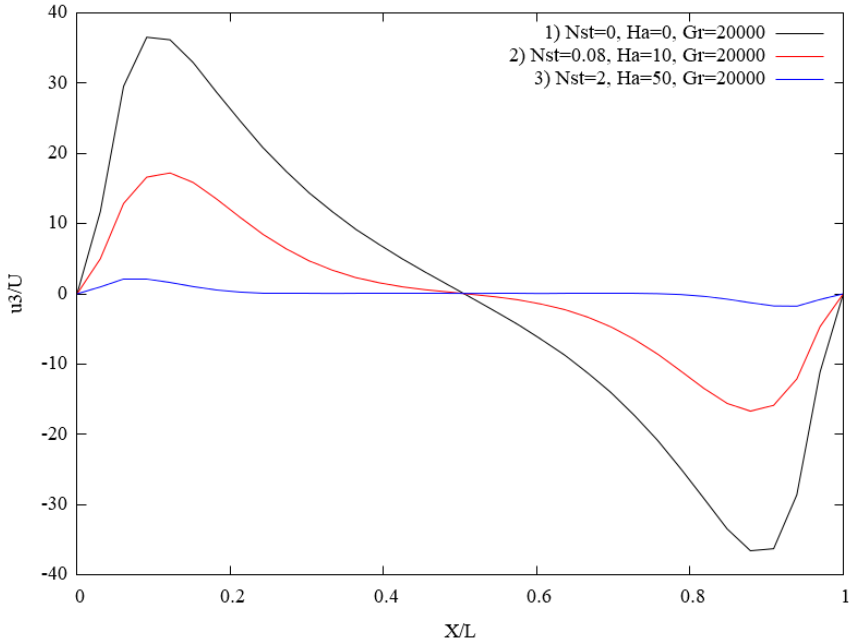

Figure 7 – Velocity profile for different Stuart values
1) $N = 0$; 2) $N = 0.09$; 3) $N = 2.16$ at $Gr = 20000$.

Conclusion

MHD natural convection in a three dimensional area at different Stuart numbers with temperature distribution on side wall has been considered by finite difference method with spectral method.

To solve the equations of flow motion and temperature, the finite difference method is used in combination with a pentadiagonal matrix, and solved by using the Adams-Bashfort scheme. The Poisson equation is solved by spectral method using the fast Fourier transform.

Thus, the following conclusions are drawn: isothermal surfaces change considerably and gradient of the boundary layer declines with increasing of Stuart number, so heat transfer rate, which depends on the temperature gradient, gradually decreases with increasing magnetic field, which indicates a weakening of the overall heat transfer effect. As for the physics of the influence of MHD on the structure of natural convection flows and heat transfer, this is due to the fact that in MHD flows the motion of vortex structures perpendicular to magnetic fields, i.e. horizontally oriented vortex cells, strongly suppressed due to the anisotropic effect of the magnetic field. The effect of the vertical magnetic field is that when the magnetic fields are stronger, the vortex structures will be more regular and will be shown parallel to each other. Consequently, thermal convection caused by the movement of the vortex cells will decrease due to the amplification of magnetic fields.

As result of modelling, isothermal surfaces, velocity and temerature contoures, also profiles for different Sturart numbers are obtained.

Acknowledgement

Theauthors were supported by the Ministry of Education and Science of the Republic of Kazakhstan Grant No. AP05133516.

References

1. Abouei Mehrizi, Farhadi, M., Hassanzadeh Afrouzi, H., Shayamehr, S.,Lotfizadeh, H.“Lattice Boltzmann simulation of natural convection flow around a horizontal cylinder located beneath an insulation plate.”*J. Theoret. Appl. Mech.* 51(2013): 729–739.

2. Sajjadi, H., Hosseinizadeh, S.F., Gorji, M., Kefayati, Gh.R.“Numerical analysis of turbulent natural convection flow in a square cavity using Large-Eddy Simulation in Lattice Boltzmann.”*Iran.J. Sci. Technol., Trans. Mech. Eng.* 35(2011):133–142.

3. Kefayati, G.H.R., Gorji, M., Sajjadi, H., Ganji, D.D.“Lattice Boltzmann simulation of MHD mixed convection in a lid-driven square cavity with linearly heated wall.”*Scientia Iranica, Trans. B – Mech. Eng.* 19(2012):1053–1065.

4. Hamid Reza Ashorynejad, Kurosh Sedighi, Mousa Farhadi, Ehsan Fattahi."Simulating magnetohydrodynamic natural convection ow in a horizontal cylindrical annulus using the lattice Boltzmann method".*Heat Transf. Asian Res*. 41 (2012): 468–483.

5. Ashorynejad, H.R., Abdulmajeed, A., Mohsen Sheikholeslami, M.“Magnetic field effects on natural convection flow of a nanofluid in a horizontal cylindrical annulus using Lattice Boltzmann method.”*Int. J. Therm. Sci.* 64(2013):240–250.

6. Xu, B.Q. Li, D.E. Stock.“An experimental study of thermally induced convection of molten gallium in magnetic fields.”*Int. J. Heat Mass Transf.* 49(2006): 2009–2019.

7. Grosan, T., Revnic, C., Pop, I., Ingham, D.B. “Magnetic field and internal heat generation effects on the free convection in a rectangular cavity filled with a porous medium.”*Int. J. Heat Mass Transfer*. 52(2009):5691–5700.

8. Sivasankaran, S., Malleswaran, A., Lee, J., Sundar, P.“Hydro-magnetic combined convection in a lid-driven cavity with sinusoidal boundary conditions on both sidewalls.” *Int. J. Heat Mass Transf.* 54(2011):512–525.

9. Oztop, H.F., Al-Salem, K., Pop, I.“MHD mixed convection in a lid-driven cavity with corner heater.” *Int. J. Heat Mass Transf.* 54(2011):3494–3504.

10. Saijadi, H., Amri Delouei, A., Sheikholeslami, M., Atashafrooz., M., Succi, S. “Simulation of the dimensional MHD natural convection using double MRT Lattice Boltzmann method.*” J.Physica A,* 515(2019): 474-496.

11. Sheikholeslami, M.“Lattice Boltzmann method simulation for MHD non-Darcy nanofluid free convection.” *J. Physica B*, 516(2017): 55–71.

12. Bhuvaneswari, M., Sivasankaran, S., Kim, Y.J.“Magneto convection in a square enclosure with sinusoidal temperature distributions on both side walls.” *Numer. Heat Transf. Part A,* 59(2011):167–184.

13. Zhang, T., Che, D.“Double MRT thermal lattice Boltzmann simulation for MHD natural convection of nanofluids in an inclined cavity with four square heat sources” *Int. J. Heat Mass Transf.* 94(2016): 87–100.

14. Sajjadi, H., Atashafrooz, M. “Double MRT Lattice Boltzmann simulation of 3-D MHD natural convection in a cubic cavity with sinusoidal temperature distribution utilizing nanofluid.” *Int. J. of Heat and Mass Trans.,* 126(2018): 489-503. https://doi.org/10.1016/j.ijheatmasstransfer.2018.05.064

15. Abdibekova, A., Zhakebayev, D., Abdigaliyeva, A., Zhubat, K. “Modeling of turbulence energy decay based on hybrid methods.”*J. Engineering Computations*, 35(2018):1965-1977.

16. Zhakebayev, D., Zhumagulov, B., Abdibekova, A. “The decay of MHD turbulence depending on the conductive properties of the environment.”*J.Magnetohydrosynamics* 50(2014):121-138.

17. Burr, U., Müller, U. “Rayleigh–Bénard convection in liquid metal layers under the influence of a horizontal magnetic field.”*J. Fluid Mech.*453 (2002):345–369.

18. Barleon, L., Burr, U., Stieglitz, R., Frank, M. “Heat transfer of a MHD flow in a rectangular duct.” *in: Proc. of the 3rd Internat. Conf. on Transfer Phenomena in Magnetohydrodynamic and Electroconducting Flows*(1997).

19. Barleon, L., Jochmann, P., Mack, K., Burr, U., Stieglitz, R. “Experimental investigations on the magneto-convective flow in a vertical gap” *Proceedings of 4th PAMIR Conference* (2000):309–314.

20. Davidson P. “Magnetic damping of jets and vortices.”*J. Fluid Mech.* 299 (1995):153–186.

IRSTI 27.29.23 https://doi.org/10.26577/ijmph-2019-i2-7

[1,2]M.K. Dauylbayev, [1]Zh. Artykbayeva, [1,2]K. Konysbaeva

[1]Al-Farabi Kazakh National University, Kazakhstan, Almaty
[2]Institute of Mathematics and Mathematical Modeling, Kazakhstan, Almaty
e-mail: Murathan.Daulbaev@kaznu.kz

Asymptotic behavior of the solution of a singularly perturbed three-point boundary value problem with boundary jumps

Abstract. In this paper, the three-point boundary value problem is considered for the third-order linear differential equation with a small parameter with at the two highest derivatives when the roots of additional characteristic equation have negative signs. The aim of this paper is to bring asymptotic estimation of the solution of a singularly perturbed three-point boundary value problem with boundary jumps and the asymptotic convergence of the solution of a singularly perturbed initial value problem to the solution of an unperturbed initial value problem. In this paper the fundamental system of solutions, initial functions of a singularly perturbed homogeneous di erential equation are constructed and their asymptotic estimates are obtained. An asymptotic behavior of the solution of the three-point boundary value problem at the points of initial jumps is established. A degenerate boundary-value problem is constructed. It is proved that the solution of the original singularly perturbed boundary value problem tends to the solution of the degenerate boundary value problem.

Key words: singular perturbation, small parameter, asymptotic, initial jumps,asymptotic estimate, boundary value problem, boundary functions, fundamental solutions.

Introduction

Equations containing a small parameter with the highest derivatives are called singularly perturbed equations. Such equations are of great applied importance. They act as mathematical models in the study of various processes in physics, chemistry, biology and technology.

The study of initial problems for singularly perturbed equations with unbounded initial data as the small parameter tends to zero, which are called Cauchy problems with an initial jump, first began with the work of M. I. Vishik, L. A. Lyusternik [1] and K. A. Kasymov [2]. A feature of such problems is that the solution of a singularly perturbed problem tends to the solution of the degenerate equation with modified initial conditions when the small parameter tends to zero. In this case, we say that there is a phenomenon of an initial jump in the solution. K. A. Kasymov and his students in [3-11] continued research on initial and two-point boundary value problems with initial jumps. Three-point boundary value problems for ordinary differential and integro-differential equations with a small parameter at only the highest derivative, which have the phenomenon of initial jumps, were considered in [12,13].

The present work is devoted to the study of the three-point boundary value problem for linear ordinary differential equations of the third order with a small parameter for two highest derivatives, which has the phenomenon of boundary jumps. The scientific novelty of this problem is that the fast variable of the solution increases unlimitedly not only at the so-called starting point, but also at the other end of the considered segment when the small parameter tends to zero.

Statement of the problem and preliminaries

We consider third-order linear differential equation with a small parameter at the two highest derivatives

$$L_\varepsilon y \equiv \varepsilon^2 y''' + \varepsilon A_0(t) y'' + A_1(t) y' + A_2(t) y = F(t) \tag{1}$$

with the boundary conditions

$$\begin{aligned} &h_1 y(t,\varepsilon) \equiv y(0,\varepsilon) = \alpha, \\ &h_2 y(t,\varepsilon) \equiv y(t_0,\varepsilon) = \beta, \\ &h_3 y(t,\varepsilon) \equiv y(1,\varepsilon) = \gamma, \end{aligned} \tag{2}$$

where $\varepsilon > 0 -$ small parametr, $0 < t_0 < 1$, and $\alpha, \beta, \gamma -$ known constants.

Let us assume that:

I. $A_i(t) \in C^2[0,1], i = \overline{0,2},\ F(t) \in C[0,1]$

II. The roots of the equation

$$\mu^2 + A_0(t)\mu + A_1(t) = 0$$

satisfy the conditions

$$\mu_1(t) < -\gamma_1 < 0, \quad \mu_2(t) > \gamma_2 > 0.$$

We consider the followinghomogeneous equation associatedwith (1):

$$\begin{aligned} L_\varepsilon y \equiv \varepsilon^2 y''' + \varepsilon A_0(t) y'' + \\ + A_1(t) y' + A_2(t) y = 0 \end{aligned} \tag{3}$$

Lemma1. If the conditions I, II are satisfied, then the fundamental set of solutionsof the equation (3) has the following asymptotic representation as $\varepsilon \to 0$ [6]:

$$y_1^{(i)}(t,\varepsilon) = \frac{1}{\varepsilon^i} e^{\frac{1}{\varepsilon}\int_0^t \mu_1(x)dx} (\mu_1^i(t) y_{10}(t) + O(\varepsilon)),$$
$$i = \overline{0,2},$$
$$y_2^{(i)}(t,\varepsilon) = \frac{1}{\varepsilon^i} e^{-\frac{1}{\varepsilon}\int_t^1 \mu_2(x)dx} (\mu_2^i(t) y_{20}(t) + O(\varepsilon)),$$
$$i = \overline{0,2}, \tag{4}$$

$$y_3^{(i)}(t,\varepsilon) = y_{30}^{(i)}(t) + O(\varepsilon),\ i = \overline{0,2},$$

where $y_3(t) = \exp\left(-\int_0^t \frac{A_2(x)}{A_1(x)} dx\right)$, and the functions $y_{i0}(t), i = 1,2$ are solutions of the problems

$$p_i(t) y'_{i0}(t) + q_i(t) y_{i0}(t) = 0,\ y_{i0}(0) = 1, \quad i = 1,2,$$

where

$$\begin{aligned} &p_i(t) = (A_0(t) + 2\mu_i(t))\mu_i(t); \\ &q_i(t) = A_2(t) + A_0(t)\mu_i'(t) + 3\mu_i(t)\mu_i'(t). \end{aligned}$$

We construct auxiliary functions:

$$\begin{aligned} K_0(t,s,\varepsilon) = \frac{P_0(t,s,\varepsilon)}{W(s,\varepsilon)}; \\ K_1(t,s,\varepsilon) = \frac{P_1(t,s,\varepsilon)}{W(s,\varepsilon)}; \end{aligned} \tag{5}$$

where $W(s,\varepsilon)$ is the Wronskianof the fundamental set of solutions of the equation (3), and $P_0(t,s,\varepsilon)$, $P_1(t,s,\varepsilon)$ are determinantsobtained from the Wronskian $W(s,\varepsilon)$ by replacing its third rows with the corresponding rows $y_1(t,\varepsilon), 0, y_3(t,\varepsilon)$ and $0, y_2(t,\varepsilon), 0$.

In view of(4),for the functions $K_0(t,s,\varepsilon), K_1(t,s,\varepsilon)$ the following asymptotic representations holdas $\varepsilon \to 0$:

$$K_0^{(j)}(t,s,\varepsilon) = \varepsilon^2 \left(\frac{y_{30}^{(j)}(t)}{y_{30}(s)\mu_1(s)\mu_2(s)} - \frac{\mu_1^j(t) y_{10}(t)}{\varepsilon^j y_{10}(s)\mu_1(s)(\mu_2(s) - \mu_1(s))} e^{\frac{1}{\varepsilon}\int_s^t \mu_1(x)dx} + O(\varepsilon) \right), \tag{6}$$
$$s \le t,$$
$$K_1^{(j)}(t,s,\varepsilon) = \varepsilon^2 \left(\frac{\mu_2^j(t) y_{20}(t)}{\varepsilon^j y_{20}(s)\mu_2(s)(\mu_2(s) - \mu_1(s))} e^{-\frac{1}{\varepsilon}\int_t^s \mu_2(x)dx} + O(\varepsilon) \right), t \le s, \quad j = \overline{0,2}.$$

From (6) for the functions $K_0(t,s,\varepsilon), K_1(t,s,\varepsilon)$ we obtainasymptotic estimates as $\varepsilon \to 0$:

$$\left|K_0^{(j)}(t,s,\varepsilon)\right| \le C\varepsilon^2 + \frac{C}{\varepsilon^{j-2}} e^{-\gamma_1 \frac{t-s}{\varepsilon}},$$
$$\left|K_1^{(j)}(t,s,\varepsilon)\right| \le \frac{C}{\varepsilon^{j-2}} e^{\gamma_2 \frac{s-t}{\varepsilon}}, \quad j=\overline{0,2}, \tag{7}$$

where $C>0, \gamma_i>0, i=1,2$ areconstants independent of ε.

Main results

Let the functions $\Phi_i(t,\varepsilon), i=1,2,3$ be a solutions of the problem

$$L_\varepsilon \Phi_i(t,\varepsilon)=0,\ h_k\Phi_i(t,\varepsilon)=\delta_{ki},\ i,k=1,2,3.$$

We call these a boundary functions and determine by the formula

$$\Phi_i(t,\varepsilon)=\frac{I_i(t,\varepsilon)}{I(\varepsilon)},\ i=1,2,3, \tag{8}$$

where

$$I(\varepsilon)=\begin{vmatrix} h_1y_1(t,\varepsilon) & h_1y_2(t,\varepsilon) & h_1y_3(t,\varepsilon) \\ h_2y_1(t,\varepsilon) & h_2y_2(t,\varepsilon) & h_2y_3(t,\varepsilon) \\ h_3y_1(t,\varepsilon) & h_3y_2(t,\varepsilon) & h_3y_3(t,\varepsilon) \end{vmatrix},$$

and $I_i(t,\varepsilon)$ are determinantsobtained from the $I(\varepsilon)$ by replacing its i-th rows with the row $y_1(t,\varepsilon), y_2(t,\varepsilon), y_3(t,\varepsilon)$.

In view of (4), for the boundary functions $\Phi_i(t,\varepsilon), i=1,2,3$ we get asymptotic representations as $\varepsilon \to 0$:

$$\Phi_1^{(j)}(t,\varepsilon)=\frac{1}{\varepsilon^j} e^{\frac{1}{\varepsilon}\int_0^t \mu_1(x)dx}\left(\mu_1^j(t)y_{10}(t)+O(\varepsilon)\right),$$

$$\Phi_2^{(j)}(t,\varepsilon)=\frac{y_{30}^{(j)}(t)}{y_{30}(t_0)}-\frac{\mu_1^j(t)y_{10}(t)}{\varepsilon^j y_{30}(t_0)} e^{\frac{1}{\varepsilon}\int_0^t \mu_1(x)dx}-$$
$$-\frac{\mu_2^j(t)y_{20}(t)y_{30}(1)}{\varepsilon^j y_{20}(1)y_{30}(t_0)} e^{-\frac{1}{\varepsilon}\int_t^1 \mu_2(x)dx}+ \tag{9}$$
$$+O\left(\varepsilon+\frac{1}{\varepsilon^{j-1}} e^{\frac{1}{\varepsilon}\int_0^t \mu_1(x)dx}+\frac{1}{\varepsilon^{j-1}} e^{-\frac{1}{\varepsilon}\int_t^1 \mu_1(x)dx}\right),$$

$$\Phi_3^{(j)}(t,\varepsilon)=\frac{1}{\varepsilon^j} e^{-\frac{1}{\varepsilon}\int_t^1 \mu_2(x)dx}\left(\frac{\mu_2^j(t)y_{20}(t)}{y_{20}(1)}+O(\varepsilon)\right).$$

From (9)for the boundary functions $\Phi_i(t,\varepsilon), i=1,2,3$, we get the following asymptotic estimates as $\varepsilon \to 0$:

$$\left|\Phi_1^{(j)}(t,\varepsilon)\right| \le \frac{C}{\varepsilon^j} e^{-\gamma_1\frac{t}{\varepsilon}}, \quad \left|\Phi_3^{(j)}(t,\varepsilon)\right| \le \frac{C}{\varepsilon^j} e^{-\gamma_2\frac{1-t}{\varepsilon}},$$

$$\left|\Phi_2^{(j)}(t,\varepsilon)\right| \le C+\frac{C}{\varepsilon^j} e^{-\gamma_1\frac{t}{\varepsilon}}+\frac{C}{\varepsilon^j} e^{-\gamma_2\frac{1-t}{\varepsilon}}, \tag{10}$$
$$j=0,1,2,$$

where $C>0, \gamma_i>0, i=1,2$ areconstants independent of ε.

We seek a solution of the boundary value problem (1), (2) in the form

$$y(t,\varepsilon)=C_1\Phi_1(t,\varepsilon)+C_2\Phi_2(t,\varepsilon)+C_3\Phi_3(t,\varepsilon)+$$
$$+\frac{1}{\varepsilon^2}\int_0^t K_0(t,s,\varepsilon)F(s)ds-\frac{1}{\varepsilon^2}\int_t^1 K_1(t,s,\varepsilon)F(s)ds$$

where $\Phi_i(t,\varepsilon), i=1,2,3-$boundary functions, and $K_0(t,s,\varepsilon),\ K_1(t,s,\varepsilon)-$auxiliary functions given by the formula (5). Now, by using condition (2) we will find the constants $C_i, i=1,2,3$. Then the following theorem is valid.

Theorem 1. Under conditions I, II, the solution of the problem (1), (2) can be represented in the form

$$y^{(j)}(t,\varepsilon)=\left(\alpha+\frac{1}{\varepsilon^2}\int_0^1 K_1(0,s,\varepsilon)F(s)ds\right)\Phi_1^{(j)}(t,\varepsilon)+$$
$$+\left(\beta+\frac{1}{\varepsilon^2}\int_0^{t_0} K_0(t_0,s,\varepsilon)F(s)ds-\frac{1}{\varepsilon^2}\int_{t_0}^1 K_1(t_0,s,\varepsilon)F(s)ds\right)\Phi_2^{(j)}(t,\varepsilon)+ \quad (11)$$
$$+\left(\gamma-\frac{1}{\varepsilon^2}\int_0^1 K_0(1,s,\varepsilon)F(s)ds\right)\Phi_3^{(j)}(t,\varepsilon)+\frac{1}{\varepsilon^2}\int_0^t K_0^{(j)}(t,s,\varepsilon)F(s)ds-\frac{1}{\varepsilon^2}\int_t^1 K_1^{(j)}(t,s,\varepsilon)F(s)ds.$$

Theorem 2. Under conditions I, II, for the solution of the problem (1), (2) the following asymptotic estimates hold as $\varepsilon\to 0$:

$$\left|y^{(j)}(t,\varepsilon)\right|\le C(|\beta|+\max_{0\le t\le 1}|F(t)|)+$$
$$+\frac{C}{\varepsilon^j}(|\alpha|+|\beta|+\max_{0\le t\le 1}|F(t)|)e^{-\gamma_1\frac{t}{\varepsilon}}+$$
$$+\frac{C}{\varepsilon^j}(|\beta|+|\gamma|+\max_{0\le t\le 1}|F(t)|)e^{-\gamma_1\frac{1-t}{\varepsilon}}+ \quad (12)$$
$$+\frac{C}{\varepsilon^{j-1}}\left|\frac{\mu_2^{j-2}(t)-\mu_1^{j-2}(t)}{\mu_2(t)-\mu_1(t)}\right|\max_{0\le t\le 1}|F(t),\ j=\overline{0,2},$$

where $C>0,\gamma_i>0,i=1,2$ areconstants independentof ε.

The proof of the Theorem 1 and Theorem 2 follow from (11), and in view of the estimates (7), (10).

By the Theorem 2, one can obtain

$$y'(0,\varepsilon)=O\left(\frac{1}{\varepsilon}\right),\ y'(1,\varepsilon)=O\left(\frac{1}{\varepsilon}\right),\ \varepsilon\to 0.$$

It means that, the solution of the boundary value problem (1), (2) has the phenomena of initial jumps of zero order at the points $t=0$ and $t=1$.

We consider the following degenerate problem

$$L_0\overline{y}\equiv A_1(t)\overline{y}'+A_2(t)\overline{y}=F(t),$$
$$\overline{y}(t_0)=\beta. \quad (13)$$

Let the initial jump condition be satisfied

III. $\Delta_0\equiv\alpha-\overline{y}(0)\ne 0,\quad \Delta_1\equiv\gamma-\overline{y}(1)\ne 0.$

Then following theorem holds true.

Theorem 3. Let the conditions I-III are satisfied, then for the difference between the solutions $y(t,\varepsilon)$ and $\overline{y}(t)$ of the singularly perturbed boundary value problem (1), (2) and the degenerate problem (13) following asymptotic estimate holds as $\varepsilon\to 0$:

$$\left|y^{(j)}(t,\varepsilon)-\overline{y}^{(j)}(t)\right|\le$$
$$\le\frac{C}{\varepsilon^j}\left(|\alpha-\overline{y}(0)|e^{-\gamma_1\frac{t}{\varepsilon}}+|\gamma-\overline{y}(1)|e^{-\gamma_2\frac{1-t}{\varepsilon}}\right)+ \quad (14)$$
$$+C\varepsilon,\ j=0,1,$$

where $C>0,\gamma_i>0,i=1,2$ areconstants independentof ε.

Proof. We denote by $u(t\varepsilon)=y(t,\varepsilon)-y(t)$. Then in view of (13), we get the singularly perturbed problem for the function $u(t,\varepsilon)$:

$$\varepsilon^2u'''+\varepsilon A_0(t)u''+A_1(t)u'+$$
$$+A_2(t)u=-\varepsilon^2\overline{y}'''-\varepsilon A_0(t)y'',$$

$$u(0,\varepsilon)=\alpha-\overline{y}(0),$$
$$u(t_0,\varepsilon)=0, \quad (15)$$
$$u(1,\varepsilon)=\gamma-\overline{y}(1).$$

The problems (15) and (1), (2) are the same type. Therefore, by using the estimates (12) for the singularly perturbed boundary value problem (15), we obtain estimates (14).

The estimates (14) imply the following limit transitions

$$\lim_{\varepsilon \to 0} y(t,\varepsilon) = y(t),\ 0 < t < 1,$$

$$\lim_{\varepsilon \to 0} y'(t,\varepsilon) = y'(t),\ 0 < t < 1,$$

where $\bar{y}(t)$ is the solution of the degenerate problem (13).

The values of the initial jumps are determined from the following equalities:

$$\Delta_0 \equiv y(0,\varepsilon) - \bar{y}(0) =$$

$$+\alpha - \beta e^{\int_0^{t_0} \frac{A_2(x)}{A_1(x)}dx} + \int_0^{t_0} \frac{F(s)}{A_1(s)} e^{\int_0^{s} \frac{A_2(s)}{A_1(s)}dx} ds,$$

$$\Delta_1 \equiv y(1,\varepsilon) - \bar{y}(1) =$$

$$= \gamma - \beta e^{-\int_{t_0}^{1} \frac{A_2(x)}{A_1(x)}dx} - \int_{t_0}^{1} \frac{F(s)}{A_1(s)} e^{-\int_{s}^{1} \frac{A_2(x)}{A_1(x)}dx} ds.$$

Conclusion

In this paper, we consider a three-point boundary value problem for a third-order linear differential equation with a small parameter at two highest derivatives when the roots of the "additional characteristic equation" have negative signs. An analytical formula and asymptotic estimates of the solution are obtained. A degenerate boundary value problem is defined.It is shown that the solution of the original singularly perturbed boundary value problem tends to the solution of the degenerate boundary value problem. It is established that the solution of this boundary value problem has the phenomenon of boundary jumps. This means that the points of the initial jump are not only the left, but also the right point of the segment. Moreover, at both boundary points, the orders of the initial jumps coincide.

Acknowledgement

The authors were supported in parts by the MESRK grant AP05132587 "Boundary value problems for singularly perturbed differential equations with a continuous and piecewise constant argument" (2018-2020) of the Committee of Science, Ministry of Education and Science of the Republic of Kazakhstan.

References

1. Vishik M.I., Lyusternik L.A. O nachal'nom skachke dlya nelinejnyh differencial'nyh uravnenij, soderzhashchih malyj parametr // Doklady AN SSSR. - 1960. - 132, № 6. - S. 1242–1245.

2. Kasymov K.A. Ob asimptotike resheniya zadachi Koshi s bol'shimi nachal'nymi usloviyami dlya nelinejnyh obyknovennyh differencial'nyh uravnenij, soderzhashchih malyj parametr // Uspekhi mat. nauk. - 1962. - 17, № 5. - S. 187–188.

3. Abil'daev E.A., Kasymov K.A. Asimptoticheskie ocenki reshenij singulyarno vozmushchennyh kraevyh zadach s nachal'nymi skachkami dlya linejnyh differencial'nyh uravnenij // Differencial'nye uravneniya - 1992. - 28, № 10. - S. 1659–1668.

4. Kasymov K.A., Dauylbaev M.K. Ob ocenke reshenij zadachi Koshi s nachal'nym skachkom lyubogo poryadka dlya linejnyh singulyarno vozmushchennyh integro-differencial'nyh uravnenij // Differencial'nye uravneniya. Moskva – Minsk. - 1999. - T. 35, - № 6. - S. 822 – 830.

5. M. K. Dauylbaev The asymptotic behavior of solutions to singularly perturbed nonlinear integro-differential equations // Siberian Mathematical Journal, Vol. 41, No. 1, 2000. P. 49-60.

6. Kasymov K.A., ZHakipbekova D. A., Nurgabyl D.N. Predstavlenie resheniya kraevoj zadachi dlya linejnogo differencial'nogo uravneniya s malym parametrom pri starshih proizvodnyh // Vestnik Kazahskogo nacional'nogo universiteta im. al'-Farabi, seriya mat., mekh., inf. - 2001. №3. -S. 73-78.

7. Kassymov K.A., Nurgabyl D.N. Asymptotic Behavior of Solutions of Linear Singularly Perturbed General Separated Boundary-Value Problems with Initial Jump // Ukrainian Mathematical Journal. Vol. 55, No. 11, 2003. pp. 1777-1792.

8. Kassymov K.A., Nurgabyl D.N. Asymptotic Estimates of Solution of a Singularly Perturbed Boundary Value Problem with an Initial Jump for Linear Differential Equations // Differential Equations,Vol.40, No.5, 2004, pp. 641-651.

9. Kasymov K.A., Nurgabyl D.N., Uaisov A.B. Asymptotic estimates for the solutions of boundary-value problems with initial jump for linear differential equations with small parameter in the coefficients of derivatives // Ukrainian

Mathematical Journal. Vol. 65, No 5, 2013, pp 694-708

10. Dauylbayev M.K. and Atakhan N.The initial jumps of solutions and integralterms in singular BVP of linear higher orderintegro-differential equations // Miskolc Math. Notes, 2015 г. Vol. 16, № 2, P. 747-761.

11. Dauylbaev M.K., Mirzakulova A.E. Boundary-Value Problems with Initial Jumps for Singularly Perturbed Integrodifferential Equations // Journal of Mathematical Sciences, April 2017, Vol. 222, Issue 3, P. 214-225.

12. Kasymov K.A., Atanbaev N.S. Asimptoticheskie ocenki reshenij singulyarno vozmushchennoj trekhtochechnoj kraevoj zadachi dlya linejnyh differencial'nyh uravnenij tret'ego poryadka // Vestnik NAN RK. – 1999. -№3. –S. 66-71.

13. Dauylbaev M.K., Azanova A.N. Ocenka reshenij trekhtochechnoj kraevoj zadachi dlya singulyarno vozmushchennyh integro-differencial'nyh uravnenij. // Vestnik Kyrgyzskogo nacional'nogo universitata im. ZH. Balasagyn. 2011. S. 47-50.

IRSTI 29.27.49 https://doi.org/10.26577/ijmph-2019-i2-8

[1,*]A.R. Abdirakhmanov, [1]Y.A. Ussenov, [1]M.K. Dosbolayev, [1]S.K. Kodanova, [1]T.S. Ramazanov

[1] Institute of Experimental and Theoretical Physics,
Al-Farabi Kazakh National University, Kazakhstan, Almaty,
*email: abdirakhmanov@physics.kz

Langmuir probe and optical diagnostics of stratified glow discharge in a magnetic field

Abstract. The article presents the preliminary results of an experimental study of the characteristics of a DC stratified glow discharge plasma in an external magnetic field. Single Langmuir probe and emissive spectrometer are used as diagnostic tools for the estimation of various plasma parameters. The main plasma parameters, such as electron temperature, density and floating potential were determined from the voltage- current (VI) characteristics of the probe in the stratified glow discharge plasmas for different magnetic field values. Increasing the value of the magnetic field leads to an increase in the concentration of plasma particles and a decrease in the temperature of electrons. Also by the optical emission spectroscopic (OES) method it was found that the intensity of spectral lines of the stratified glow discharge increases with an increase value of magnetic field. A simple interpretation was made to explain our results according to the work of Bickerton&Engel [21].
Key words: glow discharge, plasma, magnetic field, Langmuir probe, spectrometer.

Introduction

At the moment, it is difficult to overestimate the importance of studying plasma physics. A huge number of scientific groups around the world are engaged in research of plasma processes. In the future, these studiescan be widely used in industry in the form of technical applicationslike light sources, modern plasma nanotechnology; sensitive ion cleaning of the surface of materials and etc. [1-6].

Low-temperature plasma is the subject of numerous studies. Interest in it caused by the possibility of wide application in gas lasers, plasma chemical reactors, energy converters, voltage switches, etc.Successful application of plasma technology is impossible without a deep understanding and quantitative description of the processes occurring in them. The construction of physical models fully reflecting the behavior of plasma systems is based on the knowledge of the corresponding plasma parameters. In this regard, the development of plasma diagnostic methods is of great interest and practically important [7-10].

Of particular interest is the study of plasma behavior in a magnetic field. Since plasma is an ionized gas consisting of charged particles, the presence of a magnetic field has a significant effect on all processes occurring in plasma[11-16].

Important plasma parameters are density of charged particles, electron and ion temperature, and plasma potential. Also, the discharge parameters include its power and magnetic configuration, the pressure of the working gas. To study the dynamics of dust particles depending on all the above parameters, it is necessary to be able to determine them.

The Langmuir probe diagnostic method is a common method for determining the density of charged particles, as well as the energy of electrons in plasma. An electric probe is an electrode of small size placed in plasma and used to determine its local characteristics.Usually,VI characteristic (voltage-current relationship) of the probe must bemeasured. A probe immersed in plasma is surrounded by a double electrical layer (volume charge layer or "sheath") and, in fact, the probe's VAC is the VAC of the layers. The reference electrode can be either one of the electrodes of the gas-discharge system or a metal element of the gas-discharge chamber, or a specially introduced reference probe.The main task of the theory of interpretation is to establish a connection between the probe current and plasma parameters. A rigorous solution to this problem in general is very difficult and has not yet been fully achieved. For the correct interpretation of the results of probe measurements, it is necessary to construct theories corresponding to the given conditions of application of the method[17-26].

In this work, probe and optical diagnostics of a glow discharge in a magnetic field was carried out.

Description of Experimental setup& Results

The experiment was conducted in the the laboratory of Dusty plasma and Plasma technology at the IETP. The general scheme of the experimental setup is shown in Figure 1. The gas pressure was 0.23Torr. The operating discharge current was 1.3 mA. This condition was chosen to determine the parameters of the glow discharge plasma, which manifested an interesting behavior of dust structures and not observed in other similar experimental works [27]. The magnetic field is created by a Helmholtz coil. The magnetic field strength depends on the current flowing in the solenoid. When the current is set to the 1.9 A the maximum magnetic field in the center of the solenoid is equal to B=28 mT. Probe and optical diagnostics were performed in the center of the solenoid (see Figure 1).

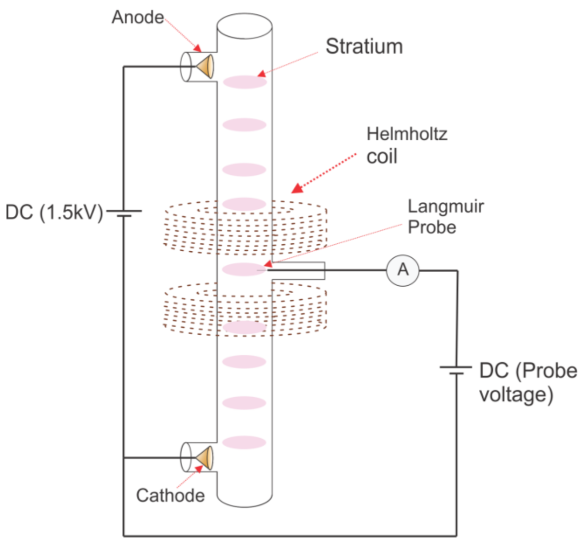

Figure 1– Experimental setup for probe diagnostics

The probe is made of tungstenire with a diameter of 100 microns. To determine the electron temperature and concentration, as well as other plasma parameters, the VI characteristic of the probe was obtained at different values of the magnetic field (Figure 2).Detailed information of the probe and the method for determining the plasma parameters are described in [28].

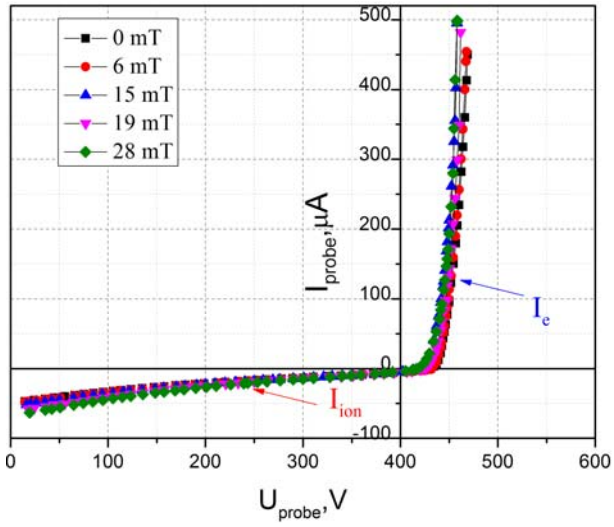

Figure 2– VI characteristic of the probe under different magnetic field conditions.(Experiment parameters: Argon, P=0.23torr, I=1.3 mA)

As can be seen from the graph, a significant difference in probe VI characteristic does not appear at different magnetic fields. This suggests that the plasma parameters do not change at weak magnetic field values. A table of plasma parameters was constructed for different magnetic field strength, which is shown in Table 1.As can be seen from the table, the measurement was carried out at five points of magnetic field values (0;6;15;19;28 mT).As the magnetic field increases, we can see that the plasma concentration increases and the electron temperature drops.When the magnetic field increases, the ambipolar diffusion decreases in the direction perpendicular to the magnetic field. The probability of collision between electrons and atoms increases; therefore, ionization also increases.As a result, electrons lose their energy more due to ionizing collisions during their drift due to the E×Beffect.This leads to a decrease in the value of the electron temperature from 4.1 to 3.45 eV.With increasing magnetic field floating potential takes less negative values.At relatively high magnetic fields, electrons become more and more restricted, and therefore the plasma potential becomes more negative to compensate the ion loss rate and maintain plasma quasi-neutrality.

Table 1 – The parameters of the stratified glow discharge for different values of the magnetic field. The results were obtained using Langmuir probe diagnostics method. (Experiment parameters: Argon, P=0.23torr, I=1.3 mA)

Induction of magnetic field	n_i, m^3	T_e, eV	V_f, V	$I_{saturation}$, mkA
0 mT	$1.41*10^{15}$	4.1	-17.8	2.35
6 mT	$1.48*10^{15}$	4.07	-17.6	2.37
15 mT	$1.49*10^{15}$	3.57	-15.6	2.59
19 mT	$1.58*10^{15}$	3.58	-15.5	2.89
28 mT	$1.74*10^{15}$	3.45	-14.9	3.16

In [21] the density of the ion current in the wall also was measured. As the field increases, the ratio of the density on the wall to the density on axis decreases with the growth of the magnetic field.For the number of electrons per unit length of the discharge to remain constant, the concentration must increase. It should be mentioned that we use a constant current (DC discharge) discharge.

Also, optical emission spectrawas obtained in stratified glow discharge at different magnetic fields (Figure 3).

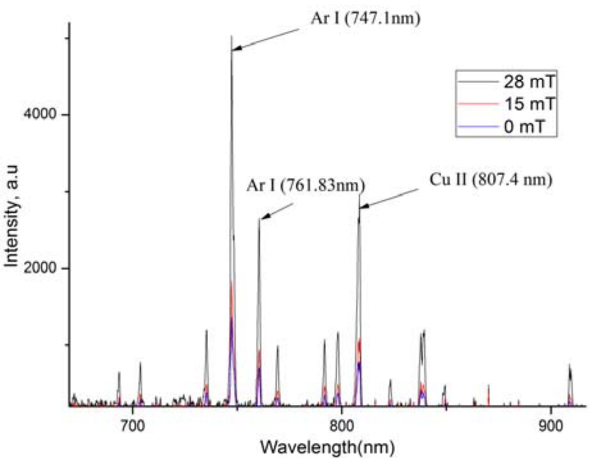

Figure 3– Optical emission spectra of stratified glow discharge at different magnetic fields

As can be seen from the graph, with increasing magnetic field the intensity of the spectral linealso increases. As mentioned above with increasing magnetic field due to diffusion the probability of collision increases, which in turn leads to enhance of ionization.Perhaps the number of excited atoms increases, leading to an increase in the intensity of the discharge.

Conclusion

In order to obtain the information about the plasma of stratified glow discharge, probe and optical diagnostics were carried out.During the experiments it was found that with increasing magnetic field plasma parameterscan be also changed.The change of these parameters is related to the processes of diffusion and collision of charged particles in ExB fields.Of course, the work requires further research in different conditions of the glow discharge.

The work was done with the support of the Ministry Education and Science of Republic Kazakhstan in the framework of the grant AP05133536.

References

1. G. Bonizzoni, E.Vassallo. “Plasma physics and technology; Industrial applications. ”*Vacuum* 64(2002): 327-336/

2. RoshanShishoo. “Plasma Treatment–Industrial Applications and Its Impact on the C&L Industry.”*Journal of Industrial Textiles* 26, (1996): 0026-10.

3. Bogaerts, A.“The glow discharge: an exciting plasma!.”*Journal of Analytical Atomic Spectrometry* 14 (1999): 1375-1384.

4. V N Tsytovich.“Elementary Excitation and the Physics of Stochastic Processes in a Plasma”, *Sov.Phys.Uspekhi*13(1970): 413–414.

5. Francis F. Chen. “Industrial applications of low-temperature plasma physics.”*Physics of Plasmas* 2,(1998): 2164.

6. . Golant V.E., Zhilinsky A.P., Sakharov I.E.“Fundamentals of Plasma Physics”, NewYork: Wiley (1980).

7. W.L.Wiese. “Spectroscopic diagnostics of low temperature plasmas: techniques and required

8. data”. *SpectrochimicaActa Part B: Atomic Spectroscopy* 46 (1991): 831-841.

9. Francis F Chen. “Langmuir probe analysis for high density plasmas.”*Physics of Plasmas* 8, (2001): 3029-3041.

10. I.H. Hutchinson. “Principles of Plasma Diagnostics.”Cambridge University Press, New York (1987).

11. G. S. Selwyn. “In situ laser diagnostic studies of plasma-generated particulate contamination.” *Journal of Vacuum Science & Technology A* 7 (1989): 2758.

12. U.Konopka, D.Samsonov, A.V. Ivlev, J.Goree, V.Steinberg, and G.Morfill. “Rigid and differential plasma crystal rotation induced by magnetic fields.”*Phys. Rev. E* 61,(2000): 1890.

13. P. K. Kaw, K. Nishikawa, and N. Sato. “Rotation in collisional stronglycoupled dusty plasmas in a magnetic field.”*Phys. Plasmas* 9, (2002):387.

14. V.Y. Karasev, A.I. Eikhvald, E.S. Dzlieva, and A. Y. Ivanov. “Rotational motion of dusty structures in glow discharge in longitudinal magnetic field.”*Phys. Rev* 74,(2006): 066403.

15. M. M. Vasiliev, L. G. D’yachkov, S. N. Antipov, R. Huijink, O. F. Petrov, V. E. Fortov. “Dynamics of dust structures in a DC discharge under action of axial magnetic field.” *EPL*93,(2011): 15001.

16. E. Jr. Thomas, B. Lynch, U. Konopka, R. L. Merlino, and M. Rosenberg. “Observations of imposed ordered structures in a dusty plasma at high magnetic field.”*Phys. Plasmas* 122, (2015): 030701.

17. V. Y. Karasev, E. S. Dzlieva, S. I. Pavlov, L. Novikov, S. Maiorov. “The rotation of complex plasmas in a stratified glow discharge in the strong magnetic field.”*IEEE Transactions on Plasma Science*46, (2018): 727-730.

18. I. Langmuir, C. G. Found, A. F. Dittmer. “A new type of electric discharge: the streamer discharge.”*Science*31, (1924): 392-394.

19. F.F. Chen, in Plasma Diagnostic Techniques, R. H. Huddleston, and S. L. Leonard, eds., Academic Press, New York (1964), Chapter 4.

20. F.F. Chen,Introduction to Plasma Physics and Controlled Fusion, Plenum Press, New York (1984).

21. J.W. Swift and M. J. R. Schwar,Electrical Probes for Plasma Diagnostics, Iliffe Book Ltd., London (1970).

22. R. J. Bickerton and A. von Engel.“The Positive Column in a Longitudinal Magnetic Field.”*Proceedings of the Physical Society* 69, (1956): 468.

23. Juan R. Sanmartin. “Theory of a Probe in a Strong Magnetic Field.”*The Physics of Fluids* 13 (1970): 103.

24. D. Bohm,“The Characteristics of Electrical Dischargesin Magnetic Fields.” A. Guthrie and R. K. Wakerling, Eds.McGraw-Hill Book Company, New York, (1949).

25. Juan Sanmartin“Theory of a Probe in a Strong Magnetic Field.”*Physics of Fluids* 13, (1970): 22-41.

26. Chung, P. M., L. Talbot, K. J. Touryan, Electrical probes in stationray and flowing plasmas, Theory and Application, Springer-Verlag, New York, (1975).

27. Demidov, V. I., S. V. Ratynskaia, and K. Rypdal, “Electric probes for plasmas: The link between theory and instrument.” *Rev. Sci. Instrum*.,73,(2002) 3409–3438.

28. A.R. Abdirakhmanov, Zh.A. Moldabekov, S. K. Kodanova , M. K. Dosbolayev , and T. S. Ramazanov. “Rotation of Dust Structures in a Magnetic Field in a DC Glow Discharge.” *IEEE Transaction on Plasma Science* (2019), doi 10.1109/TPS.2019.2906051.

29. T. S. Ramazanov, N. K. Bastykova, Y. A. Ussenov, S. K. Kodanova,K. N. Dzhumagulova, and M. K. Dosbolayev. “The behavior of dustparticles near Langmuir probe.” *Contrib. Plasma Phys*. 52,(2012): 110.

30. A.R. Abdirakhmanov, M. K. Dosbolayev, and T. S. Ramazanov. “The gas discharge dusty plasma in a uniformmagnetic field”*AIP Conference Proceedings* 1925 (2018): 020007.

31. Abdirakhmanov A.R., Dosbolayev M.K., Ramazanov T.S.*Journal of the problems of the evolution of open systems.* 18, (2016): 34–39.

IRSTI 29.19.09 https://doi.org/10.26577/ijmph-2019-i2-9

Pawitar Dulari

Department of Physics, Government Degree College Dharamshala (H.P.) INDIA-176215
*e-mail:pawitar.ibs@gmail.com

Thermoelastic properties of solids based on equation of state

Abstract. Thermoelastic properties of solids at high pressures are studied using various equations of state (EOS) such as Eularian Birch-Murnaghan EOS, Poirier-Tarantola logarithmic EOS and the generalized Vinet-Rydberg EOS. We have determined the pressure derivatives of bulk modulus upto third order which are useful for predicting the Grüneisen parameter and its volume derivatives. Expressions have been obtained for the derivative properties based on different equations of state, and extrapolated to the limit of extreme compression. It is found that all the three equations lead to a common relationship between second and third pressure derivatives of bulk modulus in the limit of extreme compression.

Keywords: Equations of state, pressure derivatives of bulk modulus, Grüneisen parameter, extreme compression behavior.

Introduction

Equations of state at high pressures have been extremely useful for studying the thermoelastic properties of solids [1-5]. Bulk modulus and its pressure derivatives are important physical quantities for understanding the thermoelastic properties [6, 7] such as the Grüneisen parameter γ and its volume derivatives. $\gamma$is related to the thermal and elastic properties of materials by the formula [8, 9].

$$\gamma = \frac{\alpha K_T V}{C_V} = \frac{\alpha K_S V}{C_P} \tag{1}$$

Where α is the coefficient of volume thermal expansion, KT and KS are isothermal and adiabatic bulk modulus, CV and CP are the specific heats at constant pressure and constant volume respectively.

The second Grüneisen constant q used in the literature is defined as [10].

$$q = \left(\frac{\partial \ln \gamma}{\partial \ln V}\right)_T \tag{2}$$

The third order Grüneisen parameter is defined as

$$\lambda = \left(\frac{\partial \ln q}{\partial \ln V}\right)_T \tag{3}$$

or

$$\lambda = 1 - q + \frac{V}{q\gamma} + \frac{d^2\gamma}{dV^2} \tag{4}$$

In order to emphasize the importance of q and λ in determining higher order thermoelastic properties we refer to the following thermodynamic identities [9].

$$\delta_S = K'_S - 1 + q - \gamma - C'_S \tag{5}$$

$$\delta_T = K'_T - 1 + q + C'_T \tag{6}$$

$$\left(\frac{\partial \delta_S}{\partial \ln V}\right)_S \text{-} K_S K''_S + q(\lambda - \gamma) + (\gamma + q) \left(\frac{\partial \ln C_v}{\partial \ln V}\right)_S - \left(\frac{\partial}{\partial \ln V}\left(\frac{\partial \ln C_v}{\partial \ln V}\right)_s\right)_s - \left(\frac{\partial}{\partial \ln V}\left(\frac{\partial \ln C_v}{\partial \ln V}\right)_s\right)_T \tag{7}$$

$$\left(\frac{\partial \delta_S}{\partial \ln V}\right)_T = -K_T K_T'' + \lambda q + \left(\frac{\partial C_T'}{\partial \ln V}\right)_T \tag{8}$$

where

δ_S is the adiabatic Anderson-Grüneisen parameter

$$\delta_S = -\frac{1}{\alpha}\left(\frac{\partial \ln K_S}{\partial T}\right)_P \tag{9}$$

δ_T is the isothermal Anderson-Grüneisen parameter

$$\delta_T = -\frac{1}{\alpha}\left(\frac{\partial \ln K_T}{\partial T}\right)_P \tag{10}$$

$$C_S' = (\partial \ln C_V / \partial \ln V)_S \tag{11}$$

and

$$C_T' = (\partial \ln C_V / \partial \ln V)_T \tag{12}$$

Thus$q$ and λ appearing in esquations [5–8] are useful parameters reduced to investigate higher order thermoelastic properties. We make use of the generalized free-volume formula for determining $q$and λ.

Generalized free-volume formulation

According to the generalized free-volume formula [8, 11], $\gamma$is related to pressure P, isothermal bulk modulus K and its pressure derivative K'as follows:

$$\gamma = \frac{\left(\frac{K'}{2}\right) - \left(\frac{1}{6}\right) - \left(\frac{t}{3}\right)\left(1 - \frac{P}{3K}\right)}{1 - 2t\left(\frac{P}{3K}\right)} \tag{13}$$

The parameter t takes different values for different derivatives of γ, based on different approximation. Thus t = 0 for Slater's formula [12], t = 1 for the formulation developed by Dugdaleand MacDonald [13], t = 2 yields the free-volume formula [9], ad t = 2.35 resulted in a molecular dynamical calculation by Barton and Stacey [14]. The assumptions and approximations on which Equation [13] is based, have been reviewed in a comprehensive manner by Stacey and Davis. Equation [13] can be applied to different types of metals, solids as well as insulators, because it is derives from the fundamental relationship between thrmal pressure and thermal energy [8]. The pressure dependence or volume dependence of γcan be studied with the help of Eq. [13] using different equations of state [10, 15]. Expressions for the volume derivatives of γ, represented by q and λ are derived from Eq. (13) considering t to be independent of pressure, i.e. $dt/dp_T = 0$. It has been found by Stacey and Davis [8] that λ varies slowly with pressure, and constant λ might be a good approximation. Although there is no fundamental reason for believing that λ is constant, it is much better assumption constant q often assumed in mineral physics [16].

It is more convenient to rewrite Eq. (13) in an equivalent form as follows (13).

$$\gamma = \frac{K'}{2} - \frac{1}{6} - \varepsilon \tag{14}$$

where

$$\varepsilon = \frac{t(K - K'P)}{(3K - 2tP)} \tag{15}$$

The following equations are then obtained from the differentiation of Eq. (13)

$$\gamma_q = \frac{-KK''}{2} + K\frac{d\varepsilon}{dP} \tag{16}$$

and

$$\gamma_q\,(q+\lambda) = $$

$$= \frac{K^2K'''}{2} + \frac{K'(KK'')}{2} - K'\left(K\frac{d\varepsilon}{dP}\right) - K^2\frac{d^2\varepsilon}{dP^2} \tag{17}$$

Eqs. (16) and (17) yield

$$(q+\lambda) = -K' - $$

$$\frac{[(K^2K'''/KK'') - (2/KK'')\,(K^2 d^2\varepsilon/dP^2)]}{1 - (2/KK'')(Kd\varepsilon/dP)} \tag{18}$$

Values of γ, q and λ can be calculate by knowing the pressure derivatives of bulk modulus. These pressure derivatives can be determined with the help of equations of state.

Analysis based on equations of state

Higher pressure derivatives of bulk modulus are determined here using some important equations of state given below:

Birch-Murnaghan fourth order EOS

This EOS has been derived from the Eulerian strain theory [17]. The expressions for P, K, K', KK'' and K^2K''' obtained from this equation of state are given below:

$$P = \frac{9K_0}{16}[-Ax^{-5/3} + Bx^{-7/3} - Cx^{-3} + Dx^{-11/3}], \quad (19)$$

$$K = \frac{9K_0}{16}[-A(5/3)x^{-5/3} + B(7/3)x^{-7/3} - C(3)x^{-3} + D(11/3)x^{-11/3}] \quad (20)$$

$$K' = \frac{9K_0}{16K}[-A(5/3)^2x^{-5/3} + B(7/3)^2x^{-7/3} - C(3)^2x^{-3} + D(11/3)^2x^{-11/3}] \quad (21)$$

$$KK'' = \frac{9K_0}{16K}[-A(5/3)^3x^{-5/3} + B(7/3)^3x^{-7/3} - C(3)^3x^{-3} + D(11/3)^3x^{-11/3}] - K^{12} \quad (22)$$

$$K^2K''' = \frac{9K_0}{16K}[-A(5/3)^4x^{-5/3} + B(7/3)^4x^{-7/3} - C(3)^4x^{-3} + D(11/3)^4x^{-11/3}] - K^{13} - 4K'KK'' \quad (23)$$

where $x = V/V_o$ and

$$A = K_0K_0'' + (K_0' - 4)(K_0' - 5) + 59/9 \quad (24)$$

$$B = 3K_0K_0'' + (K_0' - 4)(3K_0' - 13) + 129/9 \quad (25)$$

$$C = 3K_0K_0'' + (K_0' - 4)(3K_0' - 11) + 105/9 \quad (26)$$

$$D = K_0K_0'' + (K_0' - 4)(K_0' - 3) + 35/9 \quad (27)$$

Poirier-Tarantola logarithmic fourth-order EOS

Poirier and Tarantola [18] have obtained logarithmic EOS using the Henckystrain which is represented by (1/3) ($\ln V/V_o$). The expressions based on this EOS s follows:

$$P = K_0x^{-1}[-(\ln x) + \left(\frac{K_0' - 2}{2}\right)(\ln x)^2 - \frac{1}{6}Q(\ln x)^3] \quad (28)$$

$$K = K_0x^{-1}[1 - (K_0' - 1)(\ln x) + \frac{1}{2}(K_0K_0'' + K_0^{12} + 2K_0' + 1)(\ln x)^2 - \frac{1}{6}Q(\ln x)^3] \quad (29)$$

$$K' = \frac{K_0x^{-1}}{K}[K_0' - (K_0K_0'' + K_0^{12} - K_0')(\ln x) + (K_0K_0'' - k_o^{12} - 5/2K_0' + 2)(\ln x)^2 - \frac{1}{6}Q(\ln x)] \quad (30)$$

$$KK'' = 3K' + \frac{P}{k} - 3 - K^{12} + \frac{K_0}{xk}(K_0K_0'' + K_0^{12} - 3K_0' + 3) \quad (31)$$

$$K^2K''' = 3KK'' + \frac{(K - PK')}{K} - 3K'KK'' - \frac{K_0(K' - 1)}{xK}(K_0K_0'' + K_0^{12} - 3K_0' + 3) \quad (32)$$

where $x = V/V_o$ and $Q = K_0K_0'' + K_0^{12} - 3K_0' + 3$

Generalized Vinet-Rydberg Eos

Stacey [19, 20] has generalized the Vinet EOS, so as to make it compatible with infinite pressure value K_∞', for the pressure derivative of bulk modulus the equation thus formulated by Stacey is known is the generalized Rydberg EOS.

$$P = 3K_0x^{-k_\infty^1}(1 - x^{1/3})\exp[\eta(1 - x^{1/3})] \quad (33)$$

$$K = 3K_0x^{-k_\infty^1}\exp[\eta(1 - x^{1/3})][k_\infty^1(1 - x^{1/3}) + \frac{1}{3}x^{1/3} + \frac{\eta}{3}x^{1/3}(1 - x^{1/3})] \quad (34)$$

$$K' = \frac{3K_0 x^{-K'_\infty}}{K} \exp[\eta - x^{1/3})][K_\infty^{12}(1-x^{1/3}) +$$
$$+x^{1/3}\left(\frac{1+\eta}{3}\right)\left(2K'_\infty - \frac{1}{3}\right) - x^{2/3}\eta(2K'_\infty - 1) + \quad (35)$$
$$+\frac{\eta^2}{9}x^{2/3}(1-x^{1/3})]$$

$$K'' = \frac{P}{K}\left[\frac{n}{27}x^{1/3} + \frac{q}{9} + q^2 + 2q^3\right] +$$
$$+2\left(\frac{K}{P}\right)\left(K' - \frac{K}{P}\right) - K'\left(K' - \frac{K}{P}\right) \quad (36)$$

$$K''' = \frac{P}{K}\left[\frac{-n}{81}x^{1/3} + \frac{q}{27} - \frac{7}{9}q^2 + 4q^3 - 6q^4\right] -$$
$$-4KK''\left(K' - \frac{K}{P}\right) - K^{12}\left(K' - \frac{K}{P}\right) + \quad (37)$$
$$+6K'\left(\frac{K}{P}\right)\left(K' - \frac{K}{P}\right) - 6\left(\frac{K}{P}\right)^2\left(K' - \frac{K}{P}\right)$$

where x = V/V₀ and $\eta = \frac{3}{2}K_0' - 3K_\infty' + \frac{1}{2} = -3K_0 K_0'' - \frac{3}{4}K_0^{12} + \frac{1}{12}$.

$q = \dfrac{x^{1/3}}{3(1-x^{1/3})}$, for $K'_\infty = 2/3$, Eq. (33) reduces to the original Rydberg EOS.

The Birch-Murnagham EOS, the logarithmic EOS and the generalized Rydberg EOS can be written in the following form

$$K/P = K'_\infty + F(x) \quad (38)$$

Differentiating Eq (38) with the respect to 'P' successfully

$$(K' - K/P)K/P = -xF'(x) \quad (39)$$

$$[(KK'' + K'^2)(K/P) - 3K'(K/P)^2 +$$
$$+2(K/P)^3 = xF'(x) + x^2F''(x) \quad (40)$$

$$[(K^2K'''(K/P) + 4KK''(K' - K/P)(K/P) +$$
$$+K'^2(K' - K/P)(K/P) - 6K'(K' - K/P)(K/P)^2 +$$
$$+6(K' - K/P)(K/P)^3] =$$
$$= -[xF'(x) + 3x^2F''(x) + x^3F'''(x)] \quad (41)$$

Where $x = V/V_0$

In case of birch murnagham fourth order EOS the value of F(x) is

$$F(x) = \left[\frac{2Ax^2 - \left(\frac{4}{3}\right)Bx^{\frac{4}{3}} + \left(\frac{2}{3}\right)Cx^{\frac{2}{3}}}{Ax^2 - Bx^{\frac{4}{3}} + Cx^{\frac{2}{3}} - D}\right] \quad (42)$$

In case of the logarithmic fourth –order EOS the value of F(x) is

$$F(x) = \left[\frac{1 - 2A_1 \ln x + 3A_2(\ln x)^2}{-\ln x + A_1(\ln x)^2 + A_2(\ln x)^3}\right] \quad (43)$$

In case of the generalized Rydberg EOS the value of F(x) is

$$F(x) = \frac{x^{\frac{1}{3}}}{3(1-x^{\frac{1}{3}})} + \eta\frac{x^{\frac{1}{3}}}{3} \quad (44)$$

Results and Discussions

We can derive expressions for the derivatives of F(x) such as F'(x), F''(x) and F'''(x) by using Eqs. (42-44). In the limit $V \to 0$, $P \to \infty$, $K \to \infty$, but their ratio P/K remain finite such that $(P/K)_\infty = 1/K'_\infty$. Also $(1 - K'P/K)$, KK'' and K^2K''' tend to zero in the limit of infinite pressure, but their ratios $KK''(1 - K'P/K)$ and K^2K'''/KK'' remain finite [6,22]. At extreme compression $x \to 0$, we have $F(x) \to 0$, $x F'(x) \to 0$, $x^2 F''(x) \to 0$ and $x^3 F'''(x) \to 0$ for all the equations of state based on Eqs. (38-41) using the calculus, we have

$$\frac{xF'(x) + x^2F''(x)}{xF'(x)} =$$
$$= \frac{F'(x) + xF''(x) + 2xF''(x) + x^2F'''(x)}{F'(x) + xF''(x)} \quad (45)$$

In the extreme compression limit Eqs. (39) and (40) gives

$$\left[\frac{KK''}{K' - \frac{K}{P}}\right]_\infty - K'_\infty = -\frac{xF'(x) + x^2F''(x)}{xF'(x)} \quad (46)$$

Eqs. (40) and (41) gives

$$\frac{\left(\frac{K^2K'''}{KK''}\right)_\infty + K_\infty^{12}\left(\frac{K'-K/P}{KK''}\right)_\infty}{1-K'_\infty\left(\frac{K'-K/P}{KK''}\right)_\infty} =$$

$$-\frac{xF'(x)+3x^2F''(x)+x^3F'''(x)}{xF'(x)+x^2F''(x)} \qquad (47)$$

Eqs. (45 – 47) then yield

$$\left(\frac{K^2K'''}{KK''}\right)_\infty = \left(\frac{KK''}{K'-K/P}\right)_\infty - 2K'_\infty \qquad (48)$$

The Birch-Murnaghan Fourth Order EOS gives using Eqs. (19-23)

$$\left(\frac{KK''}{K'-K/P}\right)_\infty = -K'_\infty(K'_\infty - 2/3) \qquad (49)$$

$$\left(\frac{K^2K'''}{KK'''}\right)_\infty = -(K'_\infty + 2/3) \qquad (50)$$

The logarithmic fourth order EOS using Eqs. (28-32)

$$\left(\frac{KK''}{K'-K/P}\right)_\infty = -2K'_\infty \qquad (51)$$

$$\left(\frac{K^2K'''}{KK''}\right)_\infty = -K'_\infty \qquad (52)$$

The generalized Vinet-Rydberg EOS using Eqs. (33-37) gives

$$\left(\frac{KK''}{K'-K/P}\right)_\infty = -\left(K'_\infty - \frac{1}{3}\right) \qquad (53)$$

$$\left(\frac{K^2K'''}{KK''}\right)_\infty = -\left(K'_\infty + \frac{1}{3}\right) \qquad (54)$$

All these equations of states satisfies the common relation (48). This relationship can be useful for investigating further the thermoelastic properties of solids at high pressures [6, 8, 23, 24].

References

1. Anderson, O.L.; Masuda, K.; Isaak, D.G. "A new thermodynamic approach for high-pressure physics." *Physics of the Earth and Planetary Interiors* 91.1-3 (1995): 3-16.
2. Shanker,J.;Thomas, L.M. *Phys. Stat. Sol* (b) 35 (1997): 601.
3. Chauhan, R. S., Singh, C. P. "Equation of state and thermal expansivity of NaCl under high pressure and high temperature." *Physica B: Condensed Matter* 387.1-2 (2007): 352-357.
4. Shanker, J ; Singh, P K; Saurabh, S. “Analysis of infinite pressure behaviour of thermoelastic properties of materials”*Indian Journal of Pure and Applied Physics*. 539(4) (2015): 230-233.
5. Ahmad, J.F.; Alkammash, I.Y. "Theoretical study of some thermodynamical properties for solid under high pressure using finite-strain EOS." *Journal of the Association of Arab Universities for Basic and Applied Sciences* 12.1 (2012): 17-22.
6. Shanker, J., Singh, B.P. "A comparative study of Keane's and Stacey's equations of state." *Physica B: Condensed Matter* 370.1-4 (2005): 78-83.
7. Kushwah, S.S., Bhardwaj,N.K. "Analysis based on equation of state for sodium halides." *Journal of Physics and Chemistry of Solids* 70.3-4 (2009): 700-702.
8. Stacey, F.D., Davis,P.M. "High pressure equations of state with applications to the lower mantle and core." *Physics of the Earth and Planetary interiors* 142.3-4 (2004): 137-184.
9. Stacey, F.D. "High pressure equations of state and planetary interiors." *Reports on progress in physics* 68.2 (2005): 341.
10. Vocadlo, L.;Poirer, J.P.; Price, G.D. "Gruneisen parameters and isothermal equations of state." *American Mineralogist* 85.2 (2000): 390-395.
11. Zubarev, V.N.;Vashchenko,V.Ya. "O koefficienteGryunajzena " Soviet Phys. Solid State 5 (1963): 653. (inrussian).
12. J.C. Slater, *Introduction to chemical Physics*, Mc Graw – Hills, New York (1939).
13. Dugdale, J.S., MacDonald,D.K.C. "The thermal expansion of solids." *Physical Review* 89.4 (1953): 832.
14. Barton, M.A., Stacey; F.D. "The Grüneisen parameter at high pressure: a molecular dynamical study." *Physics of the earth and planetary interiors* 39.3 (1985): 167-177.

15. Holzapfel, W.B., Hartwig, M.;Sievers, W. "Equations of state for Cu, Ag, and Au for wide ranges in temperature and pressure up to 500 GPa and above." *Journal of Physical and Chemical Reference Data* 30.2 (2001): 515-529.

16. AndersonO.L.*Equations of State of Solid for Geophysics and Ceramic Science*, Oxford University Press, New York(1995).

17. Birch, F. "Elasticity and constitution of the Earth's interior." *Journal of Geophysical Research*57 (1952): 227-286.

18. Poirier,J.P.; Tarantola, A. "A logarithmic equation of state*" Physics of the Earth and Planetary Interiors*109 (1998).

19. Keane, A. "An investigation of finite strain in an isotropic material subjected to hydrostatic pressure and its seismological applications." *Australian Journal of Physics* 7.2 (1954): 322-333.

20. Stacey, F.D. "Finite strain, thermodynamics and the earth's core." *Physics of the Earth and Planetary interiors* 128.1-4 (2001): 179-193.

21. Stacey, F.D. "The K-primed approach to high-pressure equations of state." *Geophysical Journal International* 143.3 (2000): 621-628.

22. Shanker, J.; Singh,B.P.; Jitendra, K. "Extreme compression behaviour of higher derivative properties of solids based on the generalized Rydberg equation of state." *Condense Matter Phys.* 12 (2009): 205-213.

23. Shanker, J.;Dulari, P.; Singh, P.K. "Extreme compression behaviour of equations of state." *Physica B: Condensed Matter* 404.21 (2009): 4083-4085.

24. K.S. Singh. "Second order and third order Grüneisen parameters at extreme compression." *Physica B: Condensed Matter*407(2012): 668-669

IRSTI 27.25.19 https://doi.org/10.26577/ijmph-2019-i2-10

[1,*]A.A. Zhadyranova, [2]Zh.R. Myrzakul, [1]K.R. Myrzakulov

[1]1Department of General Theoretical Physics, Eurasian National University, Kazakhstan, Nur-Sultan
[2]Department of Mathematics, Nazarbayev University, Kazakhstan, Nur-Sultan,
*e-mail:a.a.zhadyranova@gmail.com

Soliton surface associated with the oriented associativity equation for n=3 case

Abstract. This paper describes the soliton surfaces approach to the Oriented Associativity equation for n=3 case. The equation of associativity arose from the 2D topological field theory. We constructed the surface associated with the Oriented Associativity equation for n=3 case equations using Sym-Tafel formula, which gives a connection between the classical geometry of manifolds immersed in R^m and the theory of solitons. The so-called Sym-Tafel formula simplifies the explicit reconstruction of the surface from the knowledge of its fundamental forms, unifies various integrable nonlinearities and enables one to apply powerful methods of the soliton theory to geometrical problems. The soliton surfaces approach is very useful in construction of the so-called integrable geometries. Indeed, any class of soliton surfaces is integrable. Geometrical objects associated with soliton surfaces (tangent vectors, normal vectors, foliations by curves etc.) usually can be identified with solutions to some nonlinear models (spins, chiral models, strings, vortices etc.). We consider the geometry of surfaces immersed in Euclidean spaces. The Oriented Associativity equation plays a fundamental role in the theory of integrable systems. Such soliton surfaces for the Oriented Associativity equation for n=3 case are considered, and first and second fundamental forms of soliton surfaces are found for this case. Also, we study an area of surfaces for the Oriented Associativity equation for n=3 case.

Key words: the Oriented Associativity equation, nonlinear equation, the Lax pair, first and second fundamental forms, soliton surfaces, area of surfaces.

Introduction

The equation of associativity relation for genus 0 Gromov-Witten (GW) invariants completely solves the classical problem of enumerating complex rational curves in the complex projective space Pn [1]. For genus-0 GW-theory, the associativity of quantum cohomology, which is equivalent to equation of associativity, led to Kontsevich's solution to the classical problem of counting degree d rational curves passing through 3d − 1 general points in P2 [2]. A system of PDE, called open WDVV, that constrains the bulkdeformed superpotential and associated open GW invariants of a Lagrangian submanifold $L \subset X$ with a bounding chain [3]. In this paper we shall consider so-called nonlinear partial differential equations of associativity in 2D topological field theories (see [4-7]) and give their description as integrable nondiagonalizable weakly nonlinear systems of hydrodynamic type. For systems of this type corresponding general differential geometric theory of integrability connected with Poisson structures of hydrodynamic type can be developed. For an arbitrary solution of the open equation of associativity, satisfying a certain homogeneity condition, constructed a descendent potential in genus 0 [8]. For any mechanics, given by the metric and the third order Codazzi tensor, it is possible to obtain the superfield Lagrangian [9] by solving a simple differential equation. Universal algebraic structure, closely related with that of the equation of associativity, govern quantum correlation functions of every quantum field theory [10]. Topological approach provides a general framework for lifting relations via morphisms between not necessarily orientable spaces [11]. For isotropic (so(n)-invariant) spaces provided admissible prepotentials for any solution to the curved equation of associativity [12]. For every flat-space equation of associativity solution subject to a simple constraint provided a curved-space solution on any isotropic space, in terms of the rotationally invariant conformal factor of the metric [13]. Flat structure was introduced by K. Saito and his collaborators at the end of 1970's. Independently the equation of associativity arose from the 2D topological field theory. B. Dubrovin unified these two notions as Frobenius manifold structure [14]. The concepts of Frobenius manifold and Lenard complex must be strictly related. They provides two ways of looking at the same object from different perspectives and by using different geometrical structures [15]. In paper [16]compared two different geometrical interpretations of the equation of associativity of 2D topological field theory. The first is the classical interpretation proposed by Boris Dubrovin, based on the concept of Frobenius manifold. The second is a novel interpretation, based on the concept of Lenard complex on a Haantjes manifold. In paper [17]. determined correlators of topological quantum field theories and provided explicit solutions to the equation of associativity.

The equation of associativity, in general, have the following form [4,18]:

$$\frac{\partial^3 F}{\partial t^i \partial t^j \partial t^p}\eta^{pq}\frac{\partial^3 F}{\partial t^q \partial t^k \partial t^r}= \\ =\frac{\partial^3 F}{\partial t^j \partial t^k \partial t^p}\eta^{pq}\frac{\partial^3 F}{\partial t^i \partial t^q \partial t^r},$$

$$\forall i,j,k,r \in \{1,...,n\},$$

where F is a prepotential, η is a metric.

The Associativity equation, or WDVV equation, plays a fundamental role in the geometric theory of Integrable Systems. Its solutions define Frobenius manifolds, which correspond to integrable systems; Frobenius manifolds also play a fundamental role in the theory of quantum cohomology and Gromov - Witten invariants. These connections were shown by B. Dubrovin in his seminal paper [19].

In this paper we shall consider so-called nonlinear partial differential equations of associativity.

The nonlinear partial differential system of equations:

$$\frac{\partial^2 c^i}{\partial a^j \partial a^m}\frac{\partial^2 c^m}{\partial a^k \partial a^n}=\frac{\partial^2 c^i}{\partial a^k \partial a^m}\frac{\partial^2 c^m}{\partial a^j \partial a^n} \quad (1)$$

on n unknown functions (c^i) of n independent variables (a^j) was introduced in [19] as a generalization of the Associativity equations. Its solution define F-manifolds, which are still in correspondence with integrable systems. The far-reaching implication of this generalization are an active subject of study: flat and bi-flat F-manifolds have interesting connections with Painlevé equations [20-22]; see also the papers [23-24] devoted to coisotropic deformations. We call the system (1) the Oriented Associativity equation.

Soliton surface associated with the Oriented Associativity equation for $n=3$ case

The Oriented Associativity equation admits the scalar linear spectral problem

$$\frac{\partial^2 h}{\partial a^i \partial a^j}=\lambda\frac{\partial^2 c^m}{\partial a^i \partial a^j}\frac{\partial h}{\partial a^m}$$

(see, for instance, [25]) that ensure that the equation is integrable as it provides a Lax pair.

We observe that the Associativity equation [26] can be obtained from (1) by the potential reduction $c^i=\eta^{im}\partial F a^m$, where η^{ks} is a constant nondegenerate symmetric matrix.

The system of quadratic equations [26]

$$\begin{aligned} u_{xx}&=v_{xt}w_{xx}-v_{xx}w_{xt}+w_{xt}^2-w_{xx}w_{tt},\\ u_{xt}&=v_{tt}w_{xx}-v_{xt}w_{xt},\\ u_{tt}&=v_{xt}^2-v_{xx}v_{tt}+v_{tt}w_{xt}-v_{xt}w_{tt}, \end{aligned} \quad (2)$$

is the Oriented Associativity equation in the simplest case $n=3$. It is endowed by the Lax pair

$$\begin{pmatrix}\psi\\ \psi_1\\ \psi_2\end{pmatrix}_x=\lambda\begin{pmatrix}0&1&0\\ u_{xx}&v_{xx}&w_{xx}\\ u_{xt}&v_{xt}&w_{xt}\end{pmatrix}\begin{pmatrix}\psi\\ \psi_1\\ \psi_2\end{pmatrix},$$

$$\begin{pmatrix}\psi\\ \psi_1\\ \psi_2\end{pmatrix}_t=\lambda\begin{pmatrix}0&0&1\\ u_{xt}&v_{xt}&w_{xt}\\ u_{tt}&v_{tt}&w_{tt}\end{pmatrix}\begin{pmatrix}\psi\\ \psi_1\\ \psi_2\end{pmatrix}$$

In the following sections we work with the system (2).

First fundamental form of a surface

The corresponding Lax pair for the Oriented Associativity equation for $n=3$ case to the system (2) is given by

$$\Phi_x = U\Phi \tag{3}$$

$$\Phi_t = V\Phi \tag{4}$$

where $U = \lambda A$ and $V = \lambda B$. Here A and B matrices defined as follows:

$$A = \begin{pmatrix} 0 & 1 & 0 \\ u_{xx} & v_{xx} & w_{xx} \\ u_{xt} & v_{xt} & w_{xt} \end{pmatrix}, \quad B = \begin{pmatrix} 0 & 0 & 1 \\ u_{xt} & v_{xt} & w_{xt} \\ u_{tt} & v_{tt} & w_{tt} \end{pmatrix}$$

Geometrical objects associated with soliton surfaces usually can be identified with solutions to some nonlinear models [27-28]. The scalar square of the total differential dr of the radius-vector of the current point of a surface is called the first fundamental form I of the surface [29]:

$$I = \mathrm{d}r^2,$$

In expanded form, it is recorded as

$$I = r_x^2 \mathrm{d}x^2 + 2r_x r_t \mathrm{d}x\mathrm{d}t + r_t^2 \mathrm{d}t^2, \tag{6}$$

where x and t are the curvatures.

To construct the surface, we now use the Sym-Tafel formula [30]. It has the form

$$r = \Phi^{-1}\Phi_\lambda,$$

where $r = \sum r_j \sigma_j$ is the matrix form of the position vector of the surface, Φ is a solution of the equations (3)-(4). We have

$$r_x = \Phi^{-1}U_\lambda\Phi, \quad r_t = \Phi^{-1}V_\lambda\Phi.$$

In terms of the Lax representation, equation (6) will be rewritten as follows:

$$I = \frac{1}{2}\left(\mathrm{tr}(U_\lambda^2)dx^2 + 2\mathrm{tr}(U_\lambda V_\lambda)dxdt + \mathrm{tr}(V_\lambda^2)dt^2\right). \tag{7}$$

We now turn to finding the first fundamental form of soliton surface for the Oriented Associativity equation for n = 3 case to the system (2)

$$tr(U_\lambda^2) \;=\; v_{xx}^2 + w_{xt}^2 + 2\left(u_{xx} + v_{xt}w_{xx}\right), \tag{8}$$

$$\begin{aligned} \mathrm{tr}(U_\lambda V_\lambda) = 2u_{xt} + v_{xt}v_{xx} + \\ + w_{xx}v_{tt} + v_{xt}w_{xt} + w_{xt}w_{tt}, \end{aligned} \tag{9}$$

$$\mathrm{tr}(V_\lambda^2) = v_{xt}^2 + w_{tt}^2 + 2\left(u_{tt} + v_{tt}w_{xt}\right). \tag{10}$$

Substituting equations (8)-(10) into equation (7) we have the first fundamental form of soliton surface for the Oriented Associativity equation to the system (2)

$$\begin{aligned} I \;=\; \frac{1}{2}\Big[&\left\{v_{xx}^2 + w_{xt}^2 + 2\left(u_{xx} + v_{xt}w_{xx}\right)\right\}\mathrm{d}x^2 + \left(2u_{xt} + v_{xt}v_{xx} + w_{xx}v_{tt} + v_{xt}w_{xt} + w_{xt}w_{tt}\right)\mathrm{d}x\mathrm{d}t + \\ &+ \left\{v_{xt}^2 + w_{tt}^2 + 2\left(u_{tt} + v_{tt}w_{xt}\right)\right\}\mathrm{d}t^2\Big] \end{aligned}$$

Second fundamental form of a surface

The scalar product of the total differential of the second order $\mathrm{d}^2 r$ of the radius-vector r of the current point of a surface by the orbit of the normal n at this point is called the second quadratic form of the surface:

$$II = -\mathrm{d}n \cdot \mathrm{d}r,$$

where

$$n = \frac{r_x \wedge r_t}{|r_x \wedge r_t|}.$$

In an expanded form, it is recorded as

$$II = b_{11}dx^2 + 2b_{12}dxdt + b_{22}dt^2, \tag{11}$$

where the coefficients b_{11}, b_{12} and b_{22} are given as

$$b_{11} \;=\; r_{xx} \cdot n, \tag{12}$$

$$b_{12} = r_{xt} \cdot n, \quad (13)$$

$$b_{22} = r_{tt} \cdot n, \quad (14)$$

or

$$b_{11} = \frac{1}{2}\mathrm{tr}(r_{xx}n),$$

$$b_{12} = \frac{1}{2}\mathrm{tr}(r_{xt}n),$$

$$b_{22} = \frac{1}{2}\mathrm{tr}(r_{tt}n),$$

here

$$r_{xx} = \Phi^{-1}(U_{\lambda x} + [U_\lambda, U])\Phi,$$

$$r_{xt} = \Phi^{-1}(U_{\lambda t} + [U_\lambda, V])\Phi,$$

$$r_{tt} = \Phi^{-1}(V_{\lambda t} + [V_\lambda, V])\Phi$$

The normal vector n is given by

$$n = \pm\frac{\Phi^{-1}[U_\lambda, V_\lambda]\Phi}{\sqrt{\frac{1}{2}tr([U_\lambda, V_\lambda]^2)}}.$$

Thus, the equation (12)-(14) is written as follows

$$b_{11} = \frac{1}{2}\frac{\mathrm{tr}\big((U_{\lambda x} + [U_\lambda, U])[U_\lambda, V_\lambda]\big)}{\sqrt{\frac{1}{2}\mathrm{tr}([U_\lambda, V_\lambda]^2)}}, \quad (15)$$

$$b_{12} = \frac{1}{2}\frac{\mathrm{tr}\big((U_{\lambda t} + [U_\lambda, V])[U_\lambda, V_\lambda]\big)}{\sqrt{\frac{1}{2}tr([U_\lambda, V_\lambda]^2)}}, \quad (16)$$

$$b_{22} = \frac{1}{2}\frac{\mathrm{tr}\big((V_{\lambda t} + [V_\lambda, V])[U_\lambda, V_\lambda]\big)}{\sqrt{\frac{1}{2}tr([U_\lambda, V_\lambda]^2)}}, \quad (17)$$

Substituting equations (15)-(17) into equation (11) we have the second fundamental form of a soliton surface for the Oriented Associativity equation to the system (2)

$$II = \frac{1}{2}\frac{\alpha\left(w_{xxt} - v_{xxx}\right) + w_{xxx}\beta + v_{xxt}\gamma}{\sqrt{\alpha^2 + \gamma\beta}}dx^2 +$$

$$+\frac{\alpha\left(w_{xtt} - v_{xxt} + 2\lambda\alpha\right) + \beta w_{xxt} + 2\lambda\beta\gamma + \gamma v_{xtt}}{\sqrt{\alpha^2 + \gamma\beta}}dxdt$$

$$+ \frac{1}{2}\frac{\alpha\left(w_{ttt} - v_{xtt}\right) + w_{xtt}\beta + v_{ttt}\gamma}{\sqrt{\alpha^2 + \gamma\beta}}dt^2$$

where

$$\alpha = \left(u_{xt} + v_{xt}w_{xt} - v_{tt}w_{xx}\right),$$

$$\beta = \left(v_{xt}^2 - u_{tt} - v_{tt}v_{xx} + v_{tt}w_{xt} - v_{xt}w_{tt}\right),$$

$$\gamma = \left(u_{xx} - w_{xt}^2 - v_{xt}w_{xx} + v_{xx}w_{xt} + w_{tt}w_{xx}\right).$$

Area of surfaces for Oriented Associativity equation for $n = 3$ case

In this section we consider the area of surfaces for the Oriented Associativity equation for $n = 3$ to the system (2). Area of surfaces is evaluated by

$$S = \iint\sqrt{\frac{1}{2}tr\left(\left\{U_{\lambda x} + \left[U_\lambda, U\right]\right\}^2\right)}\mathrm{d}x\mathrm{d}t \quad (18)$$

where the matrix A is defined as in equation (5). So, that $[U_\lambda, U] = 0$, we have

$$(U_{\lambda x})^2 = \begin{pmatrix} 0 & 0 & 0 \\ u_{xxx}v_{xxx} + w_{xxx}u_{xxt} & v_{xxx}^2 + w_{xxx}v_{xxt} & v_{xxx}w_{xxx} + w_{xxx}w_{xxt} \\ u_{xxx}v_{xxt} + w_{xxt}u_{xxt} & v_{xxx}v_{xxt} + v_{xxt}w_{xxt} & v_{xxt}w_{xxx} + w_{xxt}^2 \end{pmatrix}$$

Area of surfaces (18) for the Oriented Associativity equation to the system (2) is given by

$$S = \iint\sqrt{\frac{v_{xxx}^2 + w_{xxt}^2}{2} + v_{xxt}w_{xxx}}\,\mathrm{d}x\mathrm{d}t$$

Conclusions

In this work we considered the Oriented Associativity equation for $n = 3$ case. Soliton surfaces for the Oriented Associativity equation for $n = 3$ case was obtained. Area of surfaces for the

Oriented Associativity equation for $n = 3$ case was investigated.

References

1. Chen, X.; Zinger, A. "WDVV-type relations for disk Gromov-Witten invariants in dimension 6." *arXiv preprint arXiv:*1904.04254 (2019).
2. Fan, H.; Wu, L. "WDVV equation and its application to relative Gromov--Witten theory." *arXiv preprint arXiv:*1902.05739 (2019).
3. Solomon, J.P.; Tukachinsky, S.B. "Relative quantum cohomology." *arXiv preprint arXiv:*1906.04795 (2019).
4. Dubrovin, B. "Geometry of 2D topological field theories*." Integrable systems and quantum groups*. Springer, Berlin, Heidelberg, 1996. 120-348.
5. Dubrovin, B. "Integrable systems in topological field theory." *Nuclear physics B* 379.3 (1992): 627-689.
6. Witten, E. "On the structure of the topological phase of two-dimensional gravity." *Nuclear Physics B* 340.2-3 (1990): 281-332.
7. Dijkgraaf, R,; Verlinde, H.; Verlinde, E. "Notes on topological string theory and 2D quantum gravity." *Proc. of the Trieste Spring School.* 1990.
8. Buryak, A.; Basalaev, A. "Open WDVV equations and Virasoro constraints." *arXiv preprint arXiv:*1901.10393 (2019).
9. Kozyrev, N. "The curved WDVV equations and superfields." *Journal of Physics: Conference Series.* 1194. 1. IOP Publishing, 2019.
10. Park, J.S. "Homotopical Computations in Quantum Fields Theory." *arXiv preprint arXiv:*1810.09100 (2018).
11. Chen X. "Steenrod Pseudocycles, Lifted Cobordisms, and Solomon's Relations for Welschinger's Invariants" *arXiv preprint arXiv:*1809.08919. (2019).
12. Kozyrev, N.; Krivonos, S.; Lechtenfeld, O., Sutulin, A. "SU (2| 1) supersymmetric mechanics on curved spaces." *Journal of High Energy Physics* 2018.5 (2018): 175.
13. Kozyrev, N.; Krivonosa, S.; Lechtenfeldb, O.; Nersessianc,A.; Sutulin A. "Curved Witten-Dijkgraaf-Verlinde-Verlinde equation and N= 4 mechanics." *Physical Review D* 96.10 (2017): 101702.
14. Kato, M.; Mano,T.; Sekiguchi J. "Flat structure on the space of isomonodromic deformations*." arXiv preprint arXiv:*1511.01608 (2015).
15. Magri, F. "Haantjes manifolds and Veselov systems." *arXiv preprint arXiv:*1510.07951 (2015).
16. Magri, Franco. "WDVV equations." *arXiv preprint arXiv:*1510.07950 (2015).
17. Li, S.; Troost, J. "Twisted massive non-compact models." *Journal of High Energy Physics* 2018.7 (2018): 166.
18. Strachan, Ian AB; Stedman, R. "Generalized Legendre transformations and symmetries of the WDVV equations." *Journal of Physics A: Mathematical and Theoretical* 50.9 (2017): 095202.
19. Hertling,C.; Manin, Y.; "Weak Frobenius manifolds"*Internat. Math. Res. Notices* 6 (1999): 277-286.
20. Arsie, A.; Lorenzoni, P. "F-manifolds, multi-flat structures and Painlev\\'e transcendents." *arXiv preprint arXiv:*1501.06435 (2015).
21. Lorenzoni, P.; Pedroni, M.; Raimondo, A. "F-manifolds and integrable systems of hydrodynamic type." *Archivum Mathematicum* 47.3 (2011): 163-180.
22. Lorenzoni, P. "Darboux–Egorov system, Bi-flat F-manifolds and Painlevé VI." *International Mathematics Research Notices* 2014.12 (2014): 3279-3302.
23. Konopelchenko, B.G.; Magri, F. "Coisotropic deformations of associative algebras and dispersionless integrable hierarchies." *Communications in mathematical physics* 274.3 (2007): 627-658.
24. Konopelchenko, B.G.; Ortenzi, G."Coisotropic deformations of algebraic varieties and integrable systems." *Journal of Physics A: Mathematical and Theoretical* 42.41 (2009): 415207.
25. Pavlov, M.V.; Sergyeyev, A. "Oriented associativity equations and symmetry consistent conjugate curvilinear coordinate nets." *Journal of Geometry and Physics* 85 (2014): 46-59.
26. Pavlov, M.V.; Vitolo, R.F. "Bi-Hamiltonian structure of the oriented associativity equation." *Journal of Physics A: Mathematical and Theoretical* 52.20 (2019): 20LT01.
27. Sym, A. "Soliton surfaces." *Lettere al Nuovo Cimento (1971-1985)* 36.10 (1983): 307-312.
28. Sym, A"Soliton Surfaces and their Applications"*Geometrical Aspects of the Einstein Equations and Integrable Systems. Lecture Notes in Physics* 239, ed. Martini R, Springer- Berlin, 154-231 (1985).
29. Cieśliński, J. "The Darboux-Bianchi-B\\" acklund transformation and soliton surfaces." *arXiv preprint arXiv:*1303.5472 (2013).
30. Sym, A. "Soliton surfaces." *Lettere Al Nuovo Cimento (1971–1985)* 33.12 (1982): 394-400.

CONTENTS

International Journal of Mathematics and Physics, #2 , 2019